พฤติกรรมของเซลล์ต้นกำเนิดไขกระดูกและเซลล์ต้นกำเนิดไขมัน บนโครงเลี้ยงเซลล์ที่ทำจากเจลาตินและไคโตซาน เพื่อใช้ในงานวิศวกรรมเนื้อเยื่อกระดูก

นางสาวจุฑามาศ รัตนวราภรณ์

วิทยานิพนธ์นี้เป็นส่วนหนึ่งของการศึกษาตามหลักสูตรปริญญาวิศวกรรมศาสตรดุษฎีบัณฑิต
สาขาวิชาวิศวกรรมเคมี ภาควิชาวิศวกรรมเคมี
คณะวิศวกรรมศาสตร์ จุฬาลงกรณ์มหาวิทยาลัย
ปีการศึกษา 2552

BEHAVIOR OF BONE MARROW-DERIVED AND ADIPOSE-DERIVED STEM CELLS ON GELATIN/CHITOSAN SCAFFOLDS FOR BONE TISSUE ENGINEERING

Miss Juthamas Ratanavaraporn

A Dissertation Submitted in Partial Fulfillment of the Requirements
for the Degree of Doctor of Engineering Program in Chemical Engineering
Department of Chemical Engineering
Faculty of Engineering
Chulalongkorn University
Academic year 2009

Thesis Title	BEHAVIOR OF BONE MARROW-DERIVED AND ADIPOSE-DERIVED STEM CELLS ON GELATIN/CHITOSAN SCAFFOLDS FOR BONE TISSUE ENGINEERING
By	Miss Juthamas Ratanavaraporn
Field of Study	Chemical Engineering
Thesis Advisor	Associate Professor Siriporn Damrongsakkul, Ph.D.
Thesis Co-Advisor	Professor Yasuhiko Tabata, Ph.D.

Accepted by the Faculty of Engineering, Chulalongkorn University in Partial Fulfillment of the Requirements for the Doctoral Degree

…….. Dean of the Faculty of Engineering
(Associate Professor Boonsom Lerdhirunwong, Dr.Ing.)

THESIS COMMITTEE

…….. Chairman
(Professor Suttichai Assabumrungrat, Ph.D.)

…….. Thesis Advisor
(Associate Professor Siriporn Damrongsakkul, Ph.D.)

…….. Thesis Co-Advisor
(Professor Yasuhiko Tabata, Ph.D.)

…….. Examiner
(Assistant Professor Sorada Kanokpanont, Ph.D.)

…….. Examiner
(Assistant Professor Rath Pichyangkura, Ph.D.)

…….. External Examiner
(Borisut Sanmano Hanpanich, Ph.D.)

จุฑามาศ รัตนวราภรณ์ : พฤติกรรมของเซลล์ต้นกำเนิดไขกระดูกและเซลล์ต้นกำเนิดไขมันบนโครงเลี้ยงเซลล์ที่ทำจากเจลาตินและไคโตซานเพื่อใช้ในงานวิศวกรรมเนื้อเยื่อกระดูก. (BEHAVIOR OF BONE MARROW-DERIVED AND ADIPOSE-DERIVED STEM CELLS ON GELATIN/CHITOSAN SCAFFOLDS FOR BONE TISSUE ENGINEERING) อ.ที่ปรึกษาวิทยานิพนธ์หลัก: รศ.ดร. ศิริพร ดำรงค์ศักดิ์กุล, อ.ที่ปรึกษาวิทยานิพนธ์ร่วม: Professor Yasuhiko Tabata, PhD, 167 หน้า.

งานวิจัยนี้มีวัตถุประสงค์เพื่อที่จะศึกษาอิทธิพลของปัจจัยต่างๆอาทิ ชนิดของกรดที่ใช้เป็นตัวทำละลาย น้ำหนักโมเลกุลของวัสดุชีวภาพ และสัดส่วนในการผสมของวัสดุชีวภาพ ที่มีต่อสมบัติทางกายภาพและทางชีวภาพของโครงเลี้ยงเซลล์ที่ผลิตจากคอลลาเจน เจลาติน และไคโตซาน ในงานวิจัยนี้พบว่า ชนิดของกรดที่ใช้เป็นตัวทำละลายสารละลายคอลลาเจนส่งผลต่อสมบัติทั้งทางกายภาพและทางชีวภาพของโครงเลี้ยงเซลล์คอลลาเจนที่ผลิตได้ โดยโครงเลี้ยงเซลล์คอลลาเจนที่ผลิตจากกรดไฮโดรคลอริกจะมีขนาดรูพรุนที่ใหญ่ มีความสามารถในการทนแรงกดได้ดี และส่งเสริมการยึดเกาะของเซลล์ได้ดี ในขณะที่โครงเลี้ยงเซลล์คอลลาเจนที่ผลิตจากกรดอะซิติก จะมีความพรุนมากกว่า มีความสามารถในการอุ้มน้ำได้ดี และส่งเสริมการแบ่งตัวเพิ่มจำนวนของเซลล์ ดังนั้น การเลือกชนิดของกรดที่เหมาะสมจึงมีส่วนสำคัญที่จะทำให้สามารถผลิตโครงเลี้ยงเซลล์ที่มีสมบัติเหมาะสมสำหรับการใช้งานได้ ในงานวิจัยนี้ยังได้มีการศึกษาถึงการเปลี่ยนแปลงของน้ำหนักโมเลกุลของไคโตซาน และสัดส่วนการผสมระหว่างเจลาตินกับไคโตซาน เพื่อพัฒนาโครงเลี้ยงเซลล์ที่มีสมบัติเหมาะสมสำหรับเป็นต้นแบบในการใช้งานด้านวิศวกรรมเนื้อเยื่อกระดูก โดยพบว่าโครงเลี้ยงเซลล์ที่ผลิตจากเจลาตินและไคโตซานที่มีน้ำหนักโมเลกุลสูง (1,000 กิโลดาลตัล) มีสมบัติทางกายภาพและทางกลที่ดีเยี่ยม แต่ไม่ส่งเสริมกิจกรรมของเซลล์ต้นกำเนิดไขมันและเซลล์ต้นกำเนิดไขกระดูก ทั้งทางด้านการยึดเกาะและการแบ่งตัวเพิ่มจำนวน ในทางตรงข้าม โครงเลี้ยงเซลล์ที่ผลิตจากเจลาตินและไคโตซานที่มีน้ำหนักโมเลกุลต่ำ หรือไคโตโอลิโกแซคคาไรด์ (1.4 กิโลดาลตัล) มีความเหมาะสมสำหรับการยึดเกาะ และการแบ่งตัวเพิ่มจำนวนของเซลล์ต้นกำเนิดทั้งสองชนิด นอกจากนี้ยังพบว่า โครงเลี้ยงเซลล์ที่ผลิตจากเจลาตินและไคโตโอลิโกแซคคาไรด์ดังกล่าว โดยเฉพาะอย่างยิ่งที่สัดส่วนการผสมโดยน้ำหนักของเจลาตินต่อไคโตโอลิโกแซคคาไรด์ 70/30 ส่งเสริมการเปลี่ยนแปลงของเซลล์ต้นกำเนิดไขกระดูกไปเป็นเซลล์กระดูกได้ดี เมื่อเปรียบเทียบกับโครงเลี้ยงเซลล์เจลาติน นอกจากนี้ เมื่อเปรียบเทียบพฤติกรรมของเซลล์ต้นกำเนิดทั้งสองชนิด พบว่าเซลล์ต้นกำเนิดไขมันสามารถแบ่งตัวเพิ่มจำนวนได้เร็วกว่าเซลล์ต้นกำเนิดไขกระดูก ในขณะที่เซลล์ต้นกำเนิดไขกระดูกสามารถเปลี่ยนแปลงไปเป็นเซลล์กระดูกได้ดีกว่าเซลล์ต้นกำเนิดไขมัน ทั้งนี้ไม่ขึ้นอยู่กับชนิดของโครงเลี้ยงเซลล์

ภาควิชา วิศวกรรมเคมี ลายมือชื่อนิสิต .....

สาขาวิชา วิศวกรรมเคมี ลายมือชื่ออ.ที่ปรึกษาวิทยานิพนธ์หลัก .....

ปีการศึกษา 2552 ลายมือชื่ออ.ที่ปรึกษาวิทยานิพนธ์ร่วม .....

4971805521 : MAJOR CHEMICAL ENGINEERING

KEYWORDS : GELATIN / CHITOSAN / BONE MARROW-DERIVED STEM CELLS / ADIPOSE-DERIVED STEM CELLS / BONE TISSUE ENGINEERING

JUTHAMAS RATANAVARAPORN: BEHAVIOR OF BONE MARROW-DERIVED AND ADIPOSE-DERIVED STEM CELLS ON GELATIN/CHITOSAN SCAFFOLDS FOR BONE TISSUE ENGINEERING. THESIS ADVISOR: ASSOC. PROF. SIRIPORN DAMRONGSAKKUL, Ph.D., THESIS CO-ADVISOR: PROF. YASUHIKO TABATA, Ph.D., 167 pp.

This research aimed to study physical and biological properties of different types of scaffolds influenced by some parameters including type of acid solvent, molecular weight of biomaterials and blending ratio. Properties of collagen scaffolds were affected by different characteristics of collagen solutions prepared from different acid solvents. Collagen scaffold prepared from hydrochloric acid solution showed larger pore size, higher compressive modulus and greater cell adhesion than that prepared from acetic acid solution. However, porous structure with high swelling ability of the scaffolds obtained from acetic acid solution promoted cell proliferation. Therefore, the selection of appropriate acid type used was necessary to achieve scaffolds with suitable properties for particular applications. Also, in this work, gelatin/chitosan scaffolds for bone tissue engineering were developed by varying molecular weight of chitosan and blending ratio. Gelatin/high molecular weight chitosan (MW = 1,000 kDa) scaffolds showed excellent mechanical properties but did not support activities of rat adipose-derived and bone marrow-derived stem cells. On the other hand, gelatin/low molecular weight chitooligosaccharide (MW = 1.4 kDa) scaffolds promoted the attachment and proliferation of both stem cells. Furthermore, gelatin/low molecular weight chitooligosaccharide scaffolds, particularly at the weight blending ratio of 70/30, were found to enhance osteogenic differentiation of bone marrow-derived stem cells, compared to pure gelatin scaffold. Comparing the behaviors of rat adipose-derived and bone marrow-derived stem cells, the faster proliferative rate of adipose-derived stem cells was observed while bone marrow-derived stem cells exhibited remarkably higher osteogenic differentiation potential, regardless of scaffold type.

Department : Chemical Engineering Student's Signature .....

Field of Study : Chemical Engineering Advisor's Signature .....

Academic Year : 2009 Co-Advisor's Signature .....

ACKNOWLEDGEMENTS

This thesis would not have been possible unless the aid and support of many people. In the first place, I would like to record my gratitude to my advisor, Associate Professor Dr. Siriporn Damrongsakkul, whose encouragement, guidance and support from the early to the final stage of this research. Also, extraordinary experiences she provided throughout the work enable me to develop my ability and potential. Above all and the most needed, she inspires and enriches my attitude to become a superior researcher and scientist. I owe my deepest gratitude to my thesis co-advisor, Professor Yasuhiko Tabata, for his crucial contribution and kind support me on staying and doing research at Institute for Frontier Medical Sciences, Kyoto University. I also would like to appreciatively thank Assistant Professor Sorada Kanokpanont for her continuous encouragement, helpful suggestions and invaluable discussion for the whole period of my study.

In addition, I am indebted to Professor Suttichai Assabumrungrat, Assistant Professor Rath Pichyangkura and Dr. Borisut Sanmano Hanpanich for serving as the chairman and the thesis committees, respectively, whose comments were constructively and especially informative.

It is an honor for me to thank Assistant Professor Masaya Yamamoto and all members of Institute for Frontier Medical Sciences, Kyoto University for their kind attentions, supports and suggestions in advanced techniques as well as facilities.

I would like to thank Assistant Tanom Bunaprasert, M.D. for the use of his facilities at i-Tissue Laboratory, Faculty of Medicine, Chulalongkorn University. In addition, I am pleased to extend my grateful thanks to Master and Ph.D. students of the Department of Biochemistry, Faculty of Sciences, Chulalongkorn University for their helps with experiments on chitin/chitosan preparation.

Finally, I would like to express my sincere thanks to my parents and everyone in my family for their warm understanding and affectionate encouragement.

CONTENTS

PAGE

CHAPTER

CHAPTER

LIST OF TABLES

LIST OF FIGURES

CHAPTER I

INTRODUCTION

1.1 Background

Tissue engineering is an emerging multidisciplinary field which applies the principles of biology, materials, engineering, and medicine to develop functional tissue substitutes that can assist the regeneration and repair of damaged tissues. Three main components required for tissue engineering techniques include: (1) cells capable of differentiating potential into specific tissue, (2) a suitable scaffold which can fill the defect and deliver cells and growth factors to specific sites, and (3) growth factors which induce specific functions of tissue regeneration and development. Generally, the approaches of tissue engineering involve in the development of scaffold from biocompatible materials and sometimes combined with growth factors, cultured with cells *in vitro* to induce proliferation and differentiation, and implantation *in vivo* to observe tissue regeneration. Target organs which are currently being investigated by the method of tissue engineering throughout the world include skin, cartilage, bone, skeletal muscle, nerve, vasculature, kidney, heart, breast, and liver (Palsson et al., 2003).

Bone is one of the most critical organs that provides a support to the body and protects the internal organs from physical harm. Nowadays, a lot of patients suffer from deteriorating bone as a result of osteoporosis (the disease due to low bone mass), osteogenesis imperfecta (a genetic disorder by disrupting either the amount or quality of collagen in bones) and osteosarcoma (bone cancers). In all cases, bone must be regenerated to fill in a defect and restore structure and function to damaged site. Natural healing of bone defect is limited into minor fractures and healing time. Treatment using a bone graft, which can be derived from own patient (autograft bone marrow and bone matrix) or from cadaver (allograft bone matrix without cells) has then become a common technique to heal such defect. However, the sites of autograft is limited when bone is harvested without loss of function while allografting may induce cell mediated immune responses and may also transmit pathogens (Mistry and Mikos, 2005). To overcome the weakness of the traditional bone grafting, tissue

engineering is introduced as an alternative treatment that effectively heals large bone defects. The method of tissue engineering usually requires stem cells capable of differentiation into mature bone cells, a suitable scaffold as a template for regeneration of new bone, and growth factors that induce bone formation and vascularizttion (Viktor and Ronnie, 2005).

Stem cells are unspecialized cells that have potential to differentiate into many different cell types in the body. Then, stem cells serve as a sort of repair system for the body. Theoretically, stem cells can be divided to other cells without limit along the life of human or animal. Each new divided cell has the potential to either remain as stem cell or become another type of cell with a more specialized function. Recently, stem cell research has become powerful applications in replacing damaged tissues in patients and act as a potentially renewable replacement source which might be used to treat numerous diseases (Krampera et al., 2006). Mesenchymal stem cells are widely employed into both research and medical fields since they exhibit multipotent differentiation capacity. Mesenchymal stem cells have been initially identified in bone marrow as non-hematopoietic stem cells, called bone marrow-derived stem cells (MSCs). The osteogenic differentiation potential of MSCs was described many years ago (Maniatopoulos et al., 1988). However, MSCs are rare in bone marrow (1 cell/10^5 nucleated cells) and their quantity decreases with age (Pittenger et al., 1999). Also, difficulty of cell isolation limits their uses. Adipose tissue, which is often removed from plastic surgery, has become another source of mesenchymal stem cells. Adipose tissue has several advantages over bone marrow, such as minimal morbidity upon harvest. High number of adipose-derived stem cells (ASCs) can be extracted from adipose tissue isolates, potentially eliminating the need for *in vitro* expansion. ASCs show higher proliferation rates than MSCs while perform potential of multiple differentiation similar to MSCs (Zhang et al., 2008). Several works have showed the effective multipotential differentiation of ASCs (Strem et al., 2005; Wu et al., 2007). Comparing on multipotential differentiation between ASCs and MSCs, there are many controversial reports. Mauney et al. (2007) studied *in vitro* and *in vivo* adipogenic differentiation utilizing human ASCs and MSCs cultured on silk fibroin scaffolds. On such system, the difference of adipogenesis between hMSCs and hASCs could not be noticed. Noel et al. (2008) also reported that both stem cells underwent adipogenic differentiation with a similar extent when cultured on tissue culture plates under adipogenic differentiation.

However, some studies found that MSCs tended to have higher potentials of osteogenic and chondrogenic differentiation while ASCs preferred to differentiate into adipocytes (Im et al., 2005; Liu et al., 2007). Base on these reports, it was therefore interesting to clarify and compare the differentiation potential of both stem cells on particular materials in this study.

Scaffolds that used in bone tissue engineering are usually created to imitate the natural bone tissue which consists of organic and inorganic components. In general, an ideal bone tissue-engineered scaffold should be biocompatible and biodegradable with a controllable degradation rate. It should be highly interconnected porosity, with an appropriate pore size and alignment to facilitate oxygen, nutrient and waste transfer as well as rapid vacularization and tissue ingrowth. Suitable mechanical property of the scaffold is also required to maintain a defined 3-D structure for the regenerating tissue and to withstand contractile force exerted by tissue formation. Furthermore, the scaffold should be able to provide the appropriate molecular signals to guide cell functions and tissue growth. Lastly, it should have appropriate size and shape to match the target bone defect (Cao et al., 2005; Mistry and Mikos, 2005; Viktor and Ronnie, 2005). The role of bone tissue-engineered scaffold is to guide cells to migrate, attach, proliferate and secret their own extracellular matrix (ECM). The developing ECM is then vascularized and the scaffold is eventually degraded or eliminated by the body.

Biomaterial is considered as a key factor for scaffold fabrication in tissue engineering. Generally, materials used to produce the scaffolds should be biocompatible and biodegradable. Furthermore, it should regulate tissue functions correctly. Among various types of biomaterials, collagen, gelatin, chitosan and its derivatives have become outstanding choices due to their appropriate characteristics. Collagen is a protein mainly found in natural extracellular matrix (ECM) of skin, bone and connective tissue. Scaffolds made from collagen have been widely used because of a number of advantageous properties such as excellent biocompatibility, hemostatic effect, low antigenicity, and appropriate mechanical characteristics (O’Brien et al., 2004 & 2005). In addition, collagen scaffolds have been reported to promote cell attachment and growth since collagen molecule contains specific cell adhesion sites such as arginine-glycine-aspartate (RGD)-like sequence which actively induce cellular adhesion by binding to integrin receptors. This interaction plays an important role in cell growth, differentiation and overall regulation of cell functions (Quirk et

al., 2001). Though collagen shows numerous suitable characteristics to be used as tissue-engineered scaffolds, it has some limitations. Collagen is rather expensive and soluble only in acid condition. Gelatin which is derived from hydrolysis process of collagen has become of interest because it is much cheaper and easier to prepare the solution than collagen. Gelatin is also biocompatible, biodegradable, non-immunogenic and non-antigenic (Choi et al., 1999; Takahashi et al., 2005; Zhao et al., 2006). Moreover, gelatin molecule contains RGD-like sequence that promotes cell adhesion, migration and proliferation (Huang et al., 2005). From our previous work, gelatin was reported to be used as a base material substituting a large portion of collagen to produce scaffolds without affecting the biological properties (Ratanavaraporn et al., 2005 & 2006). Chitosan, the deacylated derivative of chitin, is a nontoxic amino polysaccharide consisting of β-(1,4)-2-acetamido-2-deoxy-D-glucose and β-(1,4)-2-amino-2-deoxy-D-glucose units. It has attracted considerable interests due to its biological properties such as antimicrobial, antitumor, and haemostatic (Sundararajan and Howard, 1999; Liu et al., 2004). In addition, chitosan is reported to accelerate wound healing and enhance bone formation (Park et al., 2005). Depending on source and production process, molecular weight of chitosan can be varied in a wide range. Our previous study has shown that the molecular weight of chitosan had significant influences on the mechanical and biological properties of collagen/chitosan scaffolds (Tangsadthakun et al., 2007). It was reported that low molecular weight chitosan was more effective to promote the proliferation of mouse fibroblasts. However, chitosan must be dissolved in acid condition which limits their use in medical applications. One of the very low molecular weight water-soluble chitosan is then introduced, so called chitooligosaccharide (COS). Chitooligosaccharide can be obtained from various methods such as enzymetic, acid and free radical hydrolysis (Chang et al., 2001) and its molecular weight is normally lower than 10 kDa (Kim and Rajapakse, 2005; Kim and Kim, 2006). It has been reported to have high functional bio-activated applications, for example, immune enhancement, anti-cancer function, anti-bacterial function, suppressive function for blood sugar increase, cholesterol control effect, calcium absorption acceleration effect and improvement of liver function (Wang et al., 2007).

There are some parameters known to affect properties of tissue-engineered scaffold, for example, type of acid solvent, molecular weight of material and blending

composition of composite material. In this study, characteristics of scaffolds influenced by those parameters were investigated. In Part I, the study on properties of collagen scaffolds affected by acid type used as solvent was focused. Collagen scaffolds prepared from hydrochloric and acetic acids were comparatively studied in terms of physical, chemical and *in vitro* biological characteristics. In Part II of this work, the investigation and development of gelatin/chitosan scaffolds for bone tissue engineering were concentrated. Gelatin was selected as a base material to fabricate scaffolds instead of collagen since it showed comparable biological properties to collagen as previously mentioned. In addition to gelatin which served as a main ECM protein in an organic bone scaffolds, chitosan was considered as a glycosaminoglycan (GAG) analog of the ECM due to its similarity of molecular structure to natural GAG (Zhao et al., 2006). In this study, chitosan with a broad range of molecular weights from 10 kDa to 1,000 kDa and chitooligosaccharide (COS) with the molecular weight of 1 kDa were blended with gelatin at different blending ratios. The influences of chitosan molecular weight and blending ratio on the properties of gelatin/chitosan scaffolds were investigated. The behaviors of rat ASCs and MSCs including attachment, proliferation and osteogenic differentiation on gelatin/chitosan scaffolds were comparatively evaluated.

1.2 Objectives

1. To study characteristics of collagen solutions and collagen scaffolds affected by acid type.
2. To study characteristics of gelatin/chitosan scaffolds affected by blending ratio and molecular weight of chitosan
3. To develop gelatin/chitosan scaffolds for *in vitro* osteogenic differentiation of rat adipose-derived and rat bone marrow-derived stem cells.
4. To compare *in vitro* osteogenic differentiation of rat adipose-derived and rat bone marrow-derived stem cells on the gelatin/chitosan systems.

1.3 Scopes of research

Part I: Effects of acid type on collagen solutions and collagen scaffolds

1. Preparation of collagen solutions and collagen scaffolds from acetic and hydrochloric acids via freeze drying and dehydrothermal crosslinking

2. Physical and chemical characterization of collagen solutions and collagen scaffolds including:
   2.1 Viscosity of collagen solutions
   2.2 Morphology of collagen scaffolds
   2.3 Compressive modulus of collagen scaffolds
   2.4 Swelling ability of collagen scaffolds
   2.5 Crosslinking degree of collagen scaffolds

3. *In vitro* biological characterization of collagen scaffolds including:
   3.1 *in vitro* degradation test
   3.2 *in vitro* cell culture with L929 mouse fibroblasts

Part II: Gelatin/chitosan scaffolds for bone tissue engineering

1. Preparation and characterization of chitosan and chitooligosaccharide
   1.1 Preparation of different molecular weight chitosans
      1.1.1 Sources: squid pen chitin
      1.1.2 Molecular weight ranges of chitosan: 10–1,000 kDa
   1.2 Preparation of chitooligosaccharide (COS)
      1.2.1 Sources: medium molecular weight chitosan
      1.2.2 Molecular weight of COS: ~1-2 kDa
   1.3 Characterization of chitosan and COS
      1.3.1 Molecular weight by Gel permeation chromatography (GPC)
      1.3.2 Deacetylation degree by Fourier transform infrared (FT-IR) spectroscopy

2. Isolation and characterization of stem cells
   - 2.1 Adipose-derived stem cells (ASCs)
     - 2.1.1 Source: subcutaneous adipose tissue of 3-week-old Wistar rats
     - 2.1.2 Isolation technique: medium selection
   - 2.2 Bone marrow-derived stem cells (MSCs)
     - 2.1.1 Source: bone marrow of 3-week-old Wistar rats
     - 2.1.2 Isolation technique: medium selection
   - 2.3 Characterization of rat ASCs and MSCs
     - 2.3.1 Adipogenic lineage of ASCs and MSCs cultured on tissue culture plates
     - 2.3.2 Osteogenic lineage of ASCs and MSCs cultured on tissue culture plates

3. Fabrication and characterization of two-dimensional gelatin/COS and gelatin/chitosan films
   - 3.1 Fabrication of two-dimensional gelatin/COS and gelatin/chitosan films
     - 3.1.1 Molecular weights of COS and chitosans: 1.4, 12 and 1,000 kDa
     - 3.1.2 Blending ratios of gelatin/COS and gelatin/chitosan: 100/0, 90/10, 70/30, 50/50, 30/70 and 0/100
   - 3.2 *In vitro* biological characterization of the films with rat ASCs and MSCs
     - 3.2.1 Attachment and proliferation tests
     - 3.2.2 Cell immunostaining and spreading observation
     - 3.2.3 Osteogenic differentiation test
   - 3.3 Characterization of surface properties of the films
     - 3.3.1 Water contact angle
     - 3.3.2 Surface element by X-ray photoelectron spectroscopy (XPS)
     - 3.3.3 Surface charge by zeta (ζ) potential
     - 3.3.4 Protein adsorption on the films

4 Fabrication and characterization of three-dimensional gelatin/COS and gelatin/chitosan scaffolds
   - 4.1 Fabrication of three-dimensional gelatin/COS and gelatin/chitosan scaffolds
     - 4.1.1 Molecular weights of COS and chitosan: 1.4 and 1,000 kDa
     - 4.1.2 Blending ratios of gelatin/COS and gelatin/chitosan: 100/0, 70/30, 50/50, 30/70 and 0/100

CHAPTER II

RELEVANT THEORY AND LITERATURE REVIEW

2.1 Relevant theory

2.1.1 Anatomy and physiology of bone

2.1.1.1 Structure and mechanics

Typically, the adult skeleton contains 80% cortical (compact) bone and 20% trabecular (cancellous) bone as presented in Figure 2.1. Cortical bone is a hard and dense part surrounding the marrow cavity of long bones. Cortical bone is only 5-10% porous and serves as a room for a small number of cells and blood vessels. The structural unit of cortical bone is a cylindrically-shaped osteon, which is composed of concentric layers of bone called lamellae. Blood vessels run through haversian canals located at the center of each osteon while nutrient diffusion flows in canaliculi canals within bone. Osteons are aligned in the longitudinal direction of bone. The strengths of cortical bone in the longitudinal direction are 79–151 MPa in tension and 131–224 MPa in compression (Yaszemski et al., 1996). The moduli range is around 17–20 GPa for both tension and compression. Spongy cancellous bone is found in the ribs, spine, and the ends of long bones. Cancellous bone is as much as 50–90% porous and serves as an interconnected network of small bone trabeculae aligned in the direction of loading stress. The porous volume contains vasculature and bone marrow, which provide little mechanical support compared to cortical bone. The strength and moduli of cancellous bone vary with density, usually around 5–10 MPa and 50–100 MPa, respectively, for both tension and compression (Yaszemski et al., 1996).

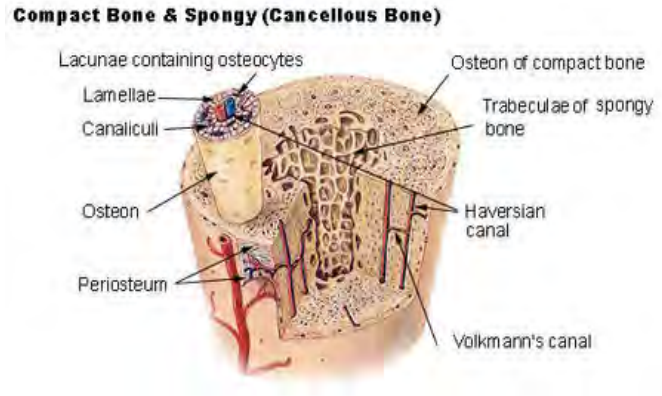

Figure 2.1 Structure of bone. (http://training.seer.cancer.gov/module.html)

Natural bone is composed of approximately 60% inorganic mineral, 30% organic material, and 10% water (Mistry and Mikos, 2005). Calcium phosphate crystals, primarily hydroxyapatite, comprise an inorganic phase while the organic extracellular matrix consists mostly of collagen crosslinked with other molecules such as glycoproteins, soluble growth factors and hormones. Collagen molecules align into triple helices that bundle into fibrils (1.5–3.5 nm in diameter), which then bundle into collagen fibers (50–70 nm in diameter). Hydroxyapatite crystals, which have 2–3 nm in thickness and tens of nanometers in length and width, are embedded in collagen fibers. Rigid hydroxyapatite crystals provide compressive strength, while collagen fibers impart energy dissipation and tensile properties to bone (Mistry and Mikos, 2005).

2.1.1.2 Cellular organization

Bone matrix contains a cellular communication network of three types of cells inhabited in the inorganic/organic composite bone structure which are osteocytes, bone-forming osteoblasts and bone-resorbing osteoclasts (Keaveny, et al., 1999). Osteoblasts are derived from mesenchymal stem cells and function in secreting collagenous proteins called osteoid that form the organic matrix of bone. Mature osteoblasts surrounded by osteoid stop secreting the matrix and become osteocytes. Osteocytes lying within the bone matrix play an important role in detecting and then converting mechanical stimuli into biochemical molecules, which signal the production or resorption of bone. Osteoclasts are derived from hematopoietic cells in bone marrow and secrete acids and proteolytic enzymes which dissolve mineral salts and digest the organic matrix of bone. Osteoblasts and osteoclasts operate in a balanced manner such that bone tissue is constantly remodeled in response to various chemical, biological, and mechanical factors. Five phases described the bone remodeling process are quiescence, activation, resorption, reversal, and formation (Mistry and Mikos, 2005). The process begins with the quiescence state in which inactive cells are present on the surface of bone. Normally, more than 80% of free bone surfaces are in this state. The activation phase arises as biochemical or physical signals attract mononuclear monocytes and macrophages to the remodeling site and promote differentiation into osteoclasts. Resorption follows as osteoclasts break down the organic and inorganic components of bone to form a cavity. During reversal, osteoclasts leave the site and mononuclear macrophage-like cells secrete a cement-

like substance on the surface. In the final phase, formation, osteoblasts fill the cavity with bone matrix and form new osteons. This begins with the rapid deposition of collagen in densely packed columns, followed by mineralization. As these processes complete, the surface returns to its quiescent state. Thus, cell–cell communication is very important for the proper maintenance of bone**.**

2.1.1.3 Function

The skeleton is designed to protect vital organs of the body and provide the frame for locomotion of the musculoskeletal system. Both the material properties of bone and the design of whole bones contribute to the exceptional stiffness and strength that give bone the ability to withstand physiological loads without breaking. Additionally, bone is a reservoir for many essential minerals such as calcium and phosphate and plays an important role in the regulation of ion concentrations in extracellular fluid. Bone marrow contains mesenchymal stem cells, which are pluripotent cells capable of differentiation into bone, cartilage, tendon, muscle, dermis, and fat tissue. Hematopoietic cells that produce the red and white blood cells are also found in bone marrow.

2.1.1.4 Bone formation

There are three forms of bone formation including endochondral bone formation, intramembranous ossification, and appositional formation (Mistry and Mikos, 2005). Endochondral ossification describes the formation of long and short bones during embryonic development, as well as bone formation into a fracture or implanted bone graft. This process begins as mesenchymal stem cells differentiate into chondrocytes, or cartilage-forming cells. These cells form a cartilaginous matrix as they mature, eventually losing the ability to proliferate. Mature chondrocytes then produce calcification proteins while phagocytic cells begin resorption of the cartilaginous matrix. Mesenchymal stem cells originating in the periosteum tissue layer surrounding long bones migrate, differentiate, and proliferate in the matrix. These cells are prone to bone (rather than cartilage) formation and subsequently construct passageways for vascularization while continuing to build bone. Osteocytes and randomly oriented collagen fibrils form soft matrix known as immature woven bone. Remodeling of woven bone into mature, lamellar bone is a slow process that yields a more organized tissue of distinct mechanical strength.

Intramembranous ossification, which applies to the formation of flat bones such as those in the skull, follows a similar process except that bone was formed directly from mesenchymal tissue without an intermediary cartilaginous network. Appositional formation occurs as layers of osteoblasts secrete sheets of matrix onto existing bone, resulting in overall bone growth. These three methods occur constantly in the development, growth, and maintenance of bones throughout the body.

2.1.1.5 Fracture healing

A fracture causes loss of function and damage to blood vessels and bone system. Fortunately, bone possesses a remarkable inherent capacity for repair and regeneration due to the local presence of osteoprogenitor cells, osteoinductive proteins, and vascularity. Thus, bone has the unique ability to go beyond repair and fully regenerate its original structure and mechanical properties (Yaszemski et al., 1996). There are three biological stages of fracture healing including inflammation, repair, and remodeling (Mistry and Mikos, 2005). The initial acute inflammatory response brings in the formation of a hematoma at the site of damaged blood vessels. Neutrophils and macrophages arrive and ingest the cellular debris of necrosis while releasing growth factors and cytokines. These biochemical signals induce the migration and differentiation of mesenchymal stem cells from surrounding bone, bone marrow and periosteum. Capillary growth and fibroblast activity create fibrovascular granulation tissue at the injury site. As mesenchymal stem cells accumulate and differentiate into osteoblasts, a repair blastema is formed. The relatively short inflammatory phase is followed by the repair phase, which begins as osteoblasts rapidly lay down new osteoid to form woven bone at the injury site, called the bony callus. Gradually, the third phase of healing, remodeling, reshapes and reorganizes collagen fibers forming mechanically strong lamellar bone. After a year of remodeling phase, especially for severe fractures, bone returns to its original, pre-fracture strength. However, if the response to bone injury does not provide enough active cells, or if a defect is too large for the natural healing response, non-union will occur at the fracture site.

2.1.2 Bone tissue engineering

Severe fractures sometimes result in non-union of injured bone and cannot be healed by the natural healing process. Traditionally, there are several methods for treating the severe fractures. The most common method involves placing a bone graft, which can be derived from own patient (autograft bone marrow and bone matrix) or from a registered bone bank (allograft bone matrix without cells) into the defect site (Sharma, et al. 2005). However, there are some limitations of these methods. For example, size of the defect, autologous bone supply and viability of the host bed can be problems of autograft. In large defects, autologous bone graft can often be resorbed before osteogenesis is complete (Sharma, et al. 2005). Furthermore, harvesting of autologous bone for grafting requires much time for surgery and is associated with donor site morbidity in the way of infection, pain, and haematoma formation. On the other hand, allograft may induce cell mediated immune responses to alloantigens, and may also transmit pathogens such as HIV. Technically, it can be difficult to shape bone grafts to fit the defect well. For these reasons, tissue engineering offers great potential for the construction and regeneration of bone. The emerging field of tissue engineering aims to combine engineering technology and the principles of biological science to develop strategies for the repair and regeneration of lost or damaged tissue. Tissue engineering concept is consisting of three general strategies: (1) cell-based strategies, (2) growth factor-based strategies and (3) matrix-based strategies (Mistry and Mikos, 2005). In practice, most experimental works combine two or more of these strategies together towards a solution. In the realm of bone tissue engineering, these strategies require interaction between osteogenic, osteoinductive, and osteoconductive elements. Osteogenic components include cells capable of bone production such as osteoprogenitor cells, stem cells or differentiated osteoblasts. Osteoinductive factors include bioactive chemicals that induce recruitment, differentiation, and proliferation of the proper cell types at an injury. A material that supports bone growth demonstrates osteoconductivity. An osteoconductive scaffold may provide mechanical support, sites for cell attachment and vascular ingrowth. It can also be served as a delivery vehicle for implanted growth factors and cells.

2.1.2.1 Cell-based strategies: Osteogenicity

Cell-based strategies for bone regeneration by tissue engineering approach involve the implantation of cells with osteogenic potential directly into a

defect site. Cell transplantation is particularly beneficial to patients with a low number of cells, as in the case of vascular disease or irradiated tissue around the site of tumor resection. The choice of cell type is important and various cells have been employed for bone regeneration. These include transplantation of fresh marrow containing osteoprogenitor cells, differentiated osteoblasts or chondrocytes, and purified mesenchymal stem cells (Bruder and Fox, 1999). These cells may not be capable of synthesizing bone matrix themselves but instead are expected to stimulate differentiation to an osteogenic phenotype through delivery of bioactive factors. Populations of differentiated osteoblasts are typically derived from mesenchymal stem cells found in bone marrow or periosteum using osteogenic cell culture supplements including β-glycerophosphate, dexamethasone, and L-ascorbic acid (Bruder and Fox, 1999). Figure 2.2 illustrates the progression from multipotent mesenchymal stem cells to committed osteoblasts. The proliferative capacity of the cells decreases as they differentiate toward a specific matrix-producing phenotype.

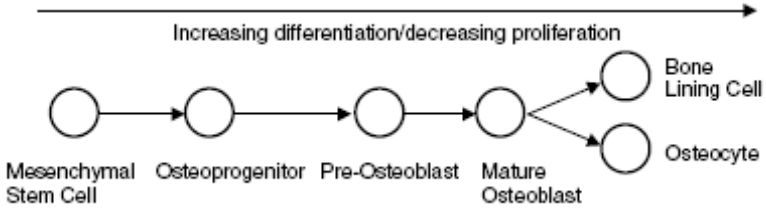

Figure 2.2 Differentiation progression from a multipotent mesenchymal stem cell to a committed osteoblast (Guldberg and Duty, 2003).

Ex vivo expanded mesenchymal stem cells provide an accessible and abundant cell source for subsequent implantation into bone defects. Mesenchymal stem cells are readily isolated from a simple bone marrow aspirate or other tissues. These can be expanded over many passages without spontaneous differentiation. Delivering cells capable of differentiating potential into bone-forming osteoblasts within an appropriate scaffold may be a particularly effective strategy for treating large defects (Figure 2.3). The osteogenic phenotype is evidenced by a change from a fibroblastic to a cuboidal morphology, expression of alkaline phosphatase (ALP), reactivity with anti-osteogenic cell surface monoclonal antibodies, osteocalcin mRNA expression, and mineralized nodule formation (Kadiyala et al., 1997).

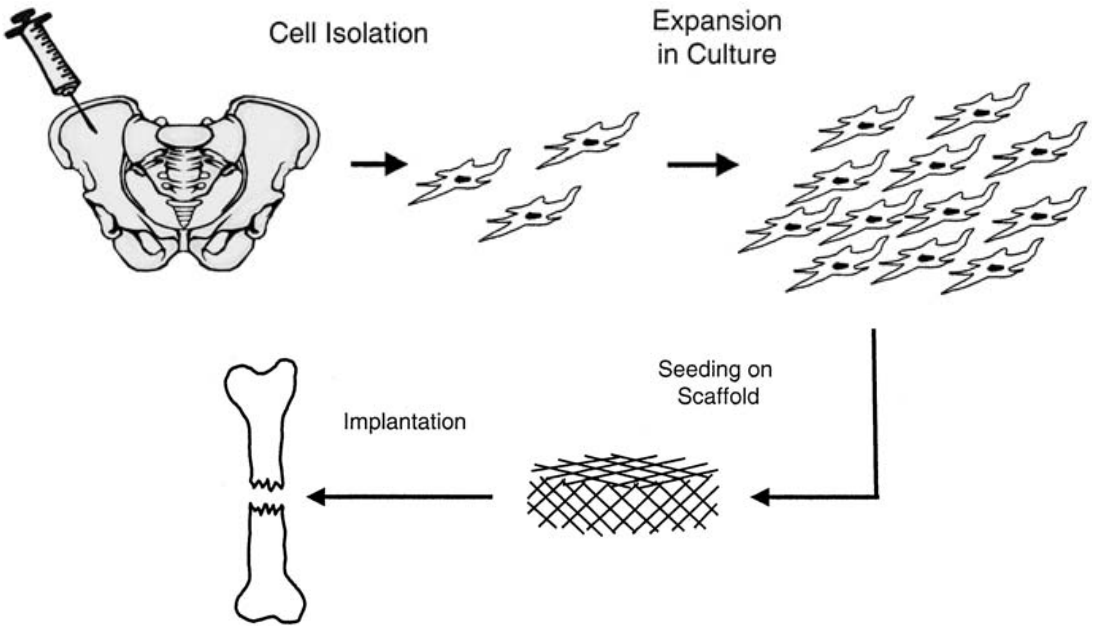

Figure 2.3 Cell transplantation: osteogenic cells are isolated from the iliac crest, expanded in cell culture, seeded onto a scaffold, and implanted into a defect (Mistry and Mikos, 2005).

2.1.2.2 Growth factor-based strategies: Osteoinductivity

An osteoinductivity explains the substances that can allow bone repair to occur in a location that would not heal if left untreated (Sharma et al., 2005). Growth factors are signaling polypeptide molecules that regulate a multitude of cellular functions including proliferation, differentiation, migration, adhesion and gene expression. Growth factors bind to specific surface receptors of target cells to induce a response, usually in the form of new mRNA or protein synthesis. These biomolecules exhibit pleiotropy, that is, a single growth factor may induce the same or different response in various cell types. In addition, many cell types secrete the same growth factors, though not always with the same effect. In some cases, growth factors produce a more significant response at higher concentrations or produce completely different responses at high and low concentrations. Growth factors also have the ability to enhance or impede the production or activity of other growth factors (Mistry and Mikos, 2005). The major challenge of working with growth factors is a relatively short biological half-life, which can be as low as 2 min. For applications in human, high doses of growth factors are required, which are unfortunately associated with high costs and limited supply. A great deal of research is being conducted on growth

factors and delivery mechanisms that sustain release, and therefore maintain activity of growth factors (Boden, 1999).

Though many osteoinductive growth factors have been identified, two of the most common groups in the transforming growth factor-β superfamily are the bone morphogenic proteins (e.g., BMP-2, BMP-7) and the transforming growth factor-βs (e.g. TGF-β1) (Mistry and Mikos, 2005). BMPs are growth factors that stimulate differentiation of mesenchymal stem cells into osteoblasts as well as proliferation and function of both chondrocytes and osteoblasts. TGF-βs are growth factors that stimulate differentiation of mesenchymal stem cells towards chondrocytes and proliferation of osteoblasts and chondrocytes. Both types of growth factors have been shown to enhance bone resorption at certain concentrations. Other growth factors with similar effects are fibroblast growth factors (FGFs), insulin-like growth factors (IGFs), platelet-derived growth factors (PDGFs), and epidermal growth factors (EGFs). Vascular endothelial growth factor (VEGF) is also as important as osteoinductive growth factors for bone applications because it promotes vascularization and angiogenesis by encouraging endothelial cell proliferation and migration. In fact, VEGF is unique among most angiogenic growth factors since it acts directly upon endothelial cells. Another important osteoinductive substance is dexamethasone, a potent synthetic member of the glucocorticoid class of steroid hormones. It is also known to induce osteogenic differentiation of mesenchymal stem cells *in vitro* (Sharma, et al. 2005).

Due to the short half-life of growth factors, a delivery device should be employed to sustain the release of these growth factors and achieve their maximum activities. Biodegradable polymers are widely studied as delivery vehicles for growth factors with many reasons. Protein structure is maintained in polymeric carriers, thus maintaining bioactivity. Delivery rate and duration can easily be controlled through growth factor loading, polymer properties, and processing conditions. Growth factors in polymeric systems can either be incorporated into the biomaterial during processing or loaded into the material after fabrication. If incorporated into a material, growth factors will be released in a diffusion-controlled manner as the material degrades. Alternatively, growth factors may be encapsulated in microparticles, nanoparticles, fibers, or other materials and then incorporated into a matrix for

delivery. Another option is the coating of biomaterials with growth factors to facilitate integration into bone.

2.1.2.3 Scaffold-based strategies: Osteoconductivity

Biological tissues consist of cells situated within a complex molecular framework, known as extracellular matrix, with an integrated vascular system for oxygen and nutrient supply. The important roles of extracellular matrix molecules are to provide structural support and signaling as well as the multiple binding sites for soluble growth factors. In order to mimic this structure, both physical and chemical features of the three-dimensional scaffold are substantially important. A biomaterial scaffold must be designed to fill a critical-sized defect and act as a carrier for the cells and/or growth factors used to heal the defect. Design criteria of a three-dimensional scaffold for bone tissue engineering include biocompatibility of both material itself and its degradation products, osteoconductivity, a porous architecture, controlled degradation capabilities, mechanical support and sterilizability (Mistry and Mikos, 2005).

The scaffold must be produced from biocompatible material which does not result in a significant inflammatory response and fibrous capsule formation around the implant. Toxic response of the tissue surrounding a biomaterial will cause cell death and worsen the injury. In addition to the base material used to form a scaffold, cross-linking agents, emulsifiers, solvents, and degraded by-products of the scaffold during the implant lifetime should also be compatible to surrounding tissue and body.

Osteoconductive material has ability to act as a substrate for cell adhesion and function while facilitating bone growth throughout a three-dimensional scaffold across a defect. Functional modification of biomaterial surfaces is another promising strategy being investigated to improve the efficacy of scaffolds for bone tissue engineering. Garcia et al. (1999) have proposed that the conformation of the absorbed proteins or protein fragments on material surfaces can be utilized to direct integrin receptor binding and thereby control cell proliferation and differentiation. The engineering of rationally designed surfaces that control cell function may endow osteoconductive scaffolds with the additional ability to induce osteoblast differentiation and subsequent bone regeneration (Guldberg and Duty, 2003).

Cell activities and function are regulated not only by the chemistry of the material, but also by the architecture and surface variations (Nerem, 2007). Thus, a porous architecture that allows bone ingrowth and vascularization throughout the scaffold is a necessity. Ideally, scaffolds will be designed to maximize porosity while maintaining mechanical properties with interconnected pores as shown in Figure 2.4. This type of architecture will provide a large surface area for cell attachment, growth, and function, as well as a large void space for bone formation and vascularization (Guldberg and Duty, 2003). Several works have reported the optimal range of pore size for bone ingrowth to be 150–600 microns (Cornell, 1999; Ishaug et al., 1997). However, Whang et al. (1999) demonstrated substantial bone formation in non-load-bearing defects filled with polymer scaffolds possessing a median pore size less than 50 microns and porosity greater than 90%. Whang et al. (1999) reported that the spatial requirement for vascularization and invasion of osteoprogenitor cells should be less than 20 microns based on the dimensions of blood vessels and bone cells. It was hypothesized that high porosity scaffolds with small pore sizes provided greater hematoma stabilization in the earliest phases of bone regeneration. Scaffold should also allow transport of nutrients (such as glucose, dissolved oxygen) to the cells and degradation products from the cells throughout the construct (Sharma et al., 2005). In addition, it has been demonstrated that osteoblast proliferation is sensitive to surface topography, strain or other mechanical stimuli. Thus, particle size, shape, and surface roughness of the scaffold affect cellular adhesion, proliferation and phenotype (Sharma et al., 2005).

Biodegradable biomaterials are highly preferred over nondegradable materials, though they are generally weaker. Controlled degradation of a scaffold allows gradual load transfer to bone, increasing space for bone growth, and eventual filling of a defect with natural bone. This opposed to a permanent biomaterial which may cause stress-shielding or infection. Furthermore, predictable degradation time of the scaffold is also crucial. If a scaffold degrades very slowly, as is the case with many hydroxyapatite formulations, it will restrict bone regeneration and may fail mechanically due to repetitive loading. In contrast, a scaffold that degrades very fast may lose their mechanical integrity before the defect site can be stabilized by newly formed bone. The degradation mechanism may also be important since scaffolds may experience hydrolytic, enzymatic, bulk, or surface degradation (Guldberg and Duty, 2003).

Mechanical properties of a scaffold should initially match the properties of the target tissue in order to provide structural stability to an injury site. The chosen biomaterial must be strong enough to support the physiological load of the body without absorbing the mechanical stimuli required for natural growth in the affected area.

In addition, a biomaterial should be easy to fabricate into irregularly shaped implants by molds or by direct injection into a defect site followed by in situ crosslinking. Scaffolds should also be created with specified internal architectures and complex external topologies designed to match patient-specific defect geometries (Guldberg and Duty, 2003).

Finally, a scaffold must be sterilizable without loss of function, that is, the sterilization process must not alter the scaffold's chemical composition, as this may affect its bioactivity, biocompatibility, or degradation properties. Figure 2.4 showed examples of bone tissue-engineered scaffolds.

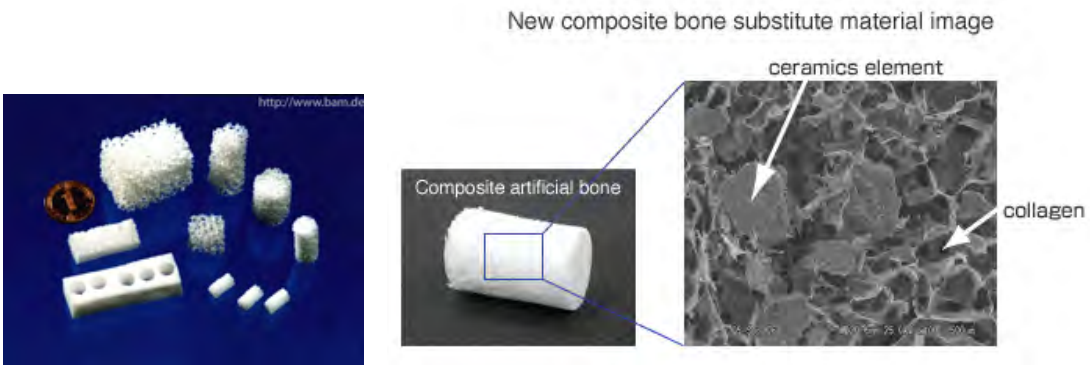

Figure 2.4. Bone tissue-engineered scaffolds.
(http://www.bam.de/en and http://www.olympus-global.com)

2.1.3 Biocompatible materials

The selection of biomaterials is greatly important in the design and development of tissue engineering product. A biomaterial must interact with tissue to repair, rather than act simply as a static replacement. Furthermore, biomaterials used directly in tissue repair or replacement applications must reach a desirable cellular response. Various types of material have been used for the construction of bone tissue-engineered scaffolds. Commonly used materials include ceramics, polymers and composites. Ceramics can be either natural or synthetic. Natural inorganic materials such as hydroxyapatite and β-tricalcium phosphate, essentially the hard part of bone, have been used as base materials for hard tissue-engineered scaffolds. Hydroxyapatite shows good osteoconductive property but have long degradation times, often a year or more. β-tricalcium phosphate is less osteoconductive but degrades faster than hydroxyapatite (Sharma et al., 2005). Due to the generally brittle nature of pure inorganic scaffolds, composite materials which combine the use of polymeric and inorganic components have been more popular (Cao et al., 2005).

Both natural and synthetic polymers offer one major advantage over ceramics that is flexibility. Synthetic polymers such as polylactic acid (PLA), polyglycolic acid (PGA) and their co-polymers (PLGA) can be easily processed into various structures and can be produced cheaply and reproducibly. Moreover, it is possible to tightly control various properties such as mechanical strength, hydrophobicity, and degradation rate. However, some synthetic polymers have an effect of long-term inflammatory response from the host tissue. Naturally derived polymers such as collagen, gelatin, fibroin, chitin, chitosan, agarose and alginate, usually isolated from biological (animal or plant) tissues, have specific biological activity and generally do not bring about unfavorable host tissue response (Sharma et al., 2005). Several biomaterials including collagen, gelatin, chitosan and chitooligosaccharide are introduced for the fabrication of scaffolds in this study.

2.1.3.1 Collagen

1. The nature of collagen

Collagen is the most abundant fibrous protein in mammals, which is found in skin, bone, teeth, tendons, cartilage, blood vessels, and connective tissue. More than 90% of the extracellular protein in tendon and bone and more than 50% in

skin consist of collagen. Collagen provides strength and elasticity to tissues. Also, it is the main component of ligaments and tendons. Collagen plays an important role in the formation of tissues and organs. It is also involved in various functional expressions of cells. Collagen is a good surface-active agent, exhibits biodegradability, weak antigenicity and superior biocompatibility compared with other natural polymers, such as albumin, alginate and cellulose.

2. Classification of collagen

Collagen can be found in many parts throughout the body. It is classified in different forms known as type. Different collagen types are necessary to confer distinct biological features to the various types of connective tissues in the body. Currently at least 13 collagen types which vary in the amino acid composition, the length of the helix, the nature and size of non-helical portions have been isolated, as listed in Table 2.1.

Table 2.1 Chain composition and body distribution of collagen types (Friess, 1998).

Collagen type	Chain composition	Tissue distribution
I	$(\alpha1(I))_2\alpha2(I)$ or trimer$(\alpha1(I))_3$	Skin, tendon, bone, cornea, dentin, fibrocartilage, large vessels, intestine, uterus, dentin, dermis, tendon
II	$(\alpha1(II))_3$	Hyaline cartilage, vitreous, nucleus pulposus, notochord
III	$(\alpha1(III))_3$	Large vessels, uterine wall, dermis, intestine, heart valve, gingiva (usually coexists with type I except in bone, tendon, cornea)
IV	$(\alpha1(IV))_2\alpha2(IV)$	Basement membranes
V	$\alpha1(V)\alpha2(V)\alpha3(V)$ or $(\alpha1(V))_2\alpha2(V)$ or $(\alpha1(V))_3$	Cornea, placental membranes, bone, large vessels, hyaline cartilage, gingiva
VI	$\alpha1(VI)\alpha2(VI)\alpha3(VI)$	Descemet's membrane, skin, nucleus pulposus, heart muscle

VII	$(\alpha1(VII))_3$	Skin, placenta, lung, cartilage, cornea
VIII	α1(VIII) α2(VIII) chain organization of unknown helix	Produced by endothelial cells, Descemet's membrane
IX	α1(IX)α2(IX)α3(IX)	Cartilage
X	$(\alpha1(X))_3$	Hypertrophic and mineralizing cartilage
XI	α1(XI)α2(XI)α3(XI)	Cartilage, intervertebral disc, vitreous humour
XII	$(a1(XII))_3$	Chicken embryo tendon, bovine periodontal ligament
XIII	Unknown	Cetal skin, bone, intestinal mucosa

3. Three dimensional structure of type I collagen

Type I collagen is predominant in higher order animals especially in the skin, tendon, and bone where extreme forces are transmitted. It is a compound of three chains, two of which are identical, termed α1(I), and one α2(I) chain with different amino acid compositions, or it can rarely represent a trimer built of three α1(I) chains. Each of the α-chains is composed of about 1,000 amino acid residues with Gly-X-Y repeating sequence. For type I collagen, X and Y residues are proline and hydroxyproline in every six residues. Only glycine residue is facing toward the center of the chain and the other hydrophobic amino acid residues are all facing outside. This is related closely to the low solubility of collagen in water. The α-chains form a helical structure by rotating counterclockwise with 3.3 amino acid residues per rotation. Helical structure is presented at the center and relaxed structure is presented at both ends of the collagen molecule as shown in Figure 2.5 (a). Furthermore, the three α-chains as a whole form a helical structure by rotating clockwise with 30-45 residues per rotation. When the triple helix is denature and becomes gelatin, polypeptides are separated to one α-chain, two β-chains, and three γ-chain.

The denaturing temperature of collagen from various animal species is different since it is related to the temperature of the environment surrounding the cells. For example, the denaturing temperature of human or higher order animals is 40°C, whereas that of the fish in Antarctic is about 5°C. Furthermore, it is known that collagen in different tissues of the same animal has different denaturing temperature. Hydroxyproline plays an important role in heat stability of the collagen molecule. Introduction of ─OH group in proline facilitates the formation of hydrogen bonds

within the molecule through water molecules. Thus, the denaturing temperature is high in collagen molecules which have high hydroxyproline content.

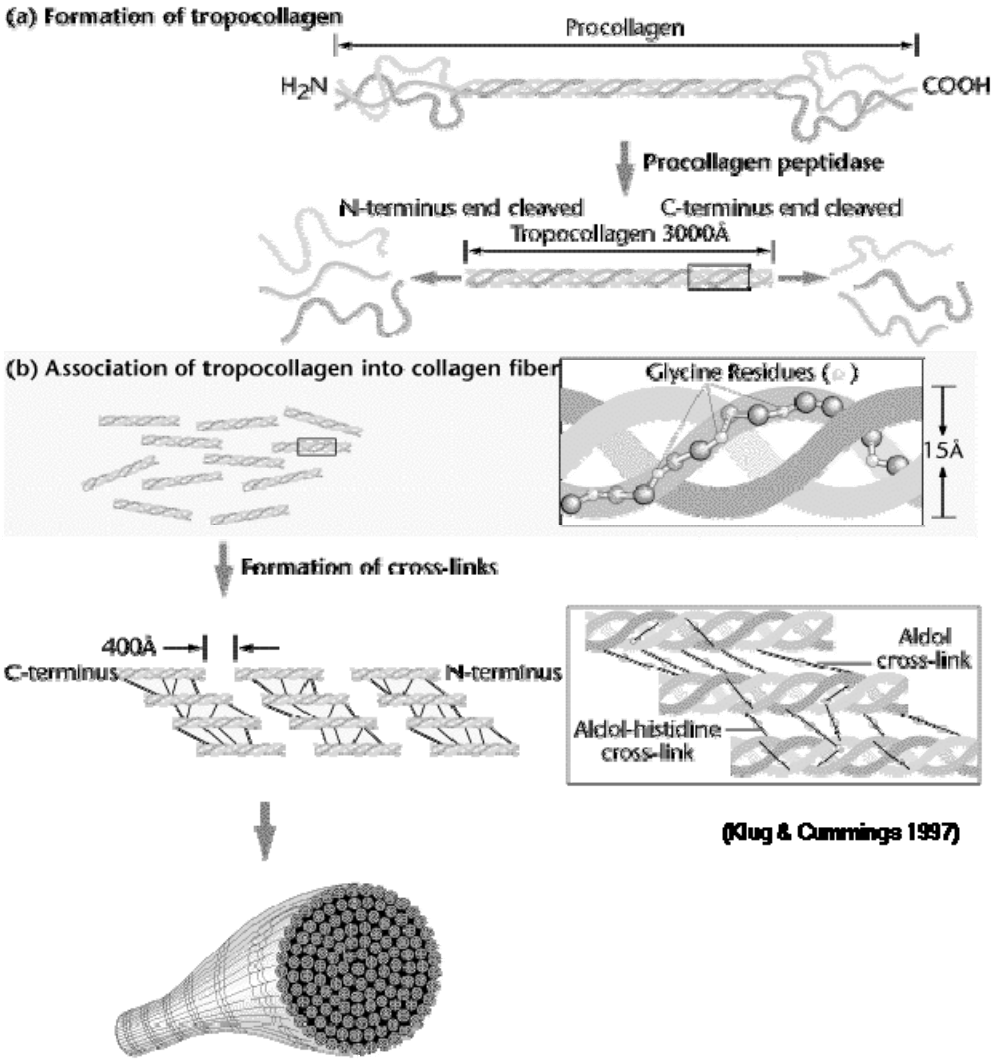

Figure 2.5 Molecular structure of type I collagen
(http://www.mun.ca/biology/scarr/collagen_structure)

4. Amino acid composition

Within collagen molecules, approximately 1/3 of the total amino acid residues is composed of glycine and 2/9 are amino acids, i.e. proline and hydroxyproline. Hydrophilic amino acid residues are very few. Telopeptide regions (non-helical regions of the molecule) are denoted for regions of 9–26 amino acids at the amino and carboxyl terminal chain ends of the molecule that are not incorporated into the helical structure. Table 2.2 represents the amino acid composition of α-chains in bovine collagen.

Table 2.2 Amino acid composition of bovine collagen α-chains (Miller and Lunde, 1973).

Amino acid	Residues/1,000 residues			
	α1(I)	α2(I)	α1(II)	α1(III)
3-Hydroxyproline	1	-	2	-
4-Hydroxyproline	85	85	91	127
Aspartic acid	45	47	43	48
Threonine	16	17	22	14
Serine	34	24	26	44
Glutamic acid	77	71	87	71
Proline	135	120	129	106
Glycine	327	328	333	366
Alanine	120	101	102	82
Cysteine	-	-	-	2
Valine	18	34	17	12
Methionine	7	4	11	7
Isoleucine	9	17	9	11
Leucine	21	34	26	15
Tyrosine	4	3	1	3
Phenylalanine	12	16	14	9
Hydroxylysine	5	11	23	7
Lysine	32	21	15	25
Histidine	3	8	2	8
Arginine	50	57	51	44

Primary structure of collagen is characterized by the presence of Gly-X-Y repeating sequence. The presence of glycine in every three residues is essential for the formation of helical structure. X and Y represent other amino acid residues. The frequency of amino acids in these positions is different in different species of collagen. For type I collagen, proline and hydroxyproline exist in X and Y, respectively. Such a regular sequence is not found in the telopeptide regions.

5. Characteristics of collagen for tissue engineering applications

Collagen is suitable as a medical material due to its alternative characteristics. Firstly, antigenicity of collagen is very low compared with other proteins. Antigenic determinant of collagen is mainly presented in the telopeptide regions. Since enzyme-solubilized collagen is lack of these regions, the antigenicity of collagen molecule is almost negligible. It is also known that the introduction of crosslinks by either chemical or physical techniques in processing of fibrils or membranes rendering the antigenicity is very low. Secondly, collagen plays a role as substratum for various types of cells. Since the affinity of collagen to tissues is very good, collagen allows the cells to grow on it when applied in the body as a medical material. The affinity of collagen to the body is much better than other synthetic high molecular weight materials. Lastly, the nature of collagen can be controlled by chemical modification of the molecule. For example, introduction of crosslinks extends the degradation time of collagen in the body.

2.1.3.2 Gelatin

Even collagen shows numerous advantages for medical applications, some disadvantages of collagen-based systems are found, for example, high cost and difficulty to process. Gelatin, a denatured form of collagen, is introduced since it shows biological properties similar to those of collagen but much cheaper and easier to prepare solution.

1. The nature of gelatin

Gelatin is a protein which does not occur in nature. It is derived from collagen, a main component found in connective tissue, skin and bone of human and animals. Gelatin can be obtained by partial hydrolysis of collagen with subsequent purification, concentration, and drying operations. Gelatin is a polypeptide, a series of amino acids joined together by peptide bonds as shown in Figure 2.6.

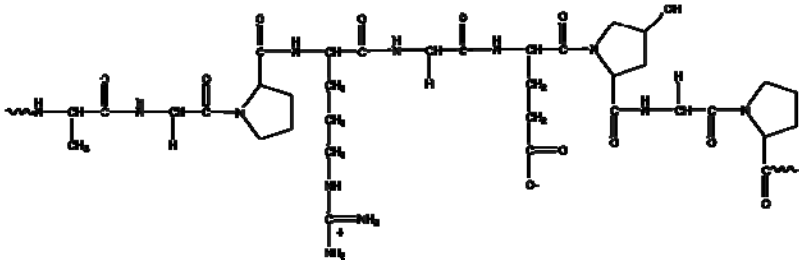

Figure 2.6 Molecular structure of gelatin.
(http://www.niroinc.com/food_chemical/spray_drying_gelatin.asp)

2. Types of gelatin

Gelatin can be divided into 2 types depending on the production process.

a) Type A gelatin is produced from an acid process. This process is mainly applied to porcine skin, in which collagen molecule is young. The isoelectric points (pI) of type A gelatin are in the range of 7-9. High gel strength (bloom strength) gelatins normally have higher pI and low bloom strength gelatins have a pI closer to 7.

b) Type B gelatin is produced from an alkaline process. It is mainly applied to cattle skin and bone, in which the triple helix collagen molecule is more densely crosslinked and complex. Type B gelatin has a pI value around 5.

The differences in properties of both gelatin types are shown in Table 2.3.

Table 2.3 Properties of type A and type B gelatin.
(http://www.gelatin-gmia.com/html/gelatin.html)

	Type A	**Type B**
pH	3.8 - 5.5	5.0 - 7.5
Isoelectric point (pI)	7.0 – 9.0	4.7 – 5.4
Gel strength (bloom)	50 -300	50 – 300
Viscosity (cp)	15 -75	20 – 75
Ash (%)	0.3 -2.0	0.5 – 2.0

3. Amino acid composition

Gelatin is a high molecular weight water-soluble protein. On a dry weight basis, gelatin consists of 98 to 99% of protein. The molecular weight of these large protein structures typically ranges between 20,000 and 250,000. Coils of amino acids are joined together by peptide bonds. As a result, gelatin contains relatively high levels of amino acids, as presented in Table 2.4. The predominant amino acid sequence is Glycine-Proline-Hydroxyproline (Gly-Pro-Hyp).

Table 2.4 Amino acid composition in gelatin.
(http://www.gmap-gelatin.com/about_gelatin_comp.html)

Amino Acid	**%**
Alanine	8.9%
Arginine	7.8%
Asperic acid	6.0%
Glutamic acid	10.0%
Glycine	21.4%
Histidine	0.8%
Hydoxylysine	1.0%
Hydroxyproline	11.9%
Isoleucine	1.5%
Leucine	3.3%
Lycine	3.5%
Methionine	0.7%
Phenylanine	2.4%
Proline	12.4%
Serine	3.6%
Theronine	2.1%
Tyrosine	0.5%
Valine	2.2%
Total	100%

4. Properties of gelatin

Gelatin is nearly tasteless and odorless. It is colorless or slightly yellow, transparent and brittle. It is soluble in hot water, glycerol, and acetic acid, and insoluble in organic solvents. Gelatin swells and absorbs water upto 5-10 times of its dry weight to form a gel in aqueous solutions at low temperature. The viscosity of the gel increases under stress and the gelation are thermally reversible. Gelatin has a unique protein structure that provides a wide range of functional properties. Gelatin is amphoteric, meaning that it is neither acidic nor alkali, depending on the nature of the

solution. The pH at which charge of gelatin in solution is neutral is known as isoelectric point (pI). The isoelectric point (pI) of a protein is the pH at which the protein will not migrate in an electric field. This is due to the fact that at that pH the molecule carries an equality of positive and negative charges. Gelatin, is rather unique as it can have an isoelectric point anywhere between pH 9 and pH 5, depending upon the source and method of production. The properties of gelatin from various sources can be different, for example, fish gelatin is distinguished from bovine or porcine gelatin by its low melting point, low gelation temperature, and high solution viscosity.

5. Characteristics of gelatin for tissue engineering applications

a) Biocompatibility
b) Biodegradability
c) Non-immunogenicity
d) Does not express antigenicity
e) Cheap and easy to obtain solution

2.1.3.3 Chitosan

1. The nature of chitosan

Chitin and chitosan are a linear polysaccharide extracted from various animals and plants. Chitin is the abundant biopolymer mainly found in cell walls of some microorganisms such as fungi, yeasts and in exoskeletons of invertebrates such as crustaceans, olluscs, crabs, shrimps, lobster, squid and insects. Chitosan, a derivative of chitin, exists naturally only in a few species of fungi. Chitin and chitosan are copolymers consisting of 2-acetamido-2-deoxy-β-D-glucose (or N-acetyl-glucosamine) and 2-amino-2-deoxy-β-D-glucose (or N-glucosamine) as repeating units. The repeating units are randomly or block distributed throughout the biopolymer chains depending on the processing method used to derive the biopolymer, as shown in Figure 2.7. When the number of N-acetyl-glucosamine units is lower than 50%, the biopolymer is referred as chitosan. The term “degree of deacetylation (DD)” is used to represent the amount of N-glucosamine units in the molecules. If the degree of deacetylation is higher than 50%, it will be classified as chitosan. In contrast, when the number of N-glucosamine units is lower than 50%, the term chitin is used.

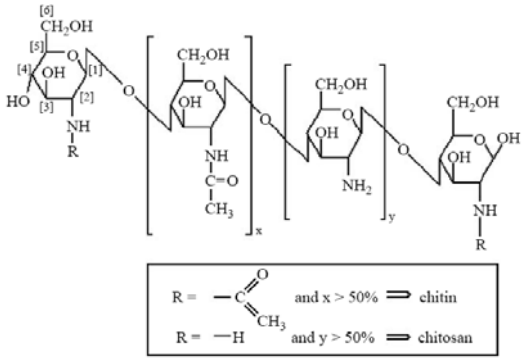

Figure 2.7 Schematic representation of the chitin and chitosan depicting the copolymer character of the biopolymers (Suh and Matthew, 2000).

2. Preparation of chitin and chitosan

Chitosan is produced from shellfish waste by a multistage process, as shown in Figure 2.8. First the salt is washed out and the shellfish is shredded. The shredded shellfish is decalcified in dilute aqueous HCl solution and deproteined in dilute aqueous NaOH solution. Then it is decolored and dried to obtain chitin. Deacetylation in hot concentrated NaOH solution is used to convert the chitin into chitosan. The chitosan obtained is then neutralized and dried. Deacetylation mechanism of chitin to chitosan is shown in Figure 2.9.

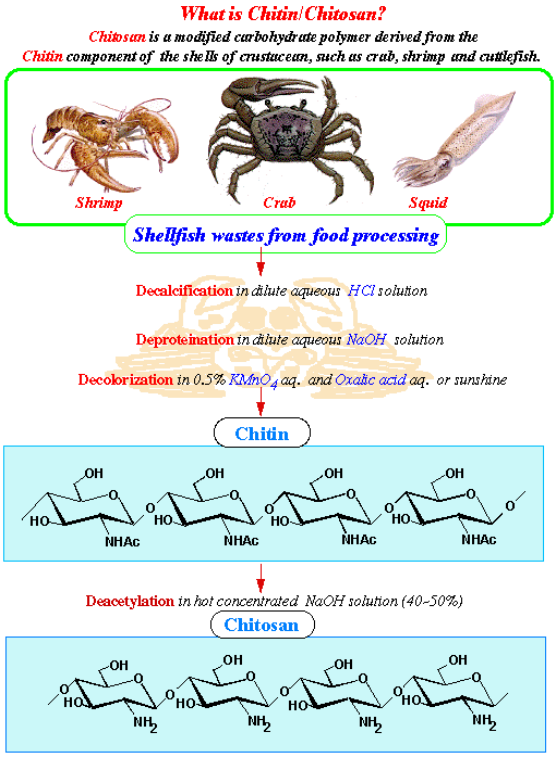

Figure 2.8 Preparation of chitin and chitosan.
(www.drugdeliverytech.com/cufm/jpg/002870.jpg)

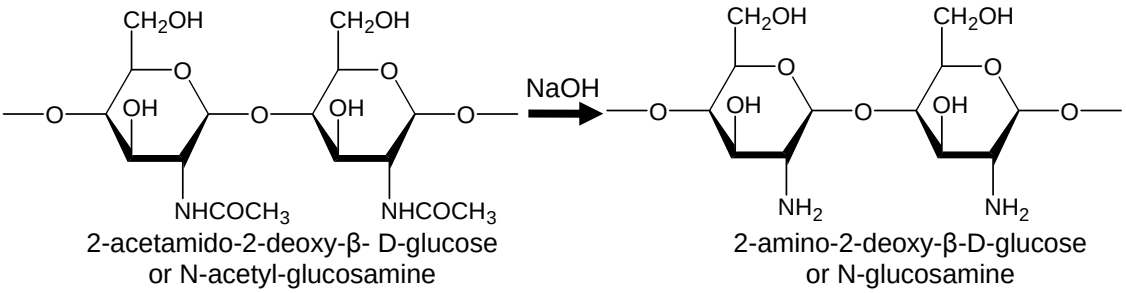

Figure 2.9 The chitosan production with deacetylation of chitin.

(http://www.ft.vslib.cz)

3. Properties of chitosan

The amino group in chitosan has a pKa value of 6.5, thus, chitosan is positively charged and soluble in acidic to neutral solution with a charge density dependent on pH and the deacetylation degree value. In other words, chitosan is bioadhesive and readily binds to negatively charged surfaces such as mucosal membranes. There are two advantages of chitosan over chitin. Firstly, chitosan is readily dissolved in agents such as 1-10% (v/v) aqueous acetic acid whereas highly toxic cosolvents such as lithium chloride and dimethylacetamide must be used to dissolve chitin. The second advantage of chitosan is the presence of the free amine group that not only renders a polyelectrolytic effect to the polymer backbone, but also presents an active site upon which many chemical reactions may be applied.

Apart of the solubility of chitosan in acidic solvent below pH 6, organic acid such as acetic, formic, and lactic acids are used for dissolving chitosan. The most commonly used solvent for chitosan is 1% acetic acid solution (pH around 4.0). Solubility in inorganic acids is quite limited. At higher pH, precipitation or gelation will occur. Chitosan solution forms polycation complex with anionic hydrocolloid and provides gel. Molecular weight and deacetylation degree of chitosan strongly affect on its properties such as solubility and biological properties. Furthermore, it was reported that deacetylation degree affects the hydrophilicity and biocompatibility of the chitosan while molecular weight affects degradation rate and the mechanical properties (Hsu et al., 2004).

4. Characteristics of chitosan for tissue engineering applications

a) Biocompatibility
b) Biodegradability
c) Nontoxicity

d) Extendability into three-dimensional structures

e) Biofunctionalities (antitrombogenic, hemostatic, immunity enhancing, antitumor activity, immunoadjuvant activity, acceleration of wound healing, antimicrobial activity)

f) Molecular affinity

g) Polyelectrolyte-forming

2.1.3.4 Chitooligosaccharide (COS)

Chitosan is a polysaccharide having high molecular weight and insoluble at neutral pH, so its use is sometimes limited, especially in human body. This problem can be overcome by water-soluble chitosan called chitooligosaccharide (COS).

COS can be obtained from chitosan by several techniques such as enzymetic, acid or free radical hydrolysis. COS is then a saccharide which composed of 2-8 β-(1-. 4)-D-glucosamine repeating units with a structure of chitosan characteristic. Structure of COS is shown in Figure 2.10. Due to its excellent absorption and water soluble, COS has been found to have high functional bio-activated applications, for example, immune enhancement, anti-cancer function, anti-bacterial function, suppressive function for blood sugar increase, cholesterol control effect, calcium absorption acceleration effect and improvement effect of liver function.

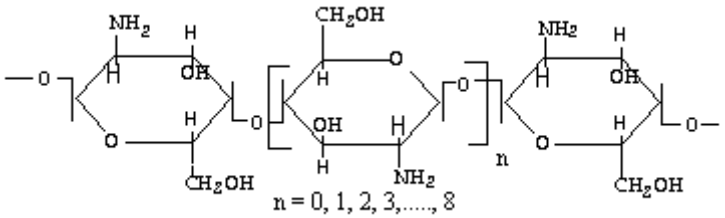

Figure 2.10 The structure of chitooligosaccharide.
(http://www.kittolife.co.kr)

2.1.4 Mesenchymal stem cells

Stem cells are cells found in all multi-cellular organisms and defined by two properties evident at division.

1. Self-renewal: the ability to go through numerous cycles of cell division while maintaining the undifferentiated state

2. Potency: the capacity to differentiate into specialized cell types yielding an organized tissue.

Mesenchymal stem cells are defined as self-renewable, multipotent progenitor cells with the capacity to differentiate into tissues of mesodermal origin such as adipocytes, osteoblasts, chondrocytes, tenocytes, skeletal myocytes and visceral stromal cells, tissues of ectodermal origin such as neurons, and tissues of endodermal origin such as hepatocytes (Krampera et al., 2006), depending on factors such as cell density, basal nutrients, spatial organization, growth factors, and cytokines (Guldberg and Duty, 2003).

2.1.4.1 Sources of mesenchymal stem cells

Mesenchymal stem cells have been initially identified in bone marrow with the amount of 1 mesenchymal stem cell per 100,000 nucleated cells (Sharma, et al. 2005). However, source of mesenchymal stem cells is not only bone marrow, but also other adult tissues such as fat, hair follicles and scalp subcutaneous tissue, periodontal ligament, thymus and spleen, as well as pre-natal tissues, such as placenta, umbilical cord blood, fetal bone marrow, blood, lung, liver and spleen (Krampera et al., 2006), as shown in Figure 2.11. In this work, mesenchymal stem cells isolated from marrow are called bone marrow-derived stem cells (MSCs) while those isolated from adipose tissue (fat) are called adipose-derived stem cells (ASCs).

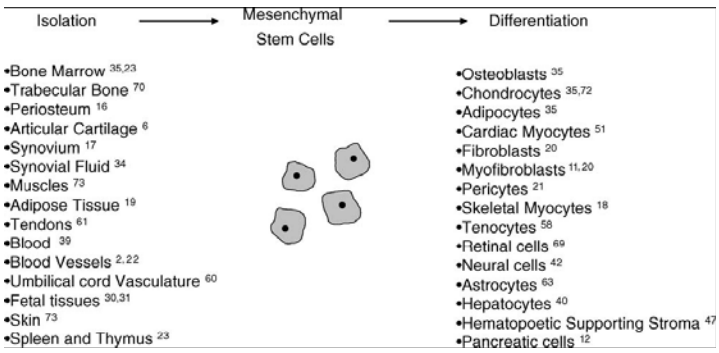

Figure 2.11. Sources and cell types derived from mesenchymal stem cells.

(Pountos and Giannoudis, 2005)

2.1.4.2 Phenotypic characteristics of mesenchymal stem cells

When stem cells are isolated and cultured *in vitro*, the adherent population indicating mesenchymal stem cells tends to form colonies of spindle-shaped cells (fibroblast-like) termed as colony-forming unit-fibroblast (CFU-F). The CFC-F property is frequently used when studying the proliferative capacity of mesenchymal stem cells in culture.

Initially, the cultured fibroblast-like cells are observed to be ALP-positive, collagen IV-positive and fibronectin-positive. In addition, type I collagen and laminin of the basement membrane are found in the extracellular matrix surrounding the cultured mesenchymal stem cells. A wide range of cell-surface antigens and peptides such as CD105, CD73 as well as other adhesion molecules and growth factor/cytokine receptors including CD29, CD90, CD117, CD166, CD54, CD102, CD121a,b, CD123, CD124, and CD49 have been targeted in these initial mesenchymal stem cells populations using a wide panel of antibodies, as presented in Table 2.5.

Table 2.5. Mesenchymal and hematopoietic stem cell surface markers (Park et al., 2007).

Mesenchymal cell-surface antigens and peptides, as well as other adhesion molecules and growth factor/cytokine receptors	**Cell markers of endothelial cells, monocytes/ macrophages, lymphocytes, leukocytes, RBC, and other hematopoietic cells as well as synthesized cytokines and growth factors**
CD9, CD29, CD44, CD81, CD106, SH2 (CD105), SH3, SH4 (CD73), SB-10, CD166, CD54, CD102, CD121a,b, CD123, CD124, and CD49	CD31, CD14, CD11a/LFA-1, CD45, glycophorin A, CD3, CD14, CD19, CD34, CD38, CD66b, stem cell factor (c-kit ligand), interleukin-7 (IL-7), IL-8, IL-11, TGF-β, cofilin, galectin-1, laminin-receptor 1, cyclophilin A and MMP-2

2.1.4.3 Growth and differentiation of mesenchymal stem cells

Mesenchymal stem cells and colony forming units-fibroblastic (CFU-F) can be induced *in vitro* to expand and differentiate into the osteoblastic lineage using dexamethasone, ascorbate, and β-glycerolphosphate. Under these conditions the cells undergo sequential: 1) growth, 2) differentiation, and 3) maturation, as presented in Figure 2.12. Growth or proliferation is marked by a many-fold increase in cell number. Synthesis of collagen I and alkaline phosphatise (ALP) indicate

differentiation. Maturation is noticed by formation of multilayer nodules, secretion of osteocalcin and mineralization of the extracellular matrix (ECM).

Arpornmaeklong et al. (2007) have studied growth and differentiation of mouse osteoblasts on chitosan/collagen scaffolds. They suggested that increase in ALP activity indicating early osteoblastic differentiation stage can be seen after 4 days, with activity peaking at 7-10 days and then slowly decreasing. Deposition of calcium and secretion of osteocalcin defined as late osteoblastic differentiation stage are usually quantified after 15 days of the culture in osteogenic medium.

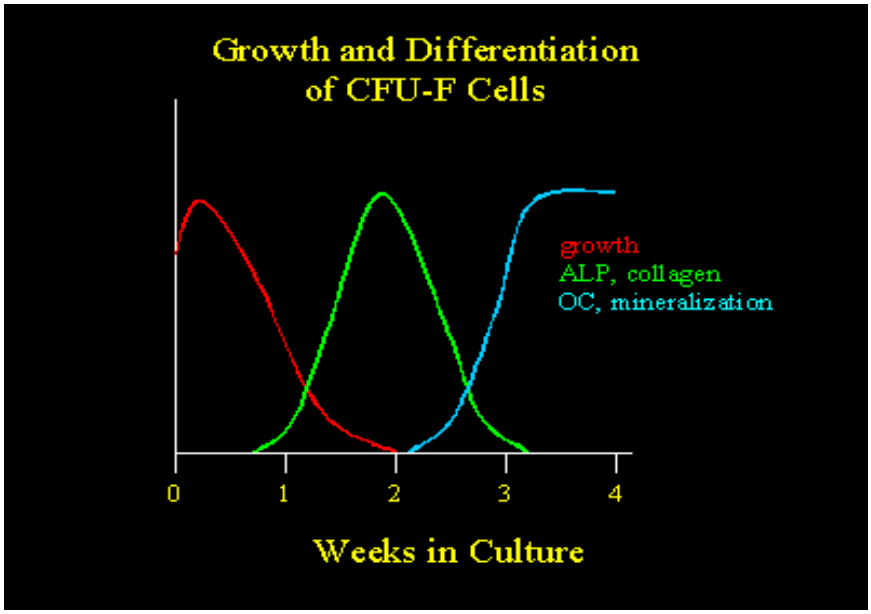

Figure 2.12. Phases of growth and differentiation of mesenchymal stem cells. (http://www.tissue.che.vt.edu/home_frame.htm)

2.2 Review of literatures

This study aimed to investigate characteristics of different scaffolds influenced by some parameters such as types of acid solvents, blending ratios and molecular weights of materials. Different types of scaffolds were prepared from natural polymers including collagen, gelatin, chitosan and chitooligosaccharide. The effects of acid types on collagen solutions and collagen scaffolds were first scoped in this work. Collagen is an excellent biocompatible material which is widely used in tissue engineering applications of skin, bone and various tissues (Chamberlain et al., 2000; Pek et al., 2004). Since collagen must be dissolved in acid condition, the characteristics of collagen in different acid solvents could be dissimilar. Among various acid types, acetic and hydrochloric acids were commonly used to solubilize collagen in order to prepare collagen solutions and scaffolds. Physical and biological properties of collagen solutions and scaffolds obtained from these two acids were of our first interest. Leffler and Muller (2000) reported the effects of acid types on the physical and drug liberation properties of chitosan/gelatin scaffolds. It was found that tartaric or citric acid used as solvent resulted in instable, soft, elastic and disintegrating scaffolds with fast drug release. Elastic but harder scaffolds were obtained from stable foams when hydrochloric or lactic acid was used. The use of acetic or formic acid enabled the production of stable foams, soft and elastic scaffolds and a slow drug release. Acid types also affected on the formation, micromeritic property, release behavior and floating phenomenon of chitosan microcapsules, as found by Lin et al. (1992). They showed that chitosan microcapsules prepared using an acetic acid as a solvent had a more compact and less porous structure and exhibited slow release action when compared to other chitosan microcapsules made from ascorbic acid and citric acid. They also revealed that acetic acid concentration significantly influenced the formation, micromeritic property and release behavior of theophylline chitosan microcapsules containing sodium carboxymethyl cellulose.

To further develop the suitable scaffolds for the specific use in bone tissue engineering, although collagen showed many appropriate characteristics, it is expensive and easy to denature at high temperature (in the form of collagen solution). Thus, gelatin, a denatured collagen, has become an alternative biomaterial because it shows biological characteristics similar to those of collagen but much cheaper. Our previous work has showed that gelatin could be used as a base material to produce

scaffolds for skin tissue engineering (Ratanavaraporn, 2005). It was found that gelatin could substitute a large portion of collagen, upto 70-90%, without any adverse effect on biological properties, comparing to pure collagen scaffold. The results from *in vitro* test showed that L929 mouse fibroblasts could proliferate on collagen/gelatin scaffolds as good as those on pure collagen scaffold. A tricalcium phosphate and glutaraldehyde crosslinked gelatin scaffold, incorporated with bone morphogenetic proteins-4 (BMP-4), was developed by Yang et al. (2005) to provide an alternative scaffold for bone tissue engineering. They investigated differences between gelatin scaffold and BMP-4 immobilized gelatin scaffold on activities of neonatal rat calvaria osteoblasts. ALP activity, calcium deposition and Gla-type osteocalcin activity of cells cultured on BMP-4 immobilized gelatin scaffold were improved from those on gelatin scaffold. These findings suggested that glutaraldehyde crosslinked gelatin scaffold provided an excellent porous structure, conductive to greater cell attachment and osteogenic differentiation, and that utility could be significantly enhanced by the inclusion of BMP-4. Yamamoto et al. (2000) have described the sustained release of transforming growth factor-β1 (TGF-β1) from gelatin hydrogel for the enhancement of bone regeneration activity. Basic TGF-β1 was adsorbed onto the acidic gelatin hydrogel by an electrostatic interaction and the ability of the hydrogels to induce bone regeneration was evaluated in a rabbit calvarial defect model. Eight weeks after treatment, the gelatin hydrogels with water contents of 90 and 95 %wt induced significantly high bone regeneration compared with those with lower and higher water contents and free TGF-β1. This indicated that the gelatin hydrogel is a promising matrix of TGF-β1 release to induce skull bone regeneration.

Though gelatin is an appropriate material to be used as a scaffold, it has some limitations in bone tissue engineering such as fast degradation rate and low mechanical property. To overcome the weak points of gelatin, in this study, chitosan was chosen to blend with gelatin. Chitosan is another promising candidate in tissue engineering due to its unique biological properties such as antibacterial, haemostatic, fungistatic, antitumoral and anticholesteremic properties (Kim et al., 2007). Martino et al. (2005) have reviewed chitosan as a versatile biopolymer for orthopaedic tissue-engineering. Chitosan showed many interesting characteristics, for example, a minimal foreign body reaction, an intrinsic antibacterial nature, and the ability to be molded in various geometries which are suitable for cell ingrowth and

osteoconduction. They reported that the presence of the *N*-acetyl-glucosamine moiety in chitosan related to its bioactivities in terms of enhanced growth and mineral deposition by ostoblasts. Cationic amino group of chitosan associated with anions on the bacterial cell wall, suppressing biosynthesis. Moreover, chitosan disrupted the mass transport across the cell wall, accelerating the death of bacteria. They also mentioned that degradation rate of chitosan was inversely related to the degree of crystallinity and deacetylation. The low deacetylated chitosan degraded rapidly while the highly deacetylated ones may last several months *in vivo*. In 2005, Li et al. reported the development of a biodegradable porous scaffold made from chitosan and alginate polymers. They found that osteoblasts readily attached, proliferated well, and deposited calcified matrix onto the chitosan/alginate scaffold. The *in vivo* result proved that the chitosan composite scaffold had a high degree of tissue compatibility, promoted rapid vascularization and deposited calcified matrix within the entire scaffold structure as early as the fourth week after implantation. Park et al. (2005) have investigated mesenchymal stem cells cultured on chitosan/alginate gel/ BMP-2 composites as an injectable material for new bone formation. After injecting the gel into the subcutaneous space on the dorsum of nude mice, subcutaneous nodules had formed by 12 weeks. Osteopontin, a protein important in bone development, was identified in the gel composite and osteocytes were positive for the antibody. This work concluded that gel composite containing chitosan was able to stimulate new bone formation.

Aylin and Jamison (2007) studied on chitosan scaffolds embedded with biphasic calcium phosphate granules in terms of distribution, morphology, and phenotypic expression of osteoblastic cells. Uniform and complete cell distribution was obtained throughout the scaffolds. It was also found that biphasic calcium phosphate layer on chitosan scaffolds altered morphology of cells initially attached to the scaffold surfaces, leading to higher expression of ALP and osteocalcin. Thus, they confirmed the use of chitosan/biphasic calcium phosphate scaffolds for culture of mesenchymal stem cells and pre-osteoblasts in bone tissue development *in vitro*. Cai et al. (2007) employed the surface modification of poly (D, L-lactic acid) scaffold with chitosan. Osteocalcin assay showed that the osteocalcin production in chitosan-modified poly (D, L-lactic acid) scaffold was significantly higher than that in the control poly (D, L-lactic acid) scaffold. The histological results from *in vivo* rabbit defect model exhibited a higher bone formation and better biocompatibility of

chitosan-modified poly (D, L-lactic acid) scaffolds, when compared with the control poly (D, L-lactic acid) scaffolds.

Recently, numerous studies have investigated molecular weight effect of chitosan on scaffold properties and cell affinity. Richardson et al. (1999) have prepared and characterized chitosans with different molecular weights in respects of their cytotoxicity, ability to cause haemolysis, ability to complex DNA as well as to protect DNA from nuclease degradation. The results displayed that all chitosans were neither toxic nor haemolytic. They also have the ability to complex DNA and protect against nuclease degradation. Furthermore, low molecular weight chitosan could be administered intravenously without liver accumulation. Thus, they suggested low molecular weight chitosans as a potential material in gene delivery system. Wang et al. (2007) examined the effects of carboxymethyl-chitosans with different molecular weights on the proliferation of skin fibroblasts and keratinocytes *in vitro*. The results demonstrated that all molecular weights of carboxymethyl-chitosans promoted the proliferation of skin fibroblasts and keratinocytes at 1-1000 ppm. However, the effects of low molecular weight carboxymethyl-chitosans were greater than those of high molecular weight one. Carboxymethyl-chitosans (M_n = 3 kDa) had the strongest promotive effects on skin fibroblasts and keratinocytes and it had equivalent effects when compared with basic fibroblast growth factor (bFGF) and epidermal growth factor (EGF). Our previous study has also shown that the molecular weight of chitosan significantly influenced on the mechanical and biological properties of collagen/chitosan scaffolds (Tangsadthakun et al., 2007). Collagen/chitosan scaffolds were prepared using chitosan samples with various molecular weights and blending compositions. The results from *in vitro* culture with fibroblasts evidenced that collagen scaffold with lower molecular weight chitosan was more effective to promote cell proliferation than pure collagen and collagen/high molecular weight chitosan scaffolds, particularly for scaffolds containing 30% of chitosan.

Although low molecular weight chitosan showed improved effectiveness in gene delivery system and cell response, it still had some limitations to be used as tissue engineering material, for example, poor solubility which limited cell penetration (Mendis et al., 2007). Therefore, in this work, very low molecular weight water-soluble chitosan called chitooligosaccharide (COS) was then chosen for the investigation on its biological characteristics, comparing to water-insoluble chitosan having various molecular weights. COS is known to possess many biological

activities such as antimicrobial, antiviral, antitumor, immunostimulant, antioxidant and radical scavenging activities (Kima and Rajapakse, 2005). In 2003, poly(3-hydroxybutyric acid-co-3-hydroxyvaleric acid) membrane grafted with chitosan or COS was fabricated by Hu et al (2003). Hyaluronic acid was further immobilized onto chitosan- or COS-grafting membranes. After chitosan- or COS- grafting, L929 fibroblasts attachment and protein adsorption were improved, while the cell number was decreased. After immobilizing hyaluronic acid, the cell proliferation was promoted, the protein adsorption was decreased, and the cell attachment was slightly lower than chitosan- or COS-grafting membranes. In 2004, Ohara et al. have studied how chitosan modulates the hard tissue forming cells by culture an osteoblastic cell line in α-MEM supplemented with 10% FBS and 0.005% COS for 3 days. The results exhibited that ALP activity was significantly high compared with the control culture group. Furthermore, COS could induce an increase in the expression of two genes, CD56 antigen and tissue-type plasminogen activator. The results suggested that a super-low concentration of COS (0.005%) could modulate the activity of osteoblastic cells through mRNA levels, concerning the regulation of proliferation and osteogenic differentiation.

To imitate an organic extracellular matrix component of natural bone, the systems of blended gelatin/chitosan and gelatin/chitooligosaccharide were studied as bone tissue-engineered scaffolds. With this manner, gelatin was considered as collagenous matrix substituting collagen and chitosan and chitooligosaccharide served as glycosaminoglycans (GAGs) because their structures were similar to natural GAGs. Numerous studies have confirmed the success of the combination between gelatin and chitosan as bone tissue-engineered materials. In 2002, Zhao et al. have fabricated hydroxyapatite/chitosan-gelatin composite scaffolds and varied the solid content and the composition of the original mixtures to control porosities and densities of the scaffolds. Scaffolds with 90.6% porosity were obtained from this study. Histological and immunohistochemical staining after culturing with neonatal rat caldaria osteoblasts indicated that osteoblasts attached and proliferated well on the scaffolds. Type I collagen and proteoglycan-like substrate were synthesized, while osteoid and bone-like tissue were formed during the culture period. In 2003, Yin et al. have developed macroporous chitosan–gelatin/β-tricalcium phosphate composite scaffolds with various suspension concentration, β-TCP amount and pre-freezing temperature. The scaffolds exhibited different pore structures and compressive

properties were improved as increasing solid concentration and β-TCP fraction. At 4 weeks after subcutaneous implantation in rabbits, formation of extracellular matrix was observed throughout the composite scaffolds with active fibroblasts. Vascular endothelial cells began to appear and blood capillaries were observed. They recommended that this composite scaffolds can be utilized in non-loading bone regeneration. Huang et al. (2005) evaluated mechanical characteristics and cell–matrix interactions of chitosan/gelatin scaffolds. Tensile and compressive properties of the scaffolds were affected by the addition of gelatin. After culture with human umbilical vein endothelial cells, they found that chitosan scaffold decreased cell-spreading area, disrupted filamentous actin and localized focal adhesion kinase in the nucleus of endothelial cells. In the blended chitosan/gelatin scaffolds, effect of gelatin was dominant, that is, filamentous actin and focal adhesion kinase distribution of the blends were comparable to those of gelatin scaffold. They summarized that there was significant influence of blending gelatin with chitosan on scaffold properties and cellular behaviours.

To explore the potentials of materials for the use in bone tissue engineering, mesenchymal stem cells are widely employed since they exhibit proliferation, self-renewal and multipotent differentiation capacities. They are able to differentiate into various cell types of mesodermal origin, such as osteoblasts, chondrocytes, adipocytes and muscle cells. Mesenchymal stem cells have been initially identified in bone marrow as non-hematopoietic stem cells, called bone marrow-derived stem cells (MSCs). The osteogenic differentiation potential of MSCs was described many years ago (Maniatopoulos et al., 1988). In 2005, MSCs isolated from rat bone marrow were cultured in osteogenic medium to obtain committed osteoprogenitor cells, then seeded onto the gelatin hydrogel and transplanted into the area of a rat tibia segmental bone defect (Srouji and Livne, 2005). After 6 weeks, radiology images revealed that calcified material was present in the site of the defect, indicating new bone formation. It was concluded that committed osteogenic MSCs contained in a biocompatible scaffold could provide a promising surgical tool for enhancement of bone defect healing. Ciapetti et al. (2006) reported *in vitro* proliferation and differentiation of MSCs derived from spare femoral bone marrow obtained during hip replacement surgery from adult donors. They found that MSCs consistently maintained an osteogenic potential. The cells turned to fully differentiated osteoblasts with a predictable set of molecular and phenotypic events of *in vitro* bone deposition. When

seeded on polycaprolactone-based scaffold or surfaces, the proliferation and mineralization of MSCs were modulated by the surface chemistry and topography. These cells were proved to be a potential source for bone regeneration, either by direct autologous re-implantation or by ex vivo expansion and re-implantation combined with a proper scaffold.

However, MSCs are rare in bone marrow (1 cell/10^5 nucleated cells) and their quantity decreases with age (Pittenger et al., 1999). Also, difficulty of cell isolation limits their uses. Adipose tissue, which is often removed from plastic surgery, has become another source of mesenchymal stem cells. Adipose-derived stem cells (ASCs) have several advantages over MSCs, such as minimal morbidity upon harvest. High number of ASCs can be isolated from adipose tissue, potentially eliminating the need for *in vitro* expansion. ASCs show higher proliferation rates than MSCs while perform potential of multiple differentiation similar to MSCs (Zhang et al., 2008). Several works have showed the effective multipotential differentiation of ASCs (Strem et al., 2005; Han et al., 2007). Girolamo et al. (2007) examined the phenotypic profile of human ASCs and compared different osteogenic-inductive media to assess ASC differentiation. They found that ASCs at passage 4 expressed mesenchymal stem cells-related cell surface antigens (CD13, CD105, CD54, CD90, CD44). Osteogenic medium containing 10 mM β-glycerol phosphate, 10 nM dexamethasone and 150 μM ascorbic acid-2-phosphate showed a higher osteogenic potential for differentiation of ASCs than osteogenic medium containing 10 mM β-glycerol phosphate, 100 nM dexamethasone, and 50 μM ascorbic acid-2-phosphate, as assessed by increased levels of calcium deposition, alkaline phospatase activity and osteopontin expression. They concluded that ASCs efficiently differentiate into osteogenic lineage, particularly when cultured in inductive medium supplemented with 10 nM dexamethasone and 150 μM ascorbic acid. In 2006, a study to assess the osteogenic potential and utility of using ASCs to regenerate bone in a rabbit calvarial defect model was designed (Dudas et al., 2006). Rabbit ASCs were seeded on gelatin scaffolds and induced in osteogenic medium containing bone morphogenetic protein-2 (BMP-2). They found that osteoinduced ASCs exhibited significantly greater healing than non-induced ASCs. Therefore, pre-implantation osteoinduction of ASCs enhanced osteogenic capacity and showed ability to heal large defect while non-induced ASCs may be secondary to use of noncritical-sized defects. Li et al. (2007) reported that ASCs genetically modified by bone morphogenetic protein-2 (BMP-2) and applied to a β-tricalcium

phosphate carrier healed critical-sized canine ulnar bone defects. After 16 weeks, radiographic, histological, and histomorphometry analysis showed that ASCs modified by BMP-2 gene produced a significant increase of newly formed bone area and healed or partly healed all of the bone defects. They concluded that ASCs modified by the BMP-2 gene could enhance the repair of critical-sized bone defects in large animals. Hao et al. (2008) explored *in vitro* and *in vivo* osteogenesis of collagen gel containing rabbit ASCs and incoporated into a porous poly (lactic-coglycolic) acid-β-tricalcium phosphate scaffold. Composites were cultured *in vitro* for 2 weeks in osteogenic medium and then implanted into the autologous muscular intervals for 8 weeks. The calcification level was radiographically evident and woven bone with a trabecular structure was formed. They concluded that homogeneous bone tissue could be successfully formed *in vivo* by using the combination of collagen gel-ASCs/poly (lactic-coglycolic) acid-β-tricalcium phosphate scaffolds.

Comparing on multipotential differentiation between ASCs and MSCs, there are many controversial reports. Mauney et al. (2007) studied *in vitro* and *in vivo* adipogenic differentiation utilizing human ASCs and MSCs cultured on silk fibroin scaffolds. On such system, the difference of adipogenesis between hMSCs and hASCs could not be noticed. Noel et al. (2008) also reported that both stem cells underwent adipogenic differentiation with a similar extent when cultured on tissue culture plates under adipogenic differentiation. However, some studies found that MSCs tended to have higher potentials of osteogenic and chondrogenic differentiation while ASCs preferred to differentiate into adipocytes (Im et al., 2005; Liu et al., 2007). On the other hand, Dragoo et al. (2003) have isolated ASCs from liposuction aspirates and examined the osteogenic potential of ASCs, MSCs and osteoblasts, when exposed to either recombinant human bone morphogenetic protein (rh-BMP-2) or adenovirus containing BMP-2. The results revealed that transduced ASCs produced more bone precursors with faster onset of calcified extracellular matrix than transduced MSCs and osteoblasts. They suggested that ASCs may be an ideal source of stem cells for gene therapy and tissue engineering.

CHAPTER III

EXPERIMENTAL WORKS

3.1 Materials

1. Type I collagen solution in HCl (6 mg/ml, pH 3.1, Nitta Gelatin Inc., Osaka, Japan)
2. Squid pen chitin (Taming Enterprise, Co., Thailand)
3. Gelatin (pI 9, Nitta Gelatin Co., Osaka, Japan)
4. Glutaraldehyde solution (25% v/v, MW 100.12 g/mol)
5. Glycine ($C_2H_5NO_2$, MW 75.07 g/mol)
6. β-Alanine ($C_3H_7NO_2$, MW 89.09 g/mol)
7. Hydroxyproline ($C_5H_9NO_3$, MW 131.13 g/mol)
8. 2,4,6-trinitrobenzene sulfonic acid (TNBS, $C_6H_3N_3O_9S$, MW 293.17 g/mol)
9. Sodium hydrogen carbonate ($NaHCO_3$, MW 84.01 g/mol)
10. Collagenase (Type I, 25 units, Sigma-Aldrich Co., USA)
11. Citric acid monohydrate ($C_6H_8O_7$, MW 210.14 g/mol)
12. Glacial acetic acid (CH_3COOH, MW 60.05 g/mol)
13. Hydrochloric acid (HCl, MW 36.46 g/mol)
14. Sodium chloride (NaCl, MW 58.44 g/mol)
15. Sodium hydroxide (NaOH, MW 40.00 g/mol)
16. Sodium acetate trihydrate ($CH_3COONa\ 3H_2O$, MW 136.08)
17. Chloramine-T ($C_7H_7ClNO_2S.Na\ .\ 3H_2O$, MW 281.70 g/mol)
18. n-propanol ($CH_3(CH_2)_2\ OH$, MW 60.1 g/mol)
19. Dimethylamino benzaldehyde ($C_9H_{11}NO$, MW 149.19 g/mol)
20. Perchloric acid ($HClO_4$, MW 100.46 g/mol)
21. Hydrogen peroxide (H_2O_2, MW 18.016 g/mol)
22. Catalase (2,000-5,000 units/mg protein, Sigma-Aldrich Co., USA)
23. Ethanol ($C2H_5OH$, MW 46.04 g/mol)
24. Formalin solution (HCHO and CH_3OH in water, MW 30.03 g/mol)
25. Sodium citrate ($HOC(COONa)(CH2COONa)_2.2H_2O$, MW 294.10 g/mol)
26. Sodium dodecylsulfate (SDS, $C_{12}H_{25}OSO_3Na$, MW 288.38 g/mol)

27. Phosphate buffer saline (PBS, pH 7.4)
28. Dulbecco's modified eagle medium (DMEM, 10%medium + L-glutamine + AB, Hyclone, USA)
29. Alpha-modified Eagle minimal essential medium (α-MEM, 10%medium + L-glutamine + AB, Hyclone, USA)
30. Medium 199 (modified, with Earle's salts, without L-glutamine, sodium bicarbonate, and phenol red, Sigma-Aldrich Co., USA)
31. Dulbecco's Modified Eagle's Medium/Ham's Nutrient Mixture F12 (DME/Ham F12, with 3151 mg/L dextrose, with 2.5 mM L-glutamine, with 15 mM HEPES, with 55 mg/L sodium pyrvuate, without sodium bicarbonate, Sigma-Aldrich Co., USA)
32. Fetal bovine serum (FBS, Hyclone, USA)
33. Penicillin/streptomycin antibiotic (100 U/ml, Hyclone, USA)
34. Trypsin-EDTA (0.25% trypsin with EDTA·Na, Gibco BRL, Canada)
35. 3-(4,5-dimethylthiazol-2-yl)-2,5-diphenyltetrazolium bromide (MTT, USB corporation, USA)
36. Dimethylsulfoxide (DMSO, $(CH_3)_2SO$, MW 78.13 g/mol)
37. bisBenzimide fluorescent dye (Hoechst 33258, $C_{25}H_{24}N_6O.3HCl$, MW 533.88 g/mol)
38. Insulin ($C_{254}H_{377}N_{65}O_{75}S_6$, MW 5733.49 g/mol)
39. 3,5,3'-triiodothyronine ($C_{15}H_{12}I_3NO_4$, MW 650.97 g/mol)
40. Transferrin
41. Calcium pantotenate ($C_{18}H_{32}CaN_2O_{10}$, MW 238.27 g/mol)
42. Biotin ($C_{10}H_{16}N_2O_3S$, MW 244.31 g/mol)
43. Dexamethasone ($C_{22}H_{29}FO_5$, MW 392.46 g/mol)
44. β-glycerol phosphate ($C_3H_7Na_2O_6P \cdot 5H_2O$, MW 306.11 g/mol)
45. L-ascorbic acid ($C_6H_8O_6$, MW 176.12 g/mol)
46. Glycerol-3-phosphate dehydrogenase (GPDH activity measurement kit, Sangi Co., Japan)
47. Oil red O ($C_{26}H_{24}N_4O$, MW 408.49 g/mol)
48. *p*-Nitrophenyl phosphate liquid substrate (Sigma, St. Louis, MO, USA)
49. *p*-Nitrophenol ($O_2NC_6H_4OH$, MW 139.11 g/mol, Sigma, St. Louis, MO, USA)
50. Ethanolamine ($NH_2CH_2CH_2OH$, MW 61.08 g/mol)

51. *o*-Cresolphthalein (OCPC, $C_{22}H_{18}O_4$, MW 346.38 g/mol)
52. Calcium carbonate ($CaCO_3$, MW 100.09 g/mol)
53. Silver nitrate ($AgNO_3$, MW 169.87 g/mol)
54. Sodium thiosulphate ($Na_2S_2O_3$, MW 158.11 g/mol)
55. Skim milk
56. Tween-20 (Sigma-Aldrich Co., USA)
57. Can get signal solution (Cosmo Bio co., Ltd.)
58. Anti-fibronectin (LSL Co., Japan)
59. Peroxidase-conjugated anti-rabbit IgG antibody (Sigma-Aldrich Co., USA)
60. o-phenylenediamine substrate ($C_6H_8N_2$, MW 108.14 g/mol, Sigma-Aldrich Co., USA)
61. Sodium peroxoborate ($NaBO_2$. $H_2O_2.3H_2O$, MW 153.88 g/mol)
62. Sulfuric acid (H_2SO_4, MW 98.08 g/mol)
63. Bovine serum albumin (pH 6.5-7.5, Sigma-Aldrich Co., USA)
64. Fluorescein 5(6)-isothiocyanate-conjugated phalloidin (Phalloidin-FITC, $C_{58}H_{63}N_{10}O_{14}S_4$, MW 1252.44 g/mol, Sigma-Aldrich Co., USA)
65. FluorSave Reagent (Calbiochem Inc., USA)
66. Fluorescein 5(6)-isothiocyanate (FITC, $C_{21}H_{11}NO_5S$, MW 389.38 g/mol)
67. Insulin-like growth factor-1 enzyme-linked immunosorbent assay (IGF-1 ELISA, R&D Systems, USA)
68. Vascular endothelial growth factor enzyme-linked immunosorbent assay (VEGF ELISA, R&D Systems, USA)
69. FITC-labeled Annexin V/propidium iodide (PI) Apoptosis Detection kit (BD Pharmingen™, BD Biosciences, USA)
70. A mouse osteocalcin ELISA kit (Biomedical Technologies Inc., USA)
71. Millipore filters (HAWPO 1300)
72. Dialysis tube (cellulose membrane in 0.1% sodium azide, MWCO 500 Da)
73. Nylon mesh (200 μm)
74. Syringe with 18-gauge needle (Corning, USA)
75. Tissue culture plates (Corning, USA)
76. Centrifugal tubes (Corning, USA))
77. Glass slip (15 mm in diameter, Matsunami, Japan)
78. Lint-freed paper (Kimwipe)
79. Ionic exchange column

3.2 Equipments

1. Freezer (-40°C, Heto, PowerDry LL3000, USA)
2. Lyophilizer (Heto, PowerDry LL3000, USA)
3. Vacuum drying oven and pump (VD23, Binder, Germany)
4. Viscometer (Rheolab MC1, Physica)
5. Scanning electron microscopy (SEM, Jeol JSM 5400)
6. Universal Testing Machine (Instron 5567, USA)
7. Spectrophotometer (Versa Max, Molecular Device Japan Co., Japan)
8. Microplate reader
9. Gel permeation chromatography (GPC, PL-GPC 110, Polymer labolatories Ltd., Shropshire SY6 6AX, UK)
10. Fourier transform infrared spectroscopy (FT-IR, Spectrum GX, Perkin Elmer, UK)
11. Water contact angle and video contact analyzer (Data Physics, OCA 15 Plus, Germany)
12. Electron spectrometer (ELS-7000AS instrument, Otsuka Electronic Co. Ltd., Japan)
13. X-ray photoelectron spectroscopy (XPS)
14. Confocal fluorescence microscope (Fluoview FV300, Olympus Optical Co., Japan)
15. Energy-dispersive X-ray spectroscopy (EDX)
16. Phase-contrast microscope (IX70, Olympus Optical Co., Japan)
17. Flow cytometer
18. Centrifuge
19. Orbital shaker
20. Sonicator
21. Digital balance
22. Water bath
23. Auto-pipettes (10, 100, 1000, 5000 μl)
24. Multi-channel pipette

3.3 Experimental procedures

Experimental work was divided into 2 parts. Part I was the study on physical, chemical and biological properties of collagen scaffolds affected by different acids used as solvent; hydrochloric (HCl) and acetic acids. Part II was the investigation on properties of gelatin/chitosan scaffolds which were influenced by the blending ratio and molecular weight of chitosan. The systems of gelatin/chitosan were developed for bone tissue engineering applications using rat adipose-derived stem cells and bone marrow-derived stem cells. This part consists of the preparation of various molecular weight chitosans, preparation and characterization of stem cells and the fabrication and characterization of gelatin/chitosan films and scaffolds.

Part I: Effects of acid type on collagen solution and collagen scaffolds

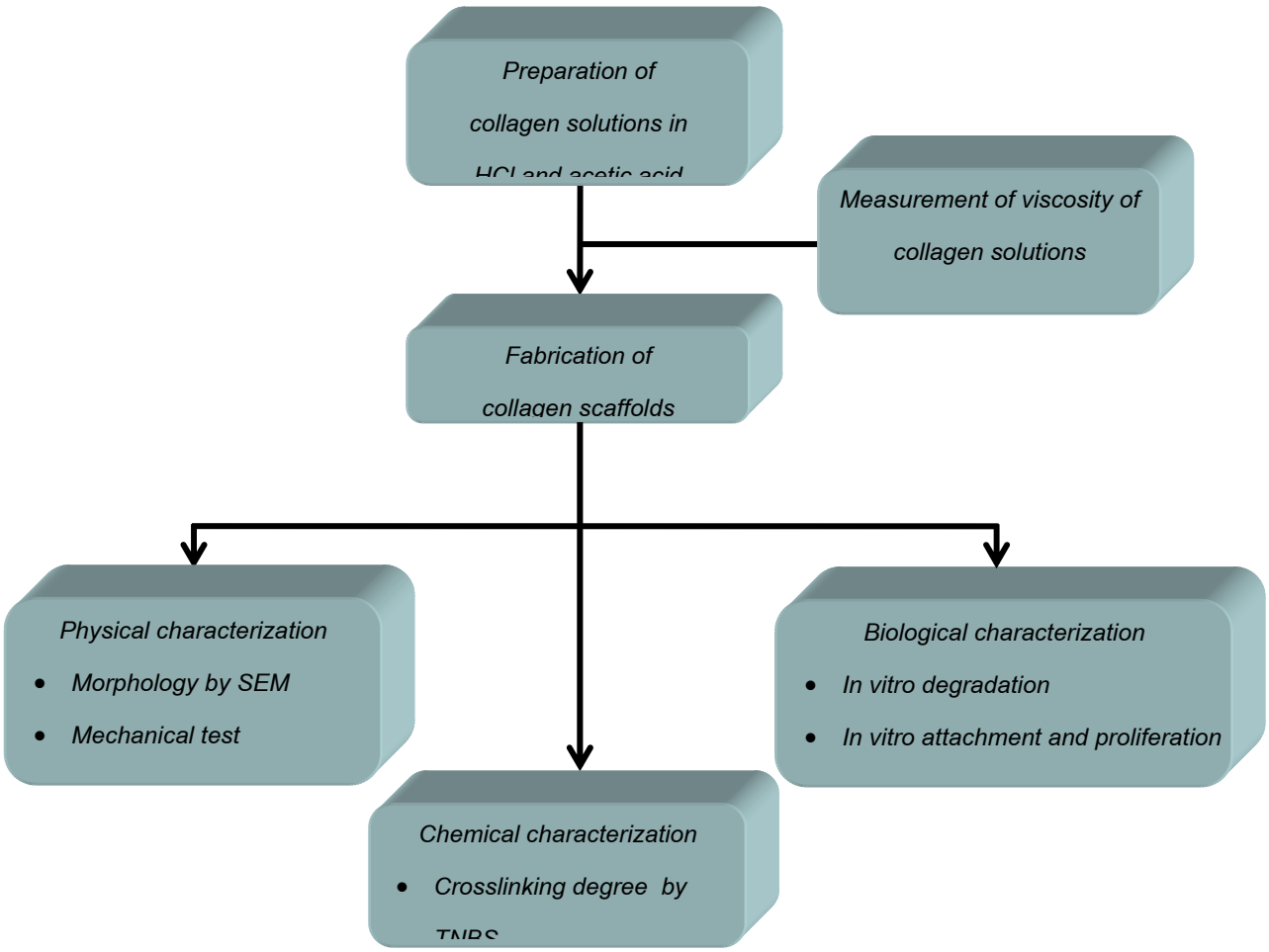

Figure 3.1 Diagram of experimental procedures (Part I).

Part II: Gelatin/chitosan scaffolds for bone tissue engineering

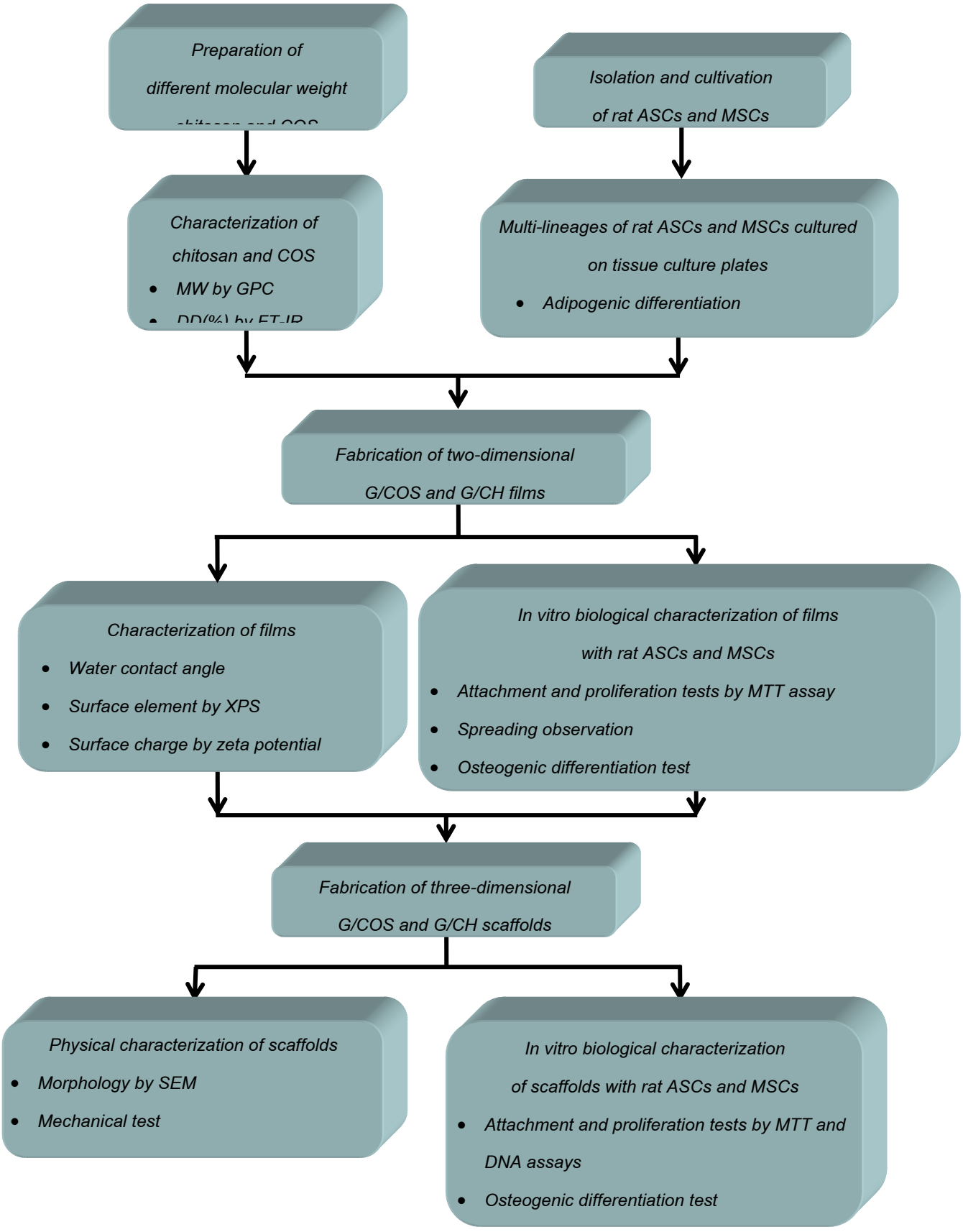

Figure 3.2 Diagram of experimental procedures (Part II).

Part I: Effects of acid type on collagen solution and collagen scaffolds

3.3.1 Fabrication of collagen scaffolds

Collagen solution in HCl (0.6% w/w, pH 3.1) was cast into polystyrene 24-well plates and frozen at −40°C overnight prior lyophilized for 24 h to produce collagen scaffold (C–HCl). For the collagen in acetic acid (C-Acetic), collagen solution in HCl was lyophilized and redissolved in 0.5 M acetic acid (Nagai et al., 2004; Song et al., 2006; Tangsadthakun et al., 2007) to obtain the solution at the same concentration (pH 2.5). The freeze-dried scaffolds were cross-linked by dehydrothermal (DHT) treatment at 140°C for 48 h (Ozeki & Tabata, 2005).

3.3.2 Physical and chemical characterization of collagen scaffolds

Viscosity of collagen solution

Viscosity of collagen solution prepared in HCl and acetic acids was determined using a viscometer equipped with TEZ-180 spindle and Z2 DIN chamber (shear rate 1000 s^{-1}).

Morphological observation

The structure of cross-sectioned collagen scaffolds was examined by scanning electron microscopy (SEM) at an accelerating voltage of 12–15 kV. The samples were sputter-coated with gold prior to SEM observation.

Mechanical test

A universal testing machine was used to determine the slope from 5% to 30% strain of the stress-stain curves of the scaffolds (13 mm in diameter and 3 mm in thickness) at a constant compression rate of 0.5 mm/min. The compressive modulus was determined and reported as the mean±standard deviation (n=5).

Swelling ability

Water sorption capacity of the swollen collagen scaffolds was determined. A known weight of the dry scaffold was immersed in PBS (pH 7.4) at 37°C for 24 h. The wet scaffold was weighed after blotting the scaffold with a lint-freed paper (Kimwipe) to remove excess water. The swelling ratio of the scaffold, W_{sw}, was calculated from the equation:

$$W_{SW} = \frac{(W_t - W_o)}{W_o}$$

W_t and W_o represented weight of the wet and dry scaffolds, respectively. The values were expressed as the mean±standard deviation (n=3).

Determination of crosslinking degree

The determination of crosslinking degree was carried out by modifying the method of Bubnis and Ofner (1992). The concept of this method was to react free amino groups of collagen molecule, which indicate the non-crosslinking groups, with 2,4,6-trinitrobenzene sulphonic acid (TNBS). The TNBS reaction was shown in Figure 3.3.

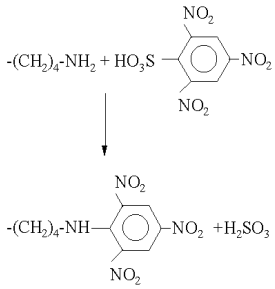

Figure 3.3 TNBS reaction

Briefly, known weight of the dry scaffold was placed into a test tube containing 1 ml of deionized (DI) water, 1 ml of 0.5% (w/v) TNBS solution and 1 ml of 4% (w/v) sodium hydrogen carbonate ($NaHCO_3$, pH 8.5). It was then reacted in a water bath maintained at 40°C for 2 h. The non-crosslinked primary amino groups of collagen molecule would react with TNBS and formed a soluble complex. This solution was further hydrolyzed with 2 ml of 6 N HCl at 60°C for 1.5 h. The absorbance of the solution was determined at 405 nm by a spectrophotometer. The crosslinking degree was then calculated by the following equation:

$$\text{Crosslinking degree (\%)} = \left(1 - \frac{A_c}{A_n}\right) \times 100$$

A_c and A_n represented absorbance of the crosslinked and non-crosslinked collagen solutions, respectively. The values were expressed as the mean±standard deviation (n=3).

3.3.3 In vitro biological characterization of collagen scaffolds

In vitro degradation test

Degradation of sterilized collagen scaffolds was evaluated after digestion with collagenase (Type I, 2 units/ml PBS) at 37°C (Powell & Boyce, 2006). Collagen content in the enzyme solution was measured using a hydroxyproline assay (Edwards & O'Brien Jr, 1980; Patiyal & Katoch, 2006). Briefly, 200 µl sample/hydroxyproline standards was mixed with 100 µl chloramin-T reagent (0.3525g Chloramine-T in 5.175 ml water, 6.5 ml n-propanol and 13.325 ml assay buffer) and incubated at room temperature for 20 min. One hundred milliliters of dimethylaminobenzaldehyde reagent (3.75 g dimethylamino benzaldehyde in 15 ml n-propanol, 6.5 ml perchloric acid) was added into each solution to react at 60°C for 15 min. The absorbance of the solution was measured immediately at 540 nm.

In vitro attachment and proliferation tests with L929

The sterilized collagen scaffolds were seeded with L929 mouse fibroblasts (3×10^4 cells/scaffold) and cultured in Dulbecco's modified eagle medium (DMEM) supplemented with 10% fetal bovine serum (FBS) and 100 U/ml penicillin/streptomycin at 37°C, 5% CO_2. The number of cells attached at 5 h and proliferated at 24 and 72 h after seeding was quantified by 3-(4,5 dimethylthiazolyl)-2,5-diphenyltetrazolium bromide (MTT) assay (Mosmann, 1983). Briefly, the samples were washed with PBS. One milliliter of MTT solution (0.5 mg/ml DMEM without phenol red) was added into each sample and incubated at 37ºC for 30 min. In this step, mitochondrial reductase, enzyme indicating the viable cells, would reduce MTT to the purple formazan crystals. After that, MTT solution was removed and DMSO was employed to dissolve the formazan crystals to the pale yellow tetrazolium rings of MTT. The absorbance of the solution was measured at 570 nm. Shrinkage of the scaffolds after 72 h culture was determined from the following equation:

$$\text{Shrinkage of the scaffold} = \frac{(D_0 - D_t)}{D_0}\times 100$$

D_0 and D_t represented the diameter of initial scaffolds and the scaffolds after 72 h culture, respectively. The values were expressed as the mean±standard deviation (n=3).

Part II: Gelatin/chitosan scaffolds for bone tissue engineering

3.3.4 Preparation of different molecular weight chitosan and COS

High and medium molecular weight chitosan were prepared by alkaline deacetylation process. Group I of squid pen chitin (20 g) was decalcified in 1 M HCl solution for 24 h and washed repeatedly with deionized (DI) water. The decalcified chitin was deproteined in 1 M NaOH solution for another 24 h and further deacetylated in concentrated NaOH solution (50% w/w) for 4 days. The obtained high molecular weight chitosan was then washed repeatedly with DI water until pH became neutral and dried at 40°C for 24 h in an oven. Group II of squid pen chitin (20 g) was first ground using a food blending machine to increase surface area before treated in the same deacetylation process described previously. With this method, medium molecular weight chitosan was obtained.

Low molecular weight chitosan was prepared according to the method of selective hydrolysis of medium molecular weight chitosan using *Bacillus* sp. PP8 crude chitosanase (Nakapong, 2004). Briefly, medium molecular weight chitosan (MW = 490 kDa) obtained from squid pen was dissolved in 1% (v/v) acetic acid to form 1% (w/w) chitosan solution. The pH of solution was adjusted to 5 by 1 M NaOH. The ratio of enzyme to chitosan solution at 1:5 was used. Crude chitosanase (200 ml) were added into chitosan solution and the solution was then incubated in a water bath at 50°C. After 24 h, the reaction was stopped and low molecular weight chitosan was precipitated by adjusting the pH of chitosan solution to 10 using 1 M NaOH. The precipitate was centrifuged and washed several times with DI water. The neutralized precipitate was then freeze-dried to get low molecular weight chitosan.

Chitooligosaccharide (COS) was produced from medium molecular weight chitosan (MW 320 kDa) by free radical degradation process using hydrogen peroxide (H_2O_2) as an oxidizing agent (Chang et al., 2001; Tian et al, 2003 & 2004). Briefly, chitosan was dissolved in 2% (v/v) acetic acid solution to form 1 g/dL solutions. H_2O_2 (30% v/v) was added to a final concentration of 1.5% (w/v) H_2O_2 in the solution (pH 3.9-4.0). The sample solution was stirred in a water bath at 50°C for 72 h. After the reaction, the solution was removed from the water bath and cooled in an ice bath to chill the reaction. The solution was then dialyzed with cellulose dialysis membrane (MWCO 500 Da) for 3 days and freeze dried to obtain COS.

3.3.5Characterization of chitosan and COS

Determination of molecular weight of chitosan and COS

Weight-averaged molecular weight of chitosan and COS was characterized using gel permeation chromatography (GPC) technique. The mobile phase was a mixture of 0.2 M acetic acid, 0.2 M sodium acetate and NaCl (pH 4). Chitosan solution was filtered through 0.45 µm Millipore filter before injection into the column at the flow rate of 0.5 ml/min. Calibration was performed using pullulans (MW 5,800-1,660,000) as standard samples. In the case of COS, catalase was added into COS solution to remove the residual H_2O_2 before injection into the GPC column (Chang et al., 2001).

Determination of deacetylation degree of chitosan and COS

The degree of decetylation (%DD) of chitosan and COS were determined using fourier transform infrared (FT-IR) spectroscopy technique (FT-IR, Spectrum GX, Perkin Elmer, UK). The degree of acetylation (%DA) and degree of deacetylation (%DD) were calculated using the following equations (Rinaudo et al., 2001).

$$DA\ (\%) = 31.92(A_{1320}/A_{1420}) - 12.20$$

where A_{1320} and A_{1420} were the absorbance peaks at the wave number of 1320 cm^{-1} and 1420 cm^{-1}, which corresponded to C-N stretching and C-H deformations, respectively.

3.3.6 Isolation and cultivation of rat adipose-derived stem cells (ASCs) and bone marrow-derived stem cells (MSCs)

Adipose-derived stem cells (ASCs) were isolated from subcutaneous adipose tissue of 3-week-old female Wistar rats according to the technique reported by Hong et al. (2007). After sacrifying, the rat was sterilized and adipose tissue was collected from subcutaneous skin of the rat. Adipose tissue was then washed with PBS, minced into small pieces and digested with 0.075% (w/v) collagenase at 37°C for 15-30 min under agitation at 100 rpm. After complete digestion, adipose tissue was filtered through 200 µm Nylon mesh and the filtrate was then centrifuged at 1,200 rpm, 4°C for 5 min to obtain ASCs at the bottom. ASCs were washed with

medium and centrifuged several times before culture in 199 medium supplemented with 10% FBS and 100 U/ml penicillin/streptomycin at 37°C, 5% CO_2. The medium was changed on the 4^{th} day after isolation and every 3 days thereafter. When the proliferated cells become subconfluent, usually for 7–10 days, the cells were trypsinized using 0.25% trypsin-EDTA. The cells of the second- and third-passages at sub-confluence were used for further experiments.

Bone marrow-derived stem cells (MSCs) were isolated from the bone shaft of femurs of the same rats according to the technique reported by Takahashi et al. (2005). After sacrifying, the rat was sterilized and both ends of rat femurs were cut away from the epiphysis. The bone marrow was flushed out using a syringe (18-gauge needle) containing 1 ml of medium. The cell suspension was then cultured in Alpha-modified Eagle minimal essential medium (α-MEM) supplemented with 15% FBS and 100 U/ml penicillin/streptomycin at 37°C, 5% CO_2. Other details were the same as in the case of ASCs.

3.3.7 Characterization of rat ASCs and MSCs

3.3.7.1 Adipogenic differentiation of rat ASCs and MSCs cultured on tissue culture plates

For adipogenic differentiation, ASCs and MSCs were seeded on 6-well tissue culture plates at $3x10^4$ cells/cm^2 and cultured in adipogenic medium (AM: DME/Ham's F12 medium containing 0.05 μM insulin, 0.2 nM 3,5,3'-triiodothyronine, 100 nM transferring, 17 μM calcium pantotenate, 33 μM biotin and 100 nM dexamethasone) (Hauner et al., 1989). 199 medium supplemented with 10% FBS was used as control medium of adipogenic differentiation (CMA). After 2 and 4 weeks of culture, the number of proliferated cells were analyzed by DNA assay (Rao & Otto, 1992). Briefly, the cells were washed with PBS, underwent a freeze and thaw process, and finally incubated in 30 mM sodium citrate-buffered saline solution (SSC, pH7.4) containing 0.2 mg/ml sodium dodecylsulfate (SDS) at 37°C for 1 h for cell lysis. Then, the cell lysate was sonicated to allow the complete lysis before assay. One hundred milliliters of cell lysate was mixed with 100 μl of Hoechst 33258 fluorescent dye solution (30 mM SSC, 1 μg/mL Hoechst 33258 dye) in 96-well black plate. The fluorescent intensity of mixed solution was immediately measured at the excitation and emission wavelengths of 355 and 460 nm, respectively. The cell number was

determined by the use of calibration curve prepared from the fluorescent measurement for the cells of known number.

In addition, adipogenic differentiating markers including glycerol-3-phosphate dehydrogenase (GPDH) activity and lipid droplet formation were assessed at 2 and 4 weeks of adipogenic culture. GPDH activity was measured to assess the biosynthesis of fat in adipocytes and adipose tissues. The activity of GPDH rapidly increases upon differentiation of precursor adipocytes to mature adipocytes. In this study, GPDH activity of both stem cells was assessed using a GPDH activity measurement kit based on the absorbance measurement of a NADH reduction (Hauner et al., 1995). The kit was designed to measure the activity of GPDH which generates glycerol 3-phosphate from dehydroxyacetone phosphate using NADH as a coenzyme. Briefly, the cell lysate was reacted with GPDH substrate and the absorbance of kinetic reaction was immediately measured at 340 nm for 10 min (1 min interval). The slope obtained from absorbance-time curve was used to calculate GPDH activity using the following equation:

$$\text{GPDH activity (U/ml)} = \text{slope (O.D. 340 nm)} \times 1.377$$

Oil red O is another key marker for adipogenic differentiation that stains lipid droplet created by stem cell underwent adipogenic differentiation (Yagi et al., 2008). Briefly, an oil red O stock solution (0.3% w/v) in isopropanol was mixed with double distilled water (DDW) at the ratio of 6:4 and the mixed solution was left at room temperature for 10 min, followed by filtration through a 0.22 μm filter to prepare the oil red O working solution. The cells were washed with PBS and fixed with 10% formalin solution in PBS at 4°C for 1 h. After that, the cells were washed with PBS and 60% (v/v) isopropanol in DDW. The aggregated lipid droplet was then stained with oil red O working solution at 37°C for 30 min. After removal of oil red O solution, the cells were washed with 60% (v/v) isopropanol in DDW. The cells and stained lipid droplet were observed under phase-contrast microscope. Stained droplet was also quantified by extracting with 100% isopropanol and the absorbance of extracting solution was measured at 540 nm by a spectrophotometer (Inoue et al., 2005). The number of cells determined by DNA assay was also used to normalize GPDH activity and oil red O absorbance.

3.3.7.2 Osteogenic differentiation of rat ASCs and MSCs cultured on tissue culture plates

For osteogenic differentiation, ASCs and MSCs were seeded on 6-well tissue culture plates at $3x10^4$ cells/cm^2 and cultured in osteogenic medium (OM: α-MEM, 10% FBS, 10 mM β-glycerol phosphate, 50 μg/ml L-ascorbic acid and 10 nM dexamethasone). α-MEM supplemented with 10% FBS was used as control medium of osteogenic differentiation (CM). After 1, 2 and 4 weeks of culture, the number of proliferated cells was analyzed by DNA assay as same as described above. Osteogenic differentiating markers including alkaline phosphatase (ALP) activity and calcium content were determined by *p*-nitrophenyl phosphate (Takahashi et al., 2005) and O-cresolphythalein methods (Haddad et al., 1997), respectively. For ALP assay, the cell lysate (20 μl) was reacted with *p*-Nitrophenyl phosphate liquid substrate (100 μl) at 37°C for 15 min. ALP would convert *p*-Nitrophenyl to the soluble yellow end product of *p*-Nitrophenol. The reaction was stopped with 0.02 N NaOH (80 μl) and absorbance of the solution was immediately measured at 405 nm by a spectrophotometer. The calibration curve was prepared from the *p*-Nitrophenol standard solution.

For calcium assay, the calcium in cell lysate was extracted with equal volume of 1 M HCl at 4°C for 4 h. The calcium extracted lysate (10 μl) was then mixed with 1 ml of 0.88 M ethanolamine buffer (pH 11) and 100 μl of 0.63 M O-cresolphythalein complex substrate (OCPC) was added into the mixed solution. The solution mixture was allowed to stand at room temperature for 5 min. OCPC substrate will combine with calcium to give a purplish red colour. The absorbance of the solution mixture was measured at 570 nm by a spectrophotometer to assess calcium amount. The calibration curve was prepared from calcium carbonate standard ($CaCO_3$). The number of cells determined by DNA assay was also used to normalize ALP activity and calcium content. Calcium deposition of both stem cells cultured on tissue culture plates was also visualized by Von Kossa staining according to the method described by Yamamoto et al. (2003). Briefly, cells were washed with PBS and fixed with 10% (v/v) formalin solution in PBS at room temperature for 10 min. After washing with DDW, the cells were incubated in 5% (w/v) silver nitrate solution under ultraviolet (UV) light for 30 min and then incubated in 5% (w/v) sodium thiosulphate solution for 3 min.

3.3.8 Fabrication of two-dimensional G/COS and G/CH films

Two-dimensional films of G/COS, G/CH12 and G/CH1000 at the weight blending ratios of 100/0, 90/10, 70/30, 50/50, 30/70 and 0/100 were fabricated. Briefly, 100 μl of sample solution (0.05% w/v) was cast onto a glass slip (15 mm in diameter) and air-dried overnight in a laminar flow hood. Thin films coated on the glass slips were then crosslinked by dehydrothermal (DHT) treatment at 140°C for 24 h (Ozeki & Tabata, 2005).

3.3.8.1 In vitro biological characteristics of two-dimensional G/COS and G/CH films with rat ASCs and MSCs

Attachment and proliferation tests

After the films were sterilized by UV irradiation for 30 min, ASCs and MSCs were seeded onto the films at $2x10^4$ cells/film and cultured in proliferating medium (α-MEM, 15% FBS, 100 U/ml penicillin/streptomycin) at 37°C, 5% CO_2. The number of cells attached on the 1st day and cells proliferated on the 3rd and 5th days after seeding was quantified by MTT assay (Mosmann, 1983), as described previously.

Cell immunostaining and spreading observation

ASCs and MSCs were seeded onto the films at $2x10^4$ cells/film and cultured in proliferating medium (α-MEM, 15% FBS, 100 U/ml penicillin/streptomycin) at 37°C, 5% CO_2. On the 1st day after seeding, cell spreading on the films was observed by immunostaining method (Inoue et al., 2008). Briefly, attached cells were washed twice with PBS and fixed with 10% formalin solution at 4°C for 20 min. After 3-time wash with PBS, cells were treated with 2% bovine serum albumin in PBS at room temperature for 20 min. Next, cells were incubated with fluorescein isothiocyanate (FITC)-conjugated phalloidin (10 μg/ml) at room temperature for 1 h to visualize the filamentous actin (F-actin) fiber. Following the PBS wash, cells were mounted in FluorSave Reagent and viewed using a confocal fluorescence microscope. In addition, photographs of 100 cells attached on each film were taken at 10X magnification using a phase-contrast microscope. Cell spreading area was quantified using Metamorph program (Universal Imaging Systems, Molecular Devices Inc., Canada) (Storrie et al., 2007).

Osteogenic differentiation test

Osteogenic differentiations of ASCs and MSCs cultured on the films under osteogenic induction were assessed. Both cells were seeded on the films at $2x10^4$ cells/cm^2 and cultured in proliferating medium (α-MEM, 15% FBS, 100 U/ml penicillin/streptomycin) at 37°C, 5% CO_2. One day after seeding, the medium was changed into osteogenic medium (OM: α-MEM, 10% FBS, 10 mM β-glycerol phosphate, 50 μg/ml L-ascorbic acid and 10 nM dexamethasone) and changed every 2 days thereafter. After 7 days cultured in OM, alkaline phosphatase (ALP) activity and calcium content were assessed by the methods referred previously. The number of cells determined by DNA assay was used to normalize the ALP activity and calcium content. Calcium deposition of both cells cultured on the films was also visualized by Von Kossa staining.

3.3.8.2 Characterization of two-dimensional G/COS and G/CH films

Measurement of water contact angle of the films

Water contact angle of G/COS and G/CH1000 films was evaluated using sessile drop method. The water contact angle was measured using video contact analyzer and imaged using SCA 20 software. Deionized (DI) water was dropped onto the film using a gastight Hamilton precision syringe. Image was captured at 60 s after dropping. The baseline and the tangent were drawn using software and the contact angle was measured from three different points.

Evaluation of surface element

Chemical information of the film surfaces was analyzed by angle resolved X-ray photoelectron spectroscopy (XPS). The XPS spectra have been obtained using a PHI spectrometer equipped with an Mg/Al dual mode source and a small area analyzer with PSD detector. An achromatic X-ray (1253.6 eV) source was operated at 300 W. The vacuum pressure was 10^{-8} Torr during spectra acquisition. The N 1s, O 1s and C 1s regions have been recorded. Ratio of N/C and N/O was quantified from the percentage of atomic concentration.

Measurement of surface charge of the films

The zeta *(ζ)* potential of film surface was measured by electron spectrometer (ELS) at 25°C and the electric field strength of 100 V/cm. The zeta *(ζ)* potential was automatically calculated using the Smoluchouski equation (Jo et al., 2007).

Protein adsorption on the films

Adsorption of fibronectin onto the films was examined by an ELISA method with a slight modification (García et al., 1999). The films were placed in α-MEM supplemented with 15% FBS and 100 U/ml penicillin/streptomycin at 37°C for 1 h. Then, the films were washed with PBS and blocked with 3% (w/v) skim milk aqueous solution for 1 h. After 3-time wash with PBS containing 0.1% (v/v) Tween-20 (PBS-T), the films were incubated in Can get signal solution 1 containing anti-fibronectin (1:1,000 dilution) at 37°C for 1 h. After 3-time wash with PBS-T, the films were incubated in Can get signal solution 2 containing peroxidase-conjugated anti-rabbit IgG antibody (1:2,000 dilution) at 37°C for 1 h. Next, the films were washed with PBS-T for 3 times and placed in O-phenylenediamine substrate (1.7 mg/ml) in sodium peroxoborate solution (0.75 mg/ml) for 15 min, followed by the addition of 2 N H_2SO_4 to stop the coloring reaction. The supernatant was transferred to a 96-well plate and the absorbance of the supernatant was measured at 495 nm by a spectrophotometer.

Determination of insulin-like growth factor-1 (IGF-1) and vascular endothelial growth factor (VEGF) concentrations

ASCs and MSCs were seeded onto the films at $1x10^5$ cells/film and cultured in proliferating medium (α-MEM, 15% FBS, 100 U/ml penicillin/streptomycin) at 37°C, 5% CO_2. The level of rat IGF-1 and VEGF concentrations in medium supernatant after 2 days of the culture was measured by enzyme-linked immunosorbent assay (ELISA) following the manufacturer's instructions.

Apoptosis test by Annexin V-FITC/PI double staining assay

MSCs were seeded on 6-well tissue culture plates at density of $4x10^5$ cells/well and cultured in proliferating medium (α-MEM, 15% FBS, 100 U/ml penicillin/streptomycin) at 37°C, 5% CO_2. One day after seeding, approximately 80% confluent, the cells were treated with COS and CH solutions. Briefly, COS and CH solutions (0.05% w/v) were added into culture medium (100 μl/1 ml medium). After 24 h treated with COS and CH, the cells were washed with PBS and trypsinized with 0.25% trypsin-EDTA. Apoptosis-mediated cell death was examined using a double staining method with FITC-labeled Annexin V/propidium iodide (PI) Apoptosis Detection kit according to the manufacturer's instructions. Flow cytometric analysis

was performed immediately after staining. Cells in early stage of apoptosis were Annexin V positive whereas cells that were both Annexin V and PI positive were in the late stage of apoptosis.

3.3.9 Fabrication of three-dimensional G/COS and G/CH scaffolds

Three-dimensional scaffolds of G/COS and G/CH1000 at different blending ratios were fabricated via freeze-drying and chemical crosslinking techniques. Briefly, G/COS and G/CH1000 solutions at the blending ratios of 100/0, 90/10, 70/30, 50/50, 30/70 and 0/100 were prepared in 1% (v/v) acetic acid at 60°C under stirring for 3 h to obtain the final solid concentration of 1% (w/v). The blended solution was added with 25% (v/v) glutaraldehyde solution (6.26 µl/ml solution) and allowed for crosslinking under stirring for 15 min (Ozeki & Tabata, 2005). The crosslinked solution was then frozen at -30°C overnight and lyophilized under vacuum for 24 h. The obtained scaffolds were immersed in 0.1 M glycine solution at room temperature for 2 h to block the non-reacted aldehyde groups and washed repeatedly with DI water before refreeze-drying.

3.3.9.1 Physical characterization of three-dimensional G/COS and G/CH scaffolds

Morphological observation

The structure of cross-sectioned scaffolds was examined by scanning electron microscopy (SEM) at an accelerating voltage of 12–15 kV. The samples were sputter-coated with gold prior to SEM observation.

Mechanical test

Compressive modulus of the dry and wet scaffolds was evaluated using a universal testing machine as explained in section 3.3.2

Swelling ability

Water sorption capacity of the swollen scaffolds was determined as explained in section 3.3.2.

3.3.9.2 In vitro biological characterization of three-dimensional G/COS and G/CH scaffolds with rat ASCs and MSCs

Attachment and proliferation tests

After the scaffolds (11 mm in diameter, 2 mm in thickness) were sterilized by ethylene oxide, ASCs and MSCs were seeded onto the scaffolds in sterile

vials at $5x10^5$ cells/scaffold using agitation seeding at 300 rpm (Takahashi and Tabata, 2003). After 6 h of agitation seeding, cells-seeded scaffolds were transferred to new 6-well tissue culture plates and cultured in proliferating medium (α-MEM, 15% FBS, 100 U/ml penicillin/streptomycin) at 37°C, 5% CO_2. The medium was refreshed every 2 days. The number of cells attached at 6 h and cells proliferated on 3, 5 and 7 days after seeding was quantified by both MTT and DNA assays, as described previously.

Osteogenic differentiation test

Osteogenic differentiation of ASCs and MSCs cultured on the scaffolds under osteogenic induction was assessed. Both cells were seeded on the scaffolds in sterile vials at $1x10^6$ cells/scaffold using agitation seeding at 300 rpm. After 6 h of agitation seeding, cells-seeded scaffolds were transferred to new 6-well tissue culture plates and cultured in proliferating medium (α-MEM, 15% FBS, 100 U/ml penicillin/streptomycin) at 37°C, 5% CO_2. The medium was refreshed every 2 days and changed into osteogenic medium (OM: α-MEM, 10% FBS, 10 mM β-glycerol phosphate, 50 μg/ml L-ascorbic acid and 10 nM dexamethasone) after 7-day culture in proliferating medium. At 7, 14, 21 and 28 days cultured in OM, alkaline phosphatase (ALP) activity and calcium content were assessed by the methods referred previously. The number of cells determined by DNA assay was used to normalize the ALP activity and calcium content. In addition, the level of osteocalcin secreted from both stem cells cultured on the scaffolds under OM for 28 days was analyzed using a mouse osteocalcin ELISA kit following the manufacturer's instructions.

Cell morphological study

The morphology of both ASCs and MSCs differentiated on the scaffolds after 28-day cultured in OM was observed by SEM. Cells/scaffold constructs were washed with PBS and fixed in 2.5% (v/v) glutaraldehyde solution at 4°C for 1 h. The scaffolds were then dehydrated in serial dilutions of ethanol (50%, 70%, 80%, 90%, 95%, 99% and 100%) for 5 min each and freeze-dried by critical point drying using butyl alcohol as a freezing agent. The scaffolds were cross-sectioned and sputter-coated with gold prior to SEM observation.

Elemental analysis of cell and scaffold surfaces

Elements, particularly calcium (Ca) and phosphorous (P), on the surface of cells and scaffolds after 28-day cultured in OM were analyzed by energy-dispersive X-ray spectroscopy (EDX). The same cells/scaffold constructs used in SEM observation were used for EDX analysis.

Fourier transform infrared analysis of cells/scaffold constructs

To confirm the presence of phosphate (PO_4^{3-}) and carbonyl (CO_3^{2-}) groups which are major components of carbonated hydroxyapaptite in bone extracellular matrix, the cells/scaffold constructs were analyzed by Fourier transform infrared (FT-IR) spectroscopy technique. The scaffolds cultured with MSCs under OM for 28 days were ground and mixed with KBr prior to the analysis. All images were taken with a spectral resolution of 8 cm^{-1} in the range 4000–650 cm^{-1} using 64 scans.

CHAPTER IV

RESULTS AND DISCUSSION

Part I: Effects of acid type on collagen solution and collagen scaffolds

In this part, physical and chemical characteristics including viscosity of collagen solution, morphology, mechanical properties and crosslinking degree of collagen scaffolds fabricated from HCl and acetic acid solutions were reported. Also, *in vitro* degradation behavior and biological properties of the scaffolds with L929 mouse fibroblast cells were elucidated.

4.1 Physical and chemical characteristics of collagen scaffolds

Physical characteristics of the solution and scaffold are known to be affected by type of acid used as solvent. Viscosity of the solution is one property that can be altered, depending on ionic strength and pH of acid (Fernandez-Kim, 2004). Herein, viscosity of collagen solution prepared from HCl and acetic acids was initially evaluated because we hypothesized that it might influence other properties of the scaffolds obtained. Viscosity of collagen solution in HCl (C–HCl) and in acetic acid (C-Acetic) was shown in Table 4.1. The viscosity of C–HCl solution (5 mPa.s) was almost 5-fold higher than that of C-Acetic solution (1.2 mPa.s). It was expected that the conformation of collagen chains was different due to the difference in ionic strength of surrounded solution. This influenced collagen self-assembly in different acids. Plausibly, the positive charge-dominated collagen molecules were more expanded in HCl solution. As a result, the viscosity of C–HCl solution was higher than that of C-Acetic solution.

After scaffolds prepared from different acids were fabricated via freeze-drying and DHT crosslinking technique, the morphology of porous collagen scaffolds was examined, as shown in Figure 4.1. The SEM images indicated homogeneous pore structure of both scaffolds. Obviously, difference in pore size of both scaffolds was noticed. The pore size of leaf-like structure of C–HCl scaffold (around 100 μm) was larger than that of C-Acetic scaffold (around 50 μm). This could possibly be the result of stronger binding of Cl^- to water molecules so that water was excluded from

collagen molecules compared to the case of acetic acid. When the C-HCl solution was frozen prior to lyophilized, large ice crystals were formed, resulting in the scaffold with larger pores.

Mechanical properties of the scaffolds including compressive modulus and swelling ability were compared. The results on mechanical strength, shown in Table 4.1, revealed that compressive modulus of the dry C–HCl scaffold was 2-fold higher than that of dry C-Acetic scaffold ($p<0.05$). It could be stated from our results that soft scaffold with small pores was obtained from low viscous C-Acetic solution while C-HCl solution was more viscous and resulted in the more rigid scaffold with larger pores. This corresponded to the result indicated by Shin et al. (2005) that higher viscous solution provided structure with a greater mechanical strength. Similarly, Leffler & Muller (2000) have reported that mechanical properties of the scaffolds were greatly influenced by the nature of acid. Elastic but harder chitosan/gelatin scaffolds were obtained when HCl or lactic acid were used. On the other hand, soft scaffolds were produced when using acetic or formic acid as solvent. They explained that viscosity of the bulk solution influenced hardness of the scaffold. Low viscous solution resulted in a decreased apparent density and hardness of the scaffold. Moreover, Pins et al. (1997) demonstrated that collagen self-assembled in a different manner could alter the mechanical properties of collagen fibers. However, in our results, the compressive modulus of both C- HCl and C-Acetic scaffolds in a wet state was not significantly different. Swelling ability of scaffolds prepared from two different acid types was also reported in Table 4.1. It was noticed that C-Acetic scaffold could uptake more water than C–HCl scaffold. This might be due to the low apparent density of scaffold produced from low viscous C-Acetic solution. Also, highly porous structure with small interconnected pores of C-Acetic scaffold could allow water to penetrate inside easily, compared to C-HCl scaffold.

In addition, the collagen scaffolds in this work were crosslinked by DHT treatment at 140°C. Crosslinking degree of different scaffolds indicated in Table 4.1 was evaluated from the reduction of free amino groups in the scaffolds by TNBS method. It was found that the crosslinking degree of both scaffolds was approximately 22–25%. This could imply that different acids used as solvent did not affect the DHT crosslinking of collagen scaffolds.

Table 4.1 Physical and chemical properties of collagen scaffolds prepared from hydrochloric acid (C-HCl) and acetic acid (C-Acetic).

Scaffold type	Viscosity (mPa·s)	Compressive modulus (kPa)		Swelling ratio (w/w)	Crosslinking Degree (%)
		Wet	Dry		
C-HCl	5.0	0.6±0.2	16.0±5.5[a]	6.4±0.2[a]	22.2±5.5
C-Acetic	1.2	0.4±0.2	8.8±1.1[a]	9.2±0.7[a]	24.7±9.1

[a] represented a significant difference between C-HCl and C-Acetic at $p<0.05$

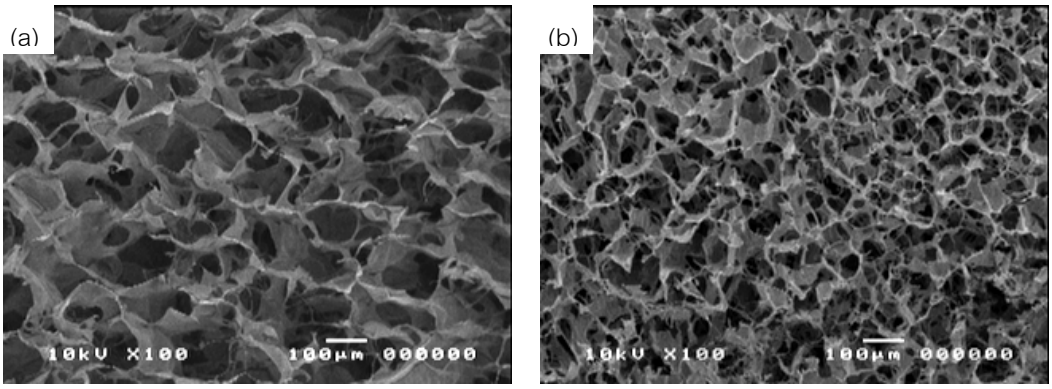

Figure 4.1 SEM photographs of freeze dried collagen scaffolds prepared from different acids (a) C-HCl and (b) C-Acetic.

4.2 In vitro biological characteristics of collagen scaffolds

Apart from physical and chemical characteristics, *in vitro* biological characteristics of C-HCl and C-Acetic scaffolds including biodegradation behavior and cell activities were also clarified. Figure 4.2 presented the percentage of hydroxyproline released from collagen scaffolds degraded in collagenase over a 24-h period. It showed that C-Acetic scaffold degraded with a slightly higher rate than C–HCl scaffold, especially in the first 6 h. This corresponded to the result on the swelling ability of the scaffolds. As the swelling ability of C-Acetic scaffold was greater than that of C–HCl scaffold, enzymatic degradation on C-Acetic scaffold could occur easier.

The results on *in vitro* tests with L929 mouse fibroblast cells illustrated in Figure 4.3 showed that C–HCl scaffold promoted initial cell adhesion at 5 h after seeding better than C-Acetic scaffold ($p < 0.05$). This could be due to the difference in stiffness of the scaffolds. C–HCl scaffold having higher compressive modulus contributed to greater cell attachment than C-Acetic scaffold, corresponding to the results reported by Brown et al. (2005). Besides the effects of mechanical properties, difference in pore structure of both scaffolds could be another reason attributed to different cell adhesion. Leaf-like structure of C–HCl scaffold might be more appropriate for cell attachment than the porous C-Acetic scaffold. However, 72 h after seeding, the number of cells proliferated on C-Acetic scaffold was significantly higher than that on C–HCl scaffold. This suggested that the higher shrinkage of C–HCl scaffold than that of C-Acetic scaffold after the culture, demonstrated in Table 4.2, was the main reason for the inhibited cell proliferation, as reported by Hiraoka et al. (2003).

4.3 Summary

It could be concluded from this part of study that the physical and mechanical properties of freeze-dried collagen scaffolds were affected by different characteristics of collagen solutions prepared from different acid solvents. Porous collagen scaffold prepared from hydrochrolic solution showed larger pore size, higher compressive modulus and lower swelling ability, compared to collagen scaffold obtained from acetic acid solution. Such physical and mechanical properties further influenced the biological characteristics of the collagen scaffolds. Leaf-like structure with high stiffness of collagen scaffold prepared from hydrochrolic solution supported

cell attachment while porous structure with high swelling ability of the scaffolds obtained from acetic acid solution promoted cell proliferation. Such information could be used to design scaffolds for particular applications.

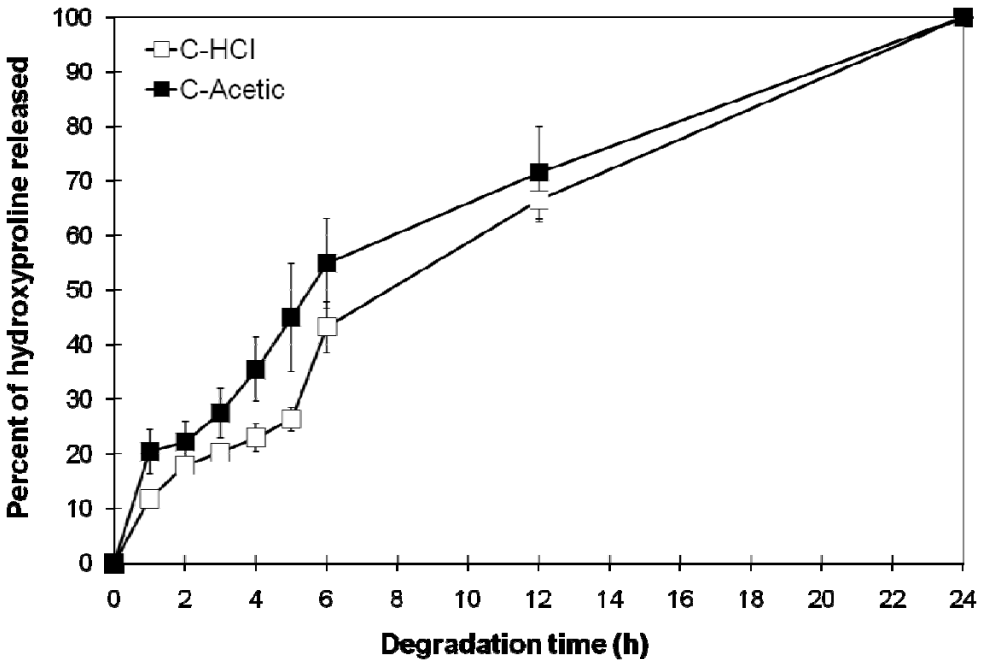

Figure 4.2 Percentage of degraded collagen scaffolds prepared different acids in collagenase Type I (2 units/ml) over a 24-h period, □C-HCl and ■C-Acetic.

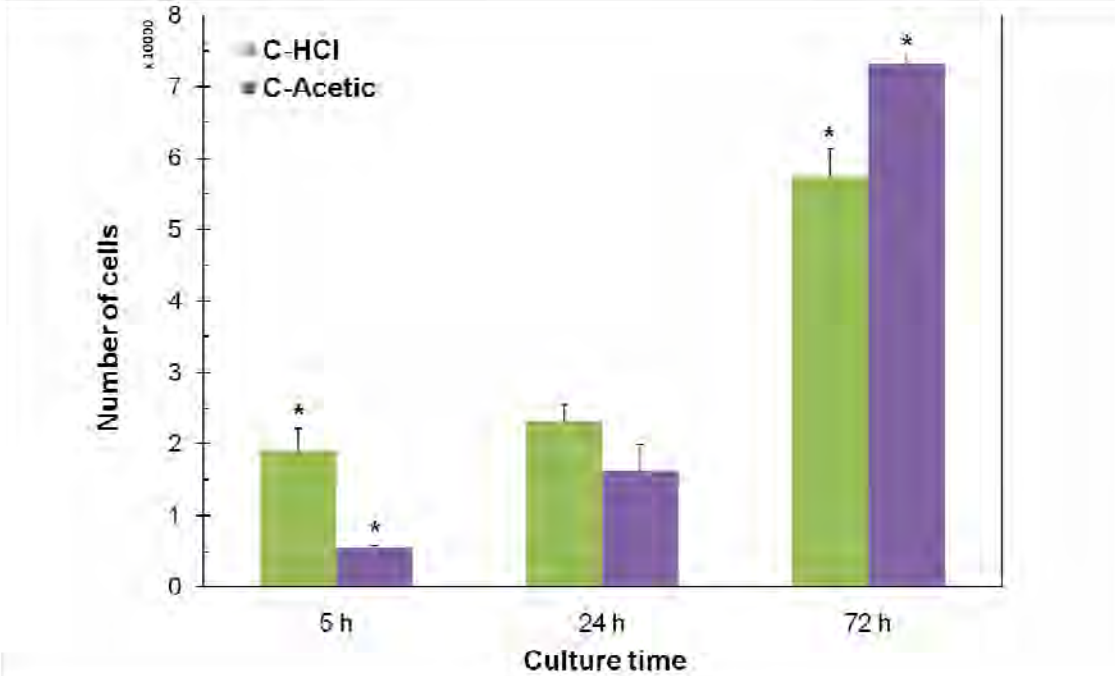

Figure 4.3 Number of L929 cell attached and proliferated on collagen scaffolds prepared from different acids at 5, 24 and 72 h after the culture, C-HCl and C-Acetic (*represented a significant difference between C-HCl and C-Acetic at $p<0.05$).

Table 4.2 Shrinkage of collagen scaffolds prepared from hydrochloric acid (C-HCl) and acetic acid (C-Acetic) after 72 h of the culture with L929 cells.

Scaffolds	**Initial diameter (D_0, mm)**	**Diameter after 72 h culture (D_t, mm)**	**% shrinkage**
C-HCl	13.62±0.08	8.01±0.19[a]	41.20 ± 1.07[a]
C-Acetic	13.53±0.05	8.98±0.11[a]	33.65 ± 0.75[a]

[a] represented a significant difference between C-HCl and C-Acetic at $p<0.05$

Part II: Gelatin/chitosan scaffolds for bone tissue engineering

In this part, the systems of gelatin/chitosan were developed for bone tissue engineering applications. Various molecular weight chitosans and very low molecular weight water-soluble chitooligosaccharide (COS) were prepared and characterized. On the other side, isolated ASCs and MSCs were first cultured on tissue culture plates under both normal and differentiating conditions to compare their adipogenic and osteogenic differentiation potentials. Behavior of both ASCs and MSCs cultured on gelatin/chitosan films at various blending ratios was elucidated. Then, gelatin/chitosan scaffolds fabricated at different blending ratios were characterized for physical and biological properties with both stem cells. Lastly, the comparison on characteristics and cell response between the systems of films and scaffolds was discussed.

4.4 Physical characteristics of chitosans and COS

Various molecular weight chitosans and very low molecular weight COS were first prepared from different methods. Molecular weight of chitosans and COS analyzed by gel permeation chromatography (GPC) was presented in Table 4.3. In this study, a wide range of molecular weight of chitosan, from 1.4 to 1,000 kDa, could be prepared. By the method of deacetylation with concentrated NaOH, the medium and high molecular weight chitosans (320 and 1,000 kDa) were obtained by varying the size of initial chitin sample. Ground squid pen chitin introduced more surface area of material contacting to NaOH, resulting in the production of chitosan with lower molecular weight. However, in this work, this technique was hardly used to produce chitosan with the molecular weight lower than 100 kDa. Enzymatic hydrolysis with *Bacillus* sp. PP8 crude chitosanase was then used to prepare low molecular weight chitosan (12 kDa) from medium molecular weight chitosan. Different molecular weight chitosans (CH12, CH320 and CH1000) obtained from the above preparation techniques were soluble only in acidic condition. In order to prepare very low molecular weight water-soluble chitosan called chitooligosaccharide (COS), the partial hydrolysis with different acids such as hydrochloric acid (HCl) and sulfuric acid (H_2SO_4) was reported for decades (Rupley, 1964; Nagasawa et al., 1971). Recently, the technique of free radical degradation of chitin and chitosan using hydrogen peroxide (H_2O_2) as oxidizing agent was introduced to prepare COS. This technique was non-toxic and could explain the phenomena of chitosan degradation *in*

vivo (Nordtveit et al., 1994; Tanioka et al., 1996). Then, the production of COS from medium molecular weight chitosan (320 kDa) using free radical degradation by H_2O_2 was applied in this study. The water-soluble COS with the molecular weight of 1.4 kDa was obtained. Deacetylation degree (%DD) of various molecular weight chitosans and COS presented in Table 4.3 and Figure 4.4 was shown to be in a similar range (78-82%). Therefore, the main variable characteristic of chitosan samples studied in this work was the molecular weight.

Table 4.3 Preparation processes and chemical characteristics of chitosans and COS.

Sample	Preparation process	MW (kDa)	DD (%)
COS	Free radical degradation by H_2O_2	1.4	80
CH12	Enzymatic hydrolysis by *Bacillus sp.* PP8 crude chitosanase	12	78
CH320	Deacetylation with concentrated NaOH	320	82
CH1000	Deacetylation with concentrated NaOH	1,000	82

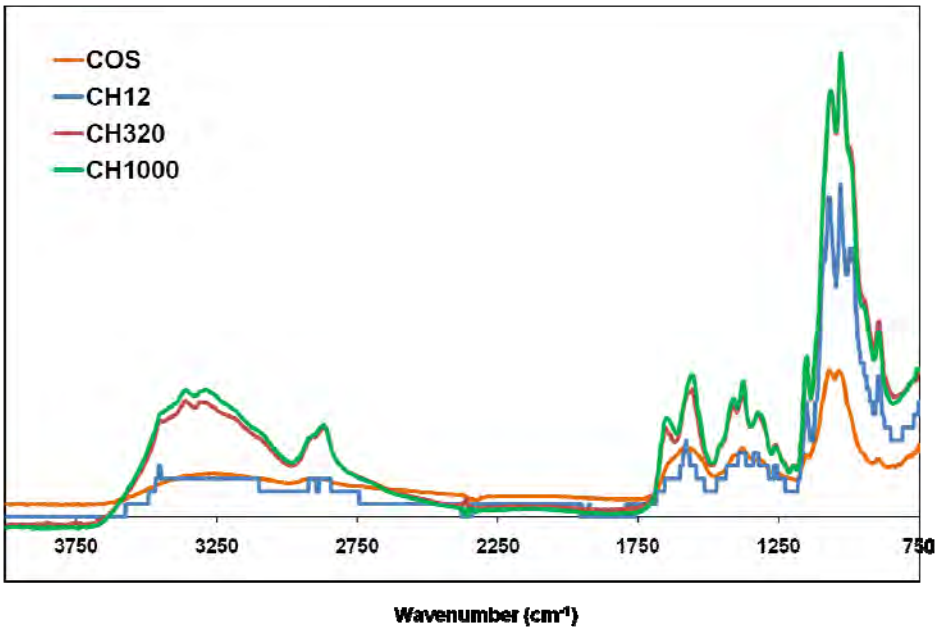

Figure 4.4 FT-IR spectra of different molecular weight chitosans and COS.

4.5 Adipogenic and osteogenic characteristics of rat ASCs and MSCs cultured on tissue culture plates

In terms of cells, ASCs and MSCs isolated from 3-week-old Wistar rats were cultured on tissue culture plates under normal condition. Cells at passages 2 and 3 were prepared for further use in this study. Due to the fact that ASCs were derived from adipose tissue and MSCs were derived from bone marrow, differentiation potential of both stem cells to adipogenic and osteogenic lineages under normal and differentiating conditions were first investigated, regardless of material effect.

For adipogenic differentiation test, both ASCs and MSCs were cultured on tissue culture plates under adipogenic medium (AM: DME/Ham's F12 medium containing 0.05 μM insulin, 0.2 nM 3,5,3'-triiodothyronine, 100 nM transferring, 17 μM calcium pantotenate, 33 μM biotin and 100 nM dexamethasone) for 2 and 4 weeks, compared to those cultured under control medium of adipogenic differentiation (CMA: 199 medium, 10% FBS). The number of both cells at 2 and 4 weeks of adipogenic culture assessed by DNA assay was shown in Figure 4.5. At 2 weeks of the culture, the number of ASCs was 2-fold higher than that of MSCs when cultured under normal condition (CMA). This represented that ASCs had faster proliferative rate than MSCs in normal culture condition. However, when cultured under adipogenic induction (AM), the number of both cells was not significantly different. Furthermore, it was found that the number of cells proliferated in AM was remarkably lower than those proliferated in CMA. Theoretically, the proliferation of stem cells decreases as the differentiation is increased (Belmonte et al., 2005). Then, the results on cell number indicated that cells in AM performed adipogenic differentiation rather than cells in CMA. After 4-week culture, a similar trend of cell number was observed but the absolute number decreased because some cells detached from plates due to too much confluence.

Gycerol-3-phosphate dehydrogenase (GPDH) activity of ASCs and MSCs cultured under the same condition was analyzed as demonstrated in Figure 4.6. The measurement of GPDH activity is widely used to assess the biosynthesis of fat in adipocytes and adipose tissue. The activity of GPDH rapidly increases upon differentiation of precursor adipocytes to mature adipocytes (Sottile & Seuwen, 2001). In this study, GPDH activity of MSCs was higher than that of ASCs both in AM and CMA. However, AM tended to promote activity of GPDH of both cells much

stronger than CMA. In addition to GPDH activity, lipid droplet formation is one of key markers for adipogenic differentiation. Oil red O was used to stain lipid droplet created by stem cell underwent adipogenic differentiation (Yagi et al., 2008). In this work, absorbance of Oil red O stained lipid droplet formed by ASCs and MSCs cultured under adipogenic induction was shown in Figure 4.7. It was exhibited that MSCs in AM formed highest amount of lipid droplet. The result was confirmed by photographs of stained lipid droplet in Figure 4.8. Large and dark stained lipid droplet aggregation was observed in the case of MSCs cultured in AM.

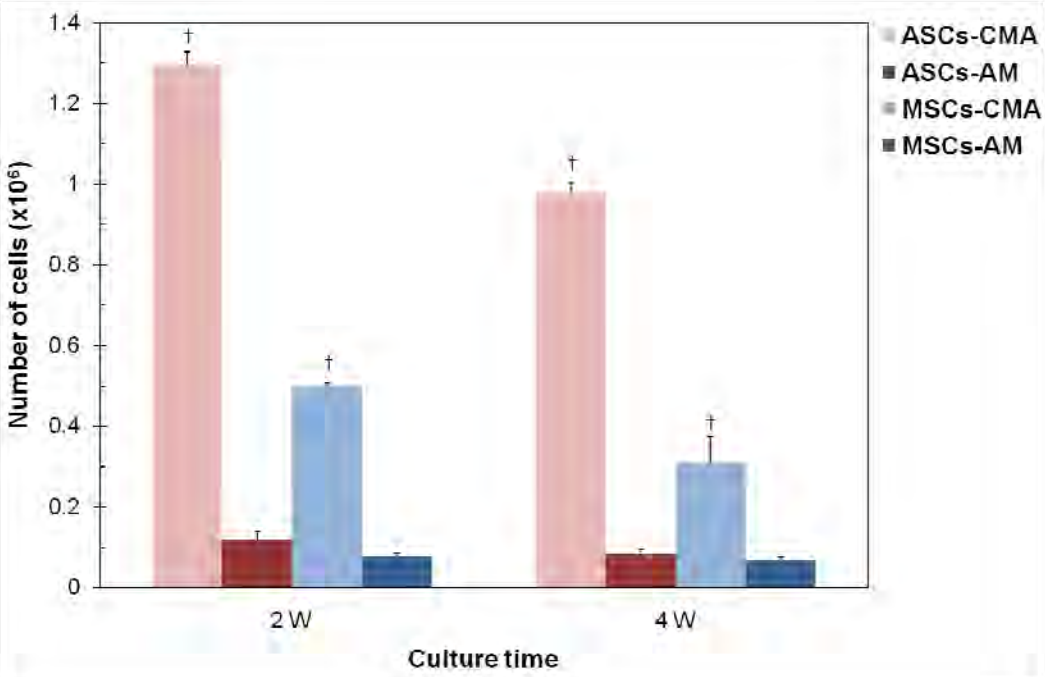

Figure 4.5 Number of ASCs and MSCs culture on 6-well tissue culture plates for 2 and 4 weeks under control medium of adipogenic differentiation (CMA: 199 medium, 10% FBS) and adipogenic medium (AM: DME/Ham's F12 medium containing 0.05 μM insulin, 0.2 nM 3,5,3'-triiodothyronine, 100 nM transferring, 17 μM calcium pantotenate, 33 μM biotin and 100 nM dexamethasone), assessed by DNA assay († and ‡ represented a significant difference between ASCs and MSCs cultured in the same medium and culture period at $p<0.05$).

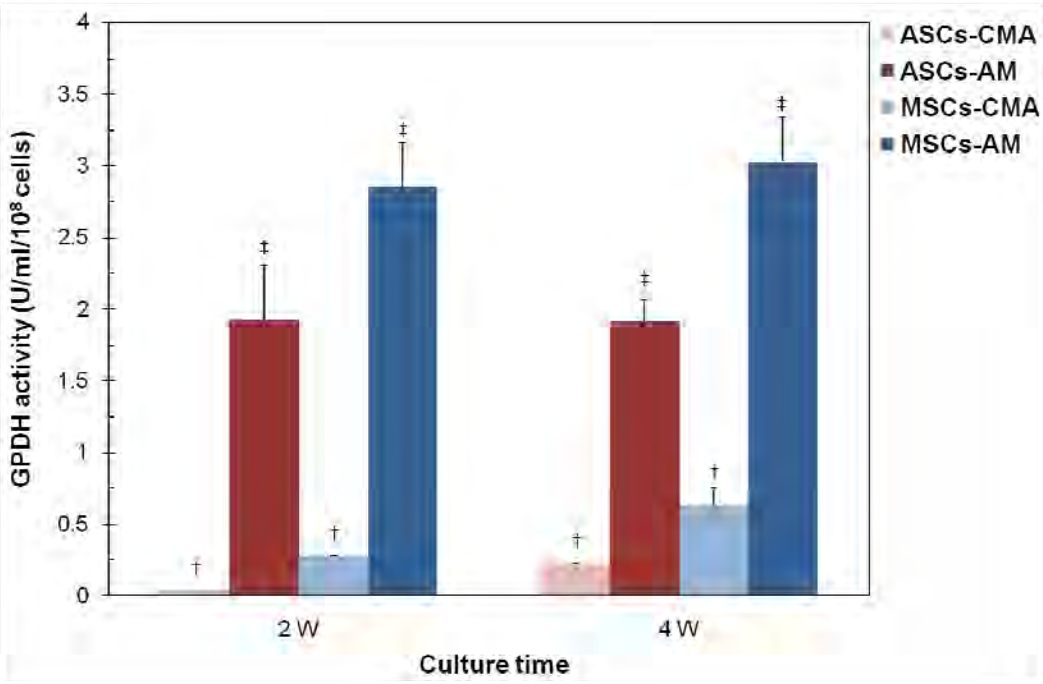

Figure 4.6 Gycerol-3-phosphate dehydrogenase (GPDH) activity of ASCs and MSCs culture on 6-well tissue culture plates for 2 and 4 weeks under control medium of adipogenic differentiation (CMA: 199 medium, 10% FBS) and adipogenic medium (AM: DME/Ham's F12 medium containing 0.05 μM insulin, 0.2 nM 3,5,3'-triiodothyronine, 100 nM transferring, 17 μM calcium pantotenate, 33 μM biotin and 100 nM dexamethasone), († and ‡ represented a significant difference between ASCs and MSCs cultured in the same medium and culture period at $p<0.05$).

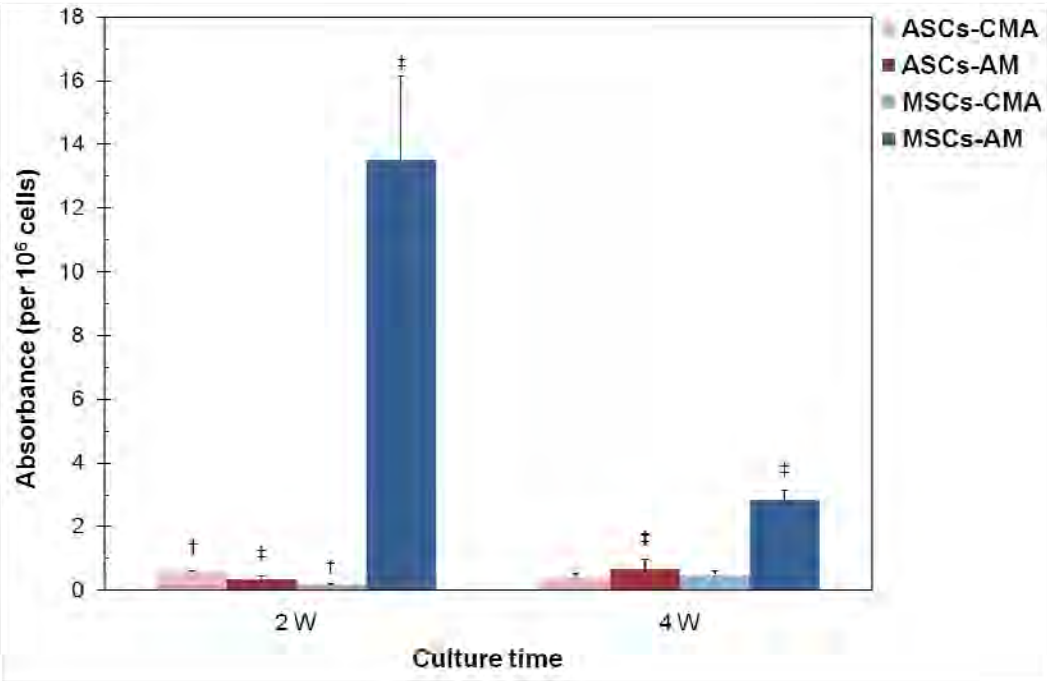

Figure 4.7 Absorbance of Oil red O stained ASCs and MSCs culture on 6-well tissue culture plates for 2 and 4 weeks under control medium of adipogenic differentiation (CMA: 199 medium, 10% FBS) and adipogenic medium (AM: DME/Ham's F12 medium containing 0.05 μM insulin, 0.2 nM 3,5,3'-triiodothyronine, 100 nM transferring, 17 μM calcium pantotenate, 33 μM biotin and 100 nM dexamethasone), († and ‡ represented a significant difference between ASCs and MSCs cultured in the same medium and culture period at $p<0.05$).

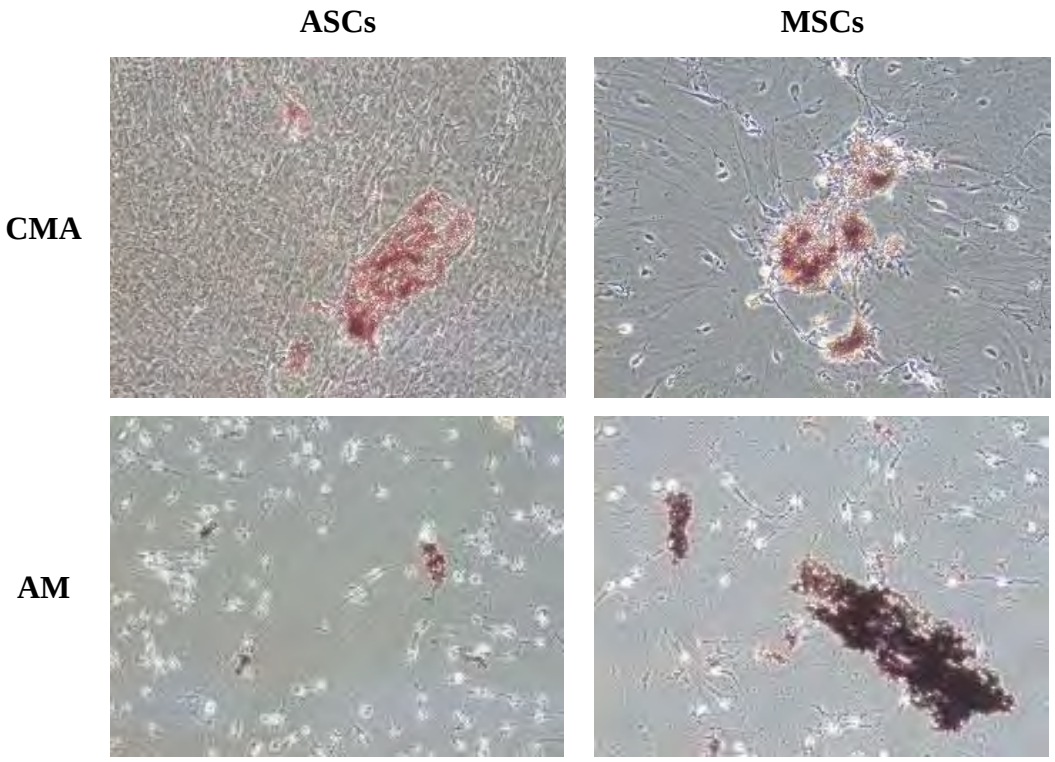

Figure 4.8 Lipid droplet formation of ASCs and MSCs culture on 6-well tissue culture plates for 4 weeks under control medium of adipogenic differentiation (CMA: 199 medium, 10% FBS) and adipogenic medium (AM: DME/Ham's F12 medium containing 0.05 μM insulin, 0.2 nM 3,5,3'-triiodothyronine, 100 nM transferring, 17 μM calcium pantotenate, 33 μM biotin and 100 nM dexamethasone), stained by Oil red O.

In the aspect of osteogenic differentiation test, both ASCs and MSCs were cultured on tissue culture plates under osteogenic medium (OM: α-MEM, 10% FBS, 10 mM β-glycerol phosphate, 50 μg/ml L-ascorbic acid and 10 nM dexamethasone) for 1, 2 and 4 weeks, compared to those cultured under control medium of osteogenic differentiation (CM: α-MEM, 10% FBS). The number of both cells at 1, 2 and 4 weeks of osteogenic culture assessed by DNA assay was shown in Figure 4.9. At the first week of the culture, the number of ASCs in CM was higher than others, indicating the lower osteogenic differentiation than other groups. During 2- to 4-week culture, the number of MSCs in OM was lowest. This implied the highest potential of osteogenic differentiation of MSCs in OM, comparing to other groups. Alkaline phosphatase (ALP) activity of ASCs and MSCs cultured under the same condition was assessed and presented in Figure 4.10. ALP activity is a marker of early osteogenic differentiation which can be detected after several days of osteogenic culture (Arpornmaeklong et al., 2007). It was clearly noticed from the results of this study that MSCs in both OM and CM produced high amount of ALP activity while ASCs in both medium types showed very low ALP activity. Particularly, MSCs cultured in OM showed highest ALP production. Furthermore, an increase in ALP activity of MSCs in both OM and CM were observed along the increased culture period.

Deposition of calcium is defined as late osteogenic differentiation stage and can normally be quantified after 15 days of osteogenic culture (Arpornmaeklong et al., 2007). Calcium content of ASCs and MSCs cultured under the same condition was presented in Figure 4.11. Small amount of calcium was noticed after the first week of MSCs cultured in OM. Calcium content of MSCs in OM rapidly increased after 2 and 4 weeks of culture. Also, calcium content of MSCs in CM was just detectable after 4-week culture. In addition, ASCs cultured in both medium types showed very low calcium production, corresponding to the ALP results. Calcium deposition of both cells was confirmed by Von Kossa staining as seen in Figure 4.12. Dark brown color was observed only in the case of MSCs cultured in OM. Also, MSCs cultured in CM for 4 weeks deposited some amount of calcium as seen from light brown color. In contrast, calcium deposition of ASCs in both medium types was not observed along culture period. The qualitative result on calcium deposition by

Von Kossa staining was in good agreement with the quantitative result on calcium content described earlier.

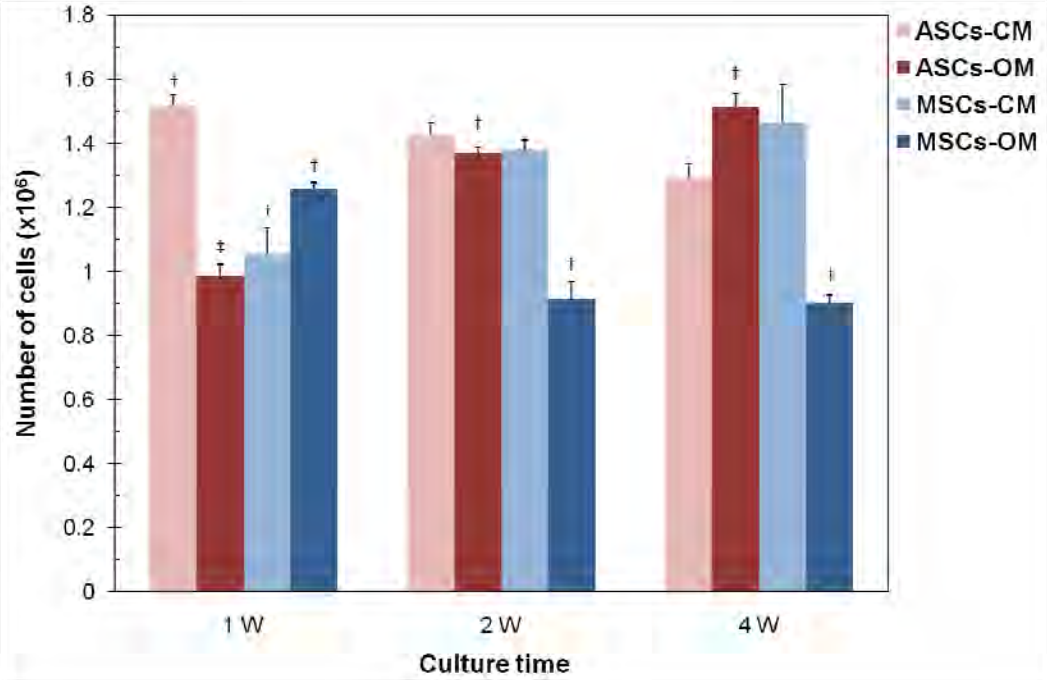

Figure 4.9 Number of ASCs and MSCs culture on 6-well tissue culture plates for 1, 2 and 4 weeks under control medium of osteogenic differentiation (CM: α-MEM, 10% FBS) and osteogenic medium (OM: α-MEM, 10% FBS, 10 mM β-glycerol phosphate, 50 μg/ml L-ascorbic acid and 10 nM dexamethasone), assessed by DNA assay († and ‡ represented a significant difference between ASCs and MSCs cultured in the same medium and culture period at $p<0.05$).

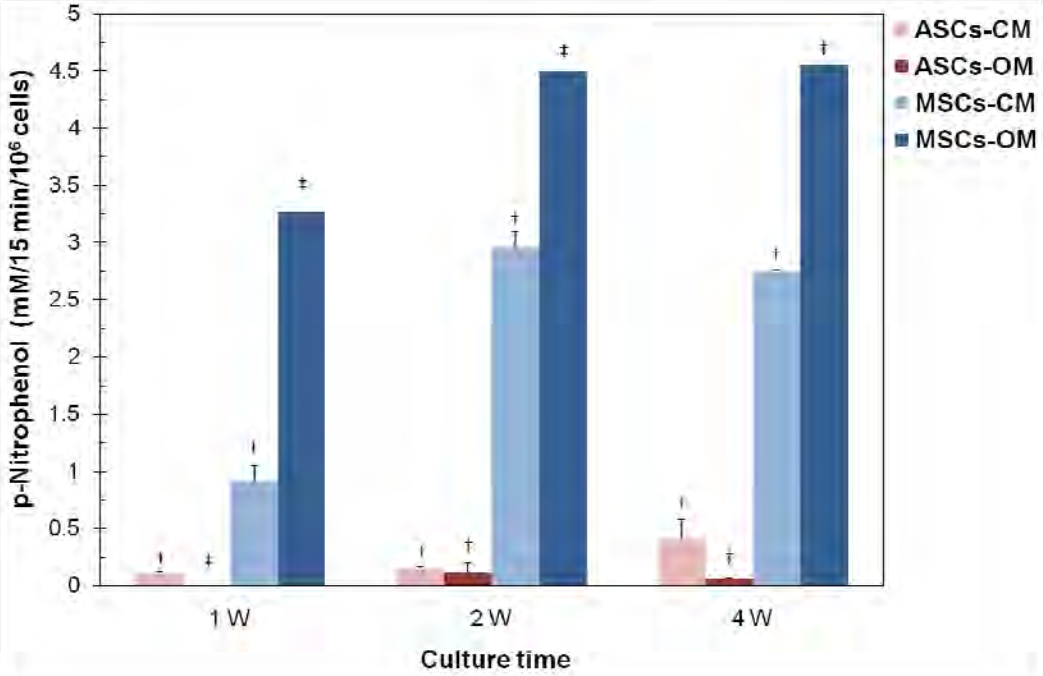

Figure 4.10 Alkaline phosphatase (ALP) activity of ASCs and MSCs culture on 6-well tissue culture plates for 1, 2 and 4 weeks under control medium of osteogenic differentiation (CM: α-MEM, 10% FBS) and osteogenic medium (OM: α-MEM, 10% FBS, 10 mM β-glycerol phosphate, 50 μg/ml L-ascorbic acid and 10 nM dexamethasone), († and ‡ represented a significant difference between ASCs and MSCs cultured in the same medium and culture period at $p<0.05$).

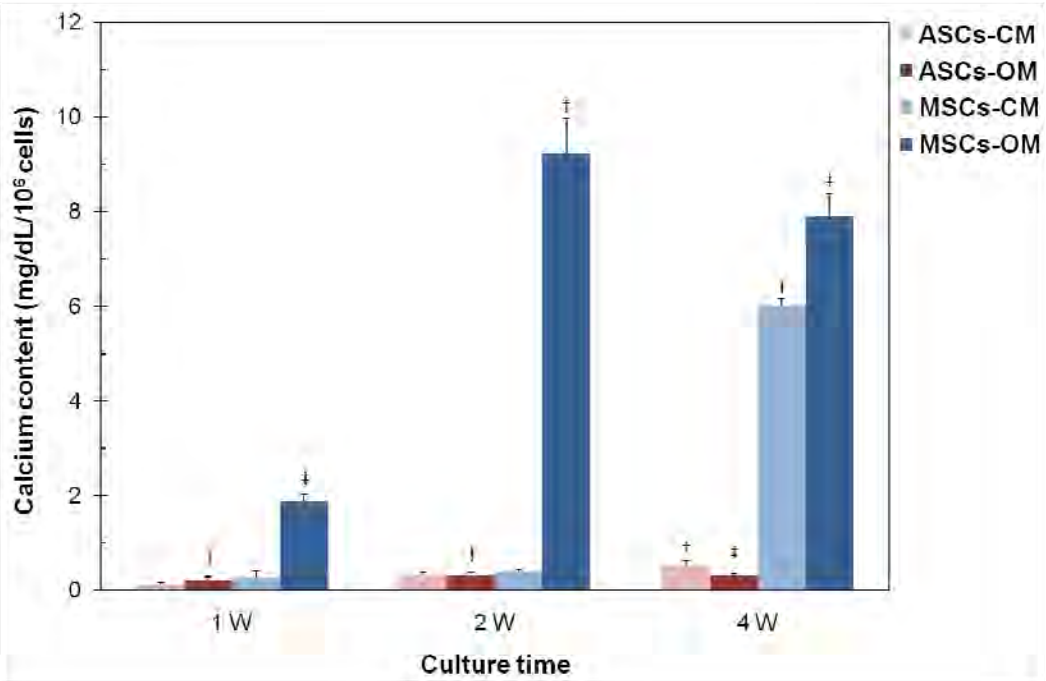

Figure 4.11 Calcium content of ASCs and MSCs culture on 6-well tissue culture plates for 1, 2 and 4 weeks under control medium of osteogenic differentiation (CM: α-MEM, 10% FBS) and osteogenic medium (OM: α-MEM, 10% FBS, 10 mM β-glycerol phosphate, 50 μg/ml L-ascorbic acid and 10 nM dexamethasone), († and ‡ represented a significant difference between ASCs and MSCs cultured in the same medium and culture period at $p<0.05$).

Culture time	Medium type	ASCs	MSCs
1 W	CM	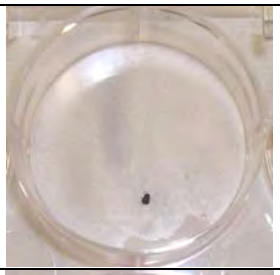	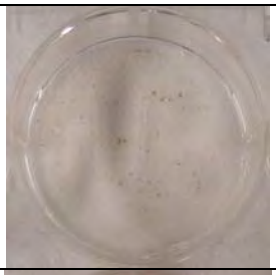
	OM		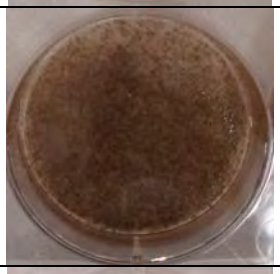
2 W	CM		
	OM	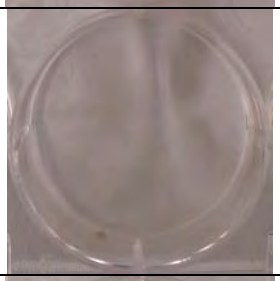	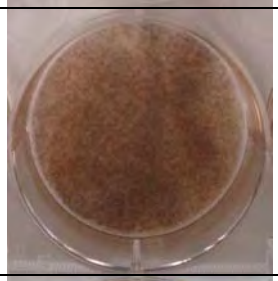
4 W	CM	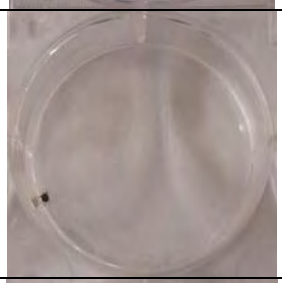	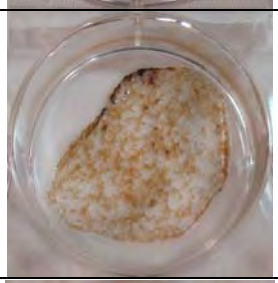
	OM		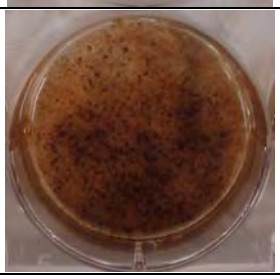

Figure 4.12 Calcium deposition of ASCs and MSCs culture on 6-well tissue culture plates for 1, 2 and 4 weeks under control medium of osteogenic differentiation (CM: α-MEM, 10% FBS) and osteogenic medium (OM: α-MEM, 10% FBS, 10 mM β-glycerol phosphate, 50 µg/ml L-ascorbic acid and 10 nM dexamethasone), stained by Von Kossa.

4.6 In vitro biological characteristics of two-dimensional G/COS and G/CH films with rat ASCs and MSCs

Films of G/COS and G/CH at different blending ratios (100/0, 90/10, 70/30, 50/50, 30/70 and 0/100) were tested with rat ASCs and MSCs in order to investigate cell spreading, proliferation and osteogenic differentiation. Surface properties and some biological characteristics of the films were also evaluated to explain the results on cell response.

4.6.1 Attachment and proliferation of ASCs and MSCs on two-dimensional G/COS and G/CH films

The systems of G/COS, G/CH12 and G/CH1000 films at different blending ratios were comparatively examined for attachment and proliferation of rat ASCs and MSCs. Behavior of both stem cells on all films was compared under the same culture condition (i.e. medium type and culture period). The number of cells attached and proliferated on G/COS, G/CH12 and G/CH1000 films was shown in Figure 4.13-4.15, respectively. From the results, it was observed that both ASCs and MSCs preferred to attach and proliferated on the blended films, particularly the films containing 70% chitosan. This might suggest the optimum ratio of the DHT-crosslinked gelatin/chitosan films which was the most suitable to promote cell activities, regardless of chitosan molecular weight. Furthermore, the difference in cell affinity between pure COS and chitosan films was noticed. Pure COS films could promote attachment and proliferation of both cells as good as the pure gelatin film while pure CH12 and CH1000 films did not support both cell attachment and proliferation. Only slight increase in cell number on pure CH12 and CH1000 films was observed after 5-day culture. The diversity of cell behavior on the systems of low molecular weight CH12 and high molecular weight CH1000 could not be detected in this work. Therefore, only the system of G/CH1000 films was selected for further biological characterization comparing to the system of G/COS films. Form this comparative study, CH1000 (MW 1,000 kDa) would serve as a representative of chitosan in which its molecular weight was almost a 1000-time higher than that of COS (MW 1.4 kDa).

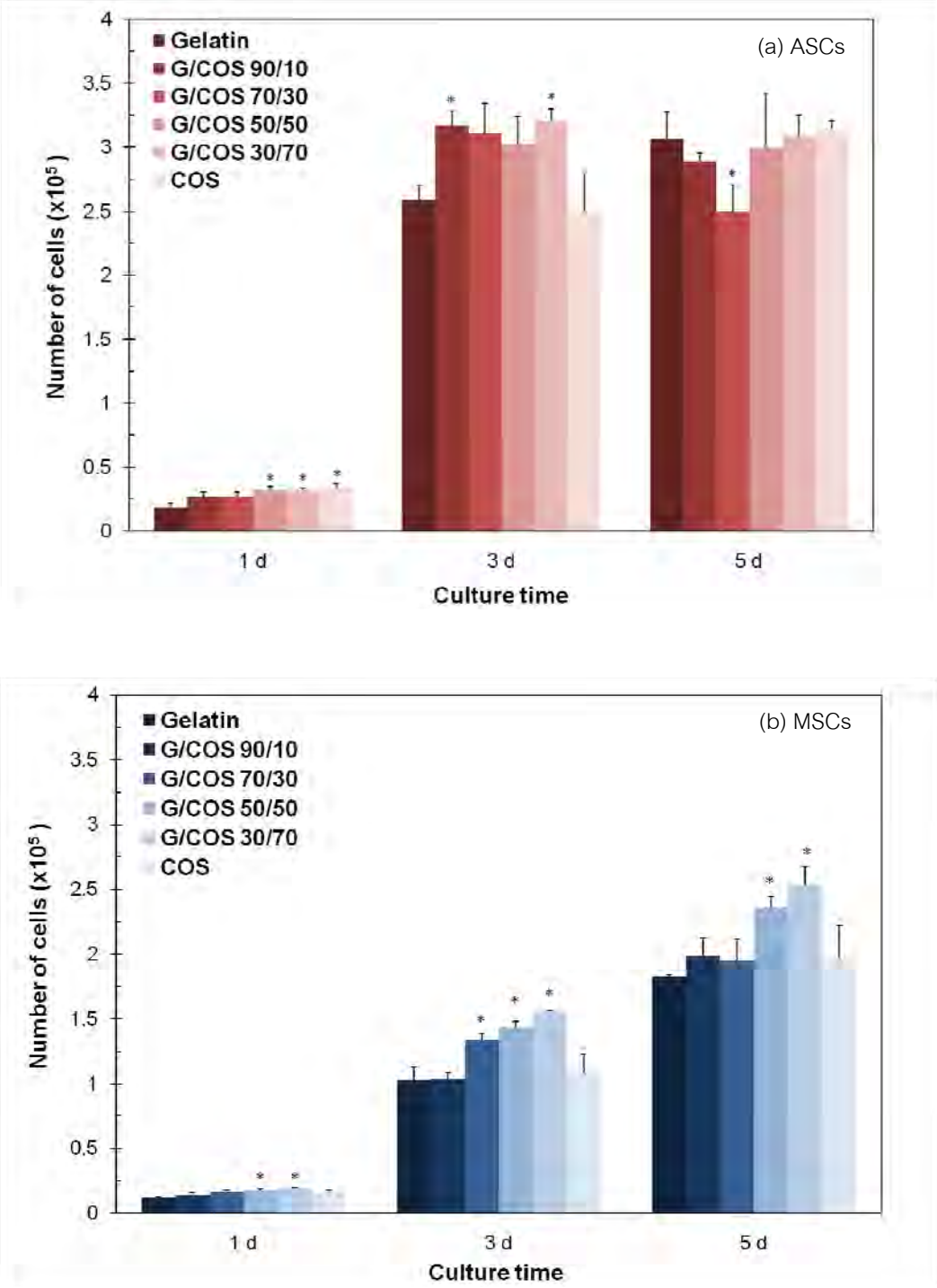

Figure 4.13 Number of (a) ASCs and (b) MSCs attached and proliferated on G/COS films at different blending ratios cultured in α-MEM + 15% FBS, assessed on the 1st, 3rd and 5th days after seeding by MTT assay (seeding: $2x10^4$ cells/film, * represented a significant difference relative to gelatin within same culture period at $p<0.05$).

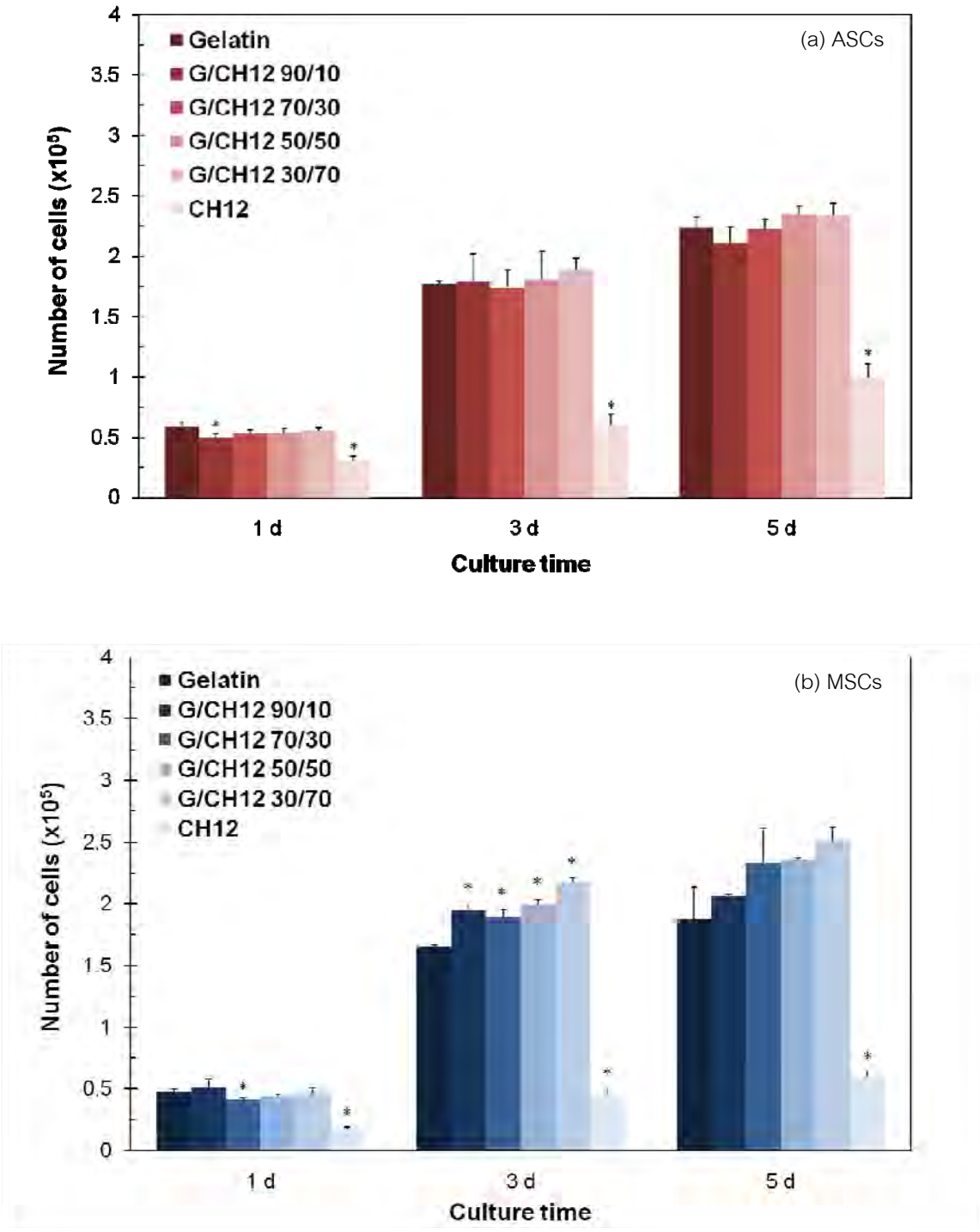

Figure 4.14 Number of (a) ASCs and (b) MSCs attached and proliferated on G/CH12 films at different blending ratios cultured in α-MEM + 15% FBS, assessed on the 1st, 3rd and 5th days after seeding by MTT assay (seeding: $2x10^4$ cells/film, * represented a significant difference relative to gelatin within same culture period at $p<0.05$).

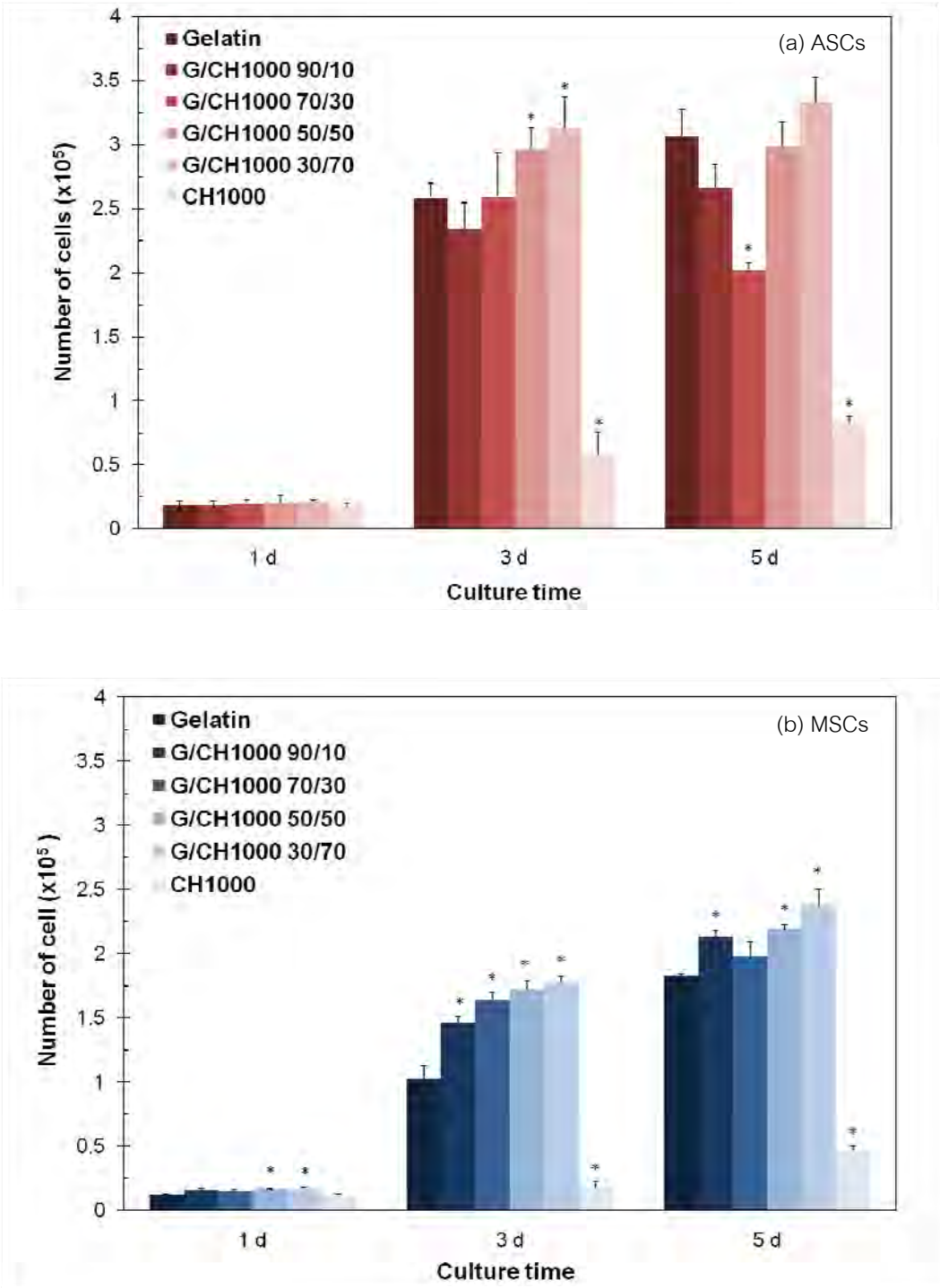

Figure 4.15 Number of (a) ASCs and (b) MSCs attached and proliferated on G/CH1000 films at different blending ratios cultured in α-MEM + 15% FBS, assessed on the 1st, 3rd and 5th days after seeding by MTT assay (seeding: $2x10^4$ cells/film, * represented a significant difference relative to gelatin within same culture period at $p<0.05$).

4.6.2 Cell immunostaining and spreading observation

Spreading and morphology of both ASCs and MSCs attached on G/COS and G/CH1000 films at 1 day after seeding were demonstrated in Figure 4.16-4.17. It could be seen that both cells could spread well on gelatin, G/COS 30/70, COS and G/CH1000 30/70 films. Also, spreading of filamentous actin was clearly observed in the cases of cells attached on the blended G/COS and G/CH1000 films, as shown in Figure 4.16 (c, d, g, h). On the other hand, morphology of both cells attached on pure CH1000 film remained round-shaped, as seen in Figure 4.16 (i, j) and 4.17 (i, j). The quantitative spreading area of both ASCs and MSCs on the films presented in Table 4.4 indicated that cells tended to have larger area on the blended G/COS and G/CH1000 films, particularly for the films containing 70% COS and CH1000. The results on cell spreading area corresponded to the results on cell number presented in Figure 4.13 and 4.15. This confirmed the optimum ratio of the DHT-crosslinked gelatin/chitosan films at 30/70 for cell activities. Wang et al. (2009) have studied the composite of chitosan/gelatin solutions and films formed from these solutions. It was found that the complex formed between chitosan and gelatin was mainly through hydrogen bond. The optimal chitosan ratio for the maximum elongation, measured by the tensile test in the swollen state, was at 69% by weight. This value was very close to the suitable blending ratio suggested from this study (70% by weight) which presented greatest cell attachment and proliferation.

Comparing between ASCs and MSCs, attachment and proliferation behaviors of both cells on each material were similar. However, ASCs showed slightly higher proliferative rate than MSCs under the same culture condition. Spreading area of both cells attached on the films was not noticeably different but that depended mainly on material types.

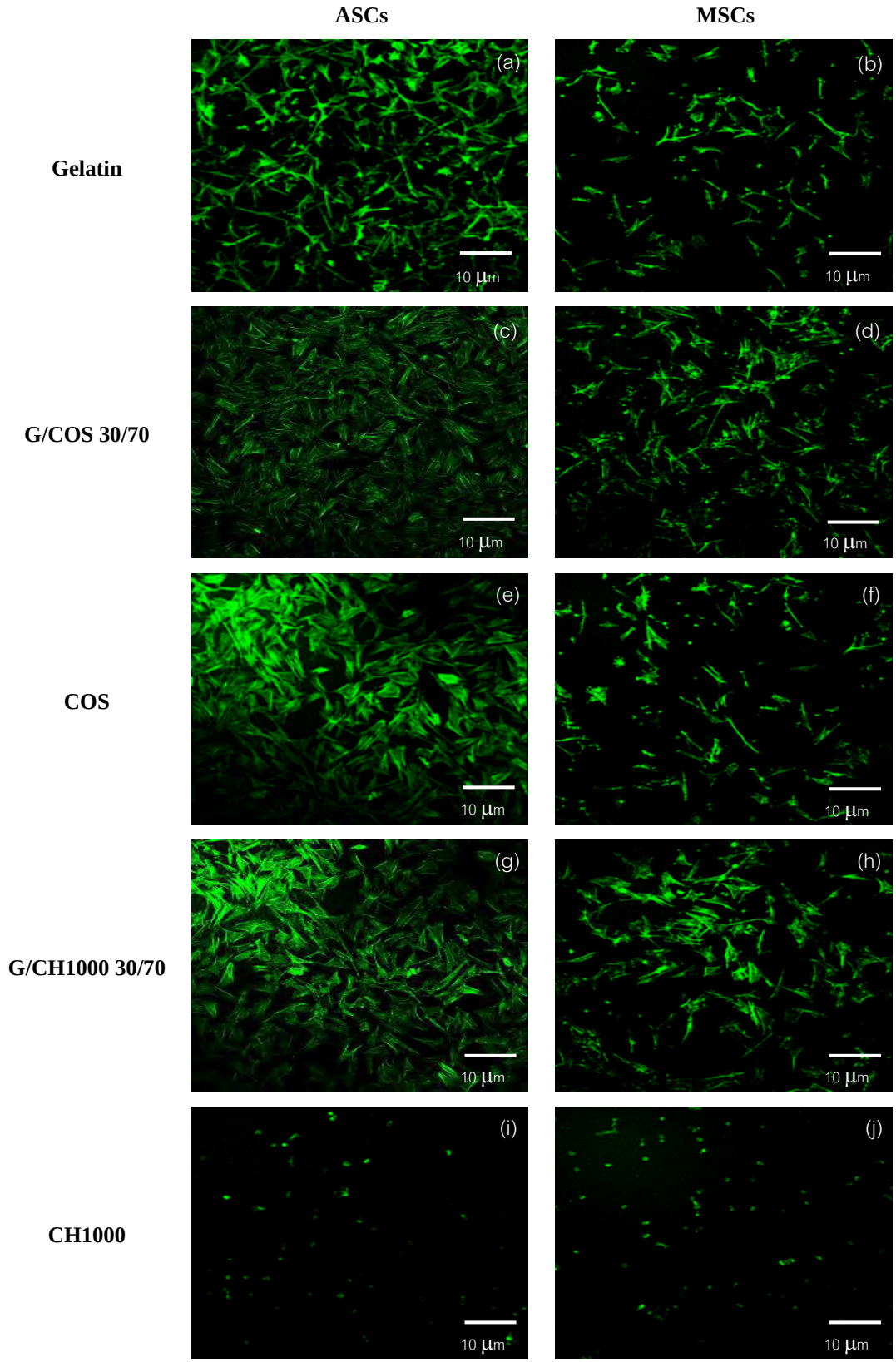

Figure 4.16 Spreading morphology of ASCs and MSCs on different films observed on the 1st day after seeding under a confocal fluorescence microscope after FITC-conjugated phalloidin immunostaining (a, b) Gelatin, (c, d) G/COS 30/70, (e, f) COS, (g, h) G/CH1000 30/70, and (i, j) CH1000.

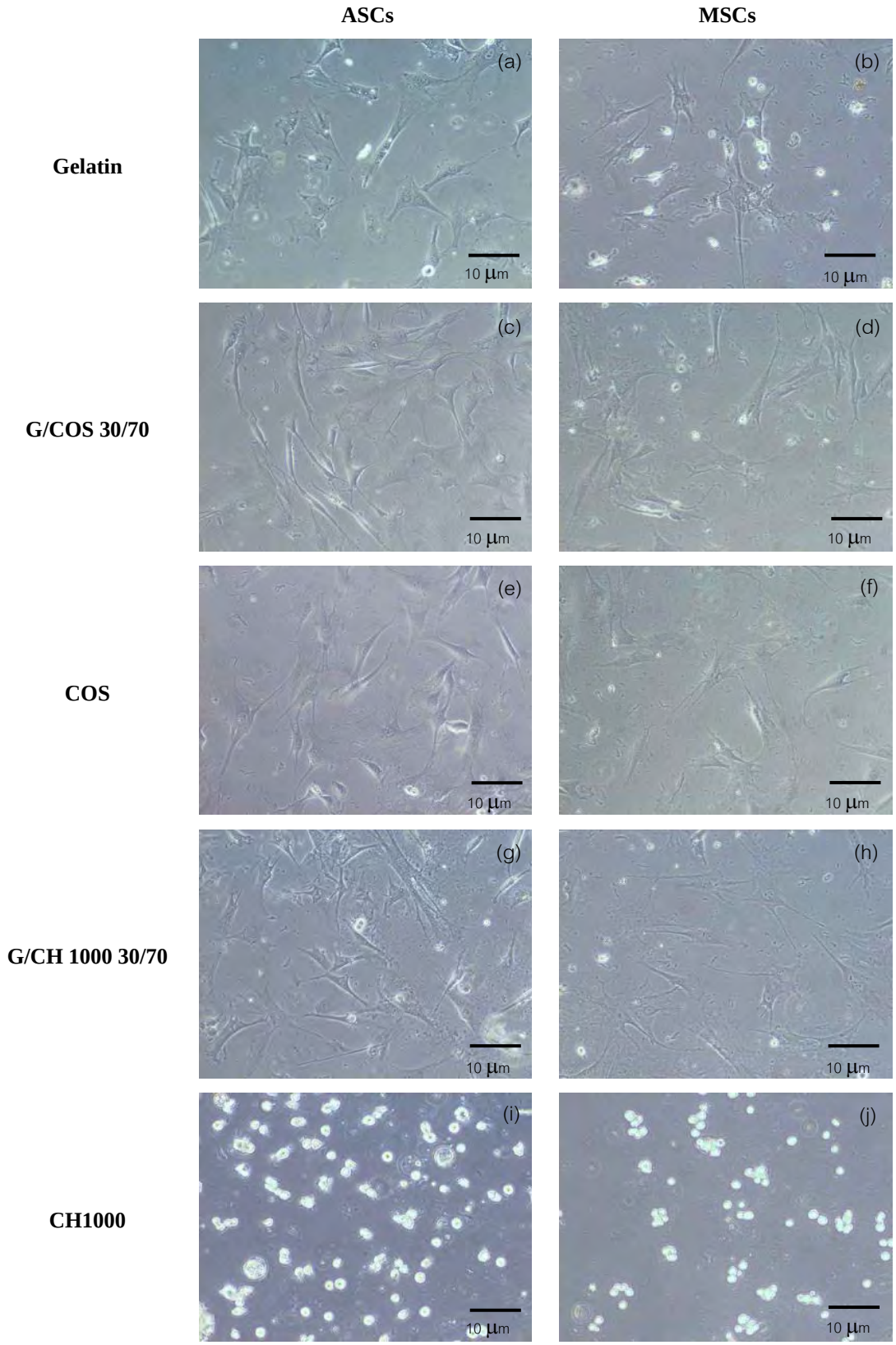

Figure 4.17 Spreading morphology of ASCs and MSCs on different films observed on the 1st day after seeding under a phase-contrast microscope at 10X magnification (a, b) Gelatin, (c, d) G/COS 30/70, (e, f) COS, (g, h) G/CH1000 30/70, and (i, j) CH1000.

Table 4.4 Spreading area of ASCs and MSCs attached on G/COS and G/CH1000 films at different blending ratios measured on the 1st day after seeding.

	Spreading area (μm^2)	
	ASCs	**MSCs**
Glass slip	77.04 ± 14.43	63.38 ± 13.51
Gelatin	66.54 ± 13.75	45.17 ± 8.66
G/COS 90/10	73.46 ± 13.43[a]	53.77 ± 10.9[a]
G/COS 70/30	82.46 ± 17.73[a]	91.44 ± 18.69[a]
G/COS 50/50	82.16 ± 14.53[a]	99.90 ± 19.99[a]
G/COS 30/70	85.23 ± 15.49[a]	99.32 ± 18.06[a]
COS	88.37 ± 17.90[a]	69.73 ± 15.95[a]
G/CH1000 90/10	65.18 ± 15.02	66.45 ± 14.95[a]
G/CH1000 70/30	71.12 ± 13.13[a]	65.61 ± 12.37[a]
G/CH1000 50/50	66.40 ± 11.71	83.52 ± 16.78[a]
G/CH1000 30/70	77.50 ± 13.67[a]	97.91 ± 21.13[a]
CH1000	12.98 ± 3.20[a]	12.72 ± 3.84[a]

[a] represented a significant difference relative to gelatin film at $p<0.01$

4.6.3 Osteogenic differentiation of ASCs and MSCs on two-dimensional G/COS and G/CH films

In addition to spreading, attachment and proliferation behaviors, osteogenic differentiation of ASCs and MSCs on G/COS and G/CH1000 films was also studied. The number of both cells cultured on the films under osteogenic medium for 7 days was presented in Figure 4.18. It was also found that the cell growth on the blended films under osteogenic induction was slightly better than that on the pure films. Moreover, pure CH1000 film did not support the growth of both cells under osteogenic induction. ALP activity of both cells cultured on G/COS and G/CH1000 films under osteogenic medium for 7 days was elucidated in Figure 4.19. In term of materials, the blended G/COS and G/CH1000 films significantly enhanced ALP production of MSCs, comparing to the pure gelatin, COS and CH1000 films. However, the optimum ratio of gelatin/chitosan that supported osteogenic differentiation of MSCs could not be noticed. Calcium content of ASCs and MSCs cultured on the films under osteogenic medium for 7 days shown in Figure 4.20 represented that both cells cultured on the blended, pure COS and CH1000 films showed higher calcium content than those on pure gelatin film. The result on calcium content was confirmed by Von Kossa staining of calcium deposition, as shown in Figure 4.21. After 7-day cultured in osteogenic medium, MSCs on the blended and pure COS films deposited high calcium, as seen from dark brown stained. In term of cells, a great difference in osteogenic differentiation potential between ASCs and MSCs was clearly observed. MSCs cultured on all film types under osteogenic medium could produce significantly higher ALP and calcium than ASCs.

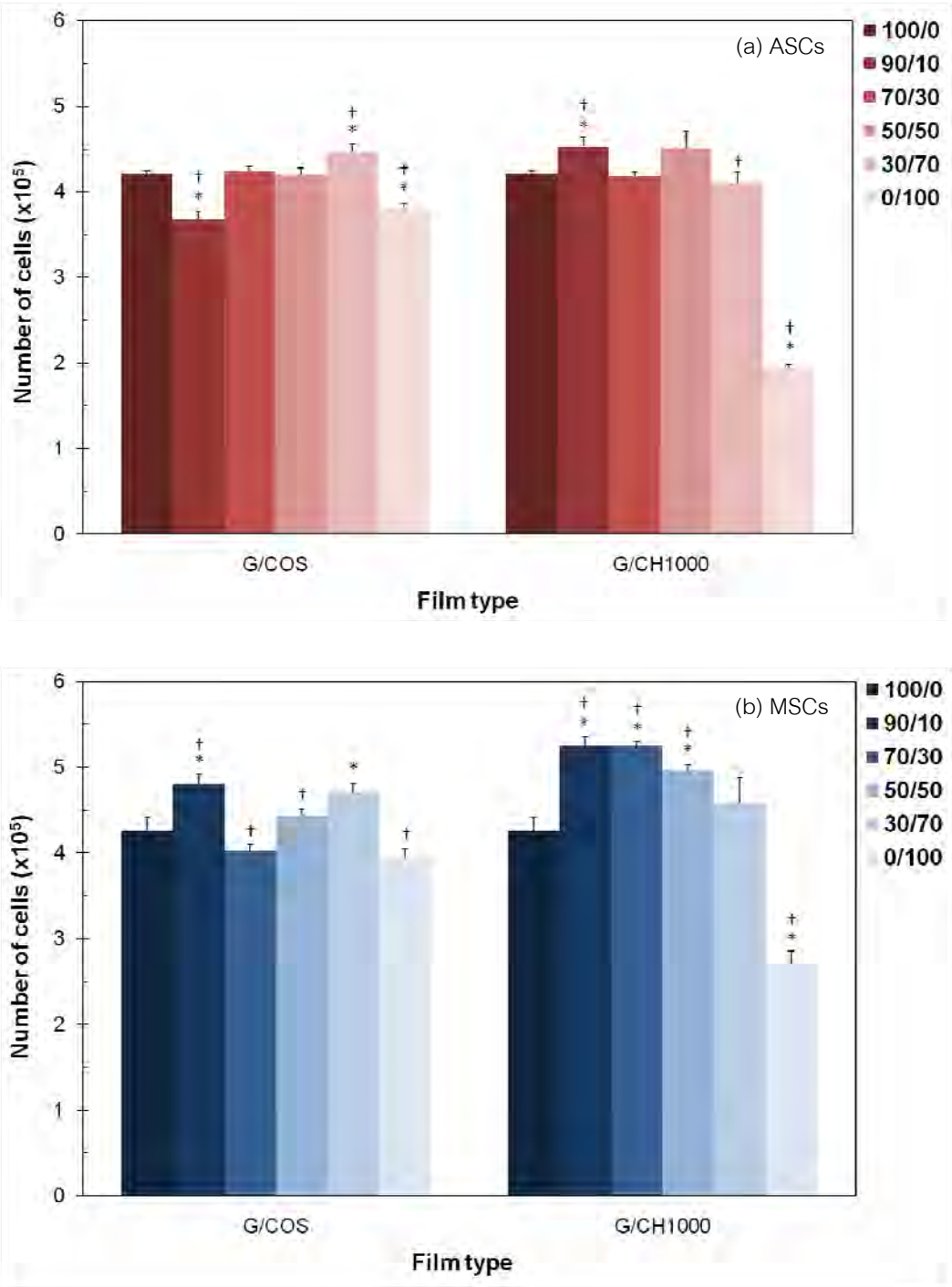

Figure 4.18 Number of (a) ASCs and (b) MSCs on G/COS and G/CH1000 films at different blending ratios cultured in osteogenic medium (OM: α-MEM, 10% FBS, 10 mM β-glycerol phosphate, 50 µg/ml L-ascorbic acid and 10 nM dexamethasone) for 7 days, assessed by DNA assay (seeding: $2x10^4$ cells/cm^2, * represented a significant difference relative to gelatin within the same group at $p<0.05$, † represented a significant difference between G/COS and G/CH1000 at same blending ratio at $p<0.05$).

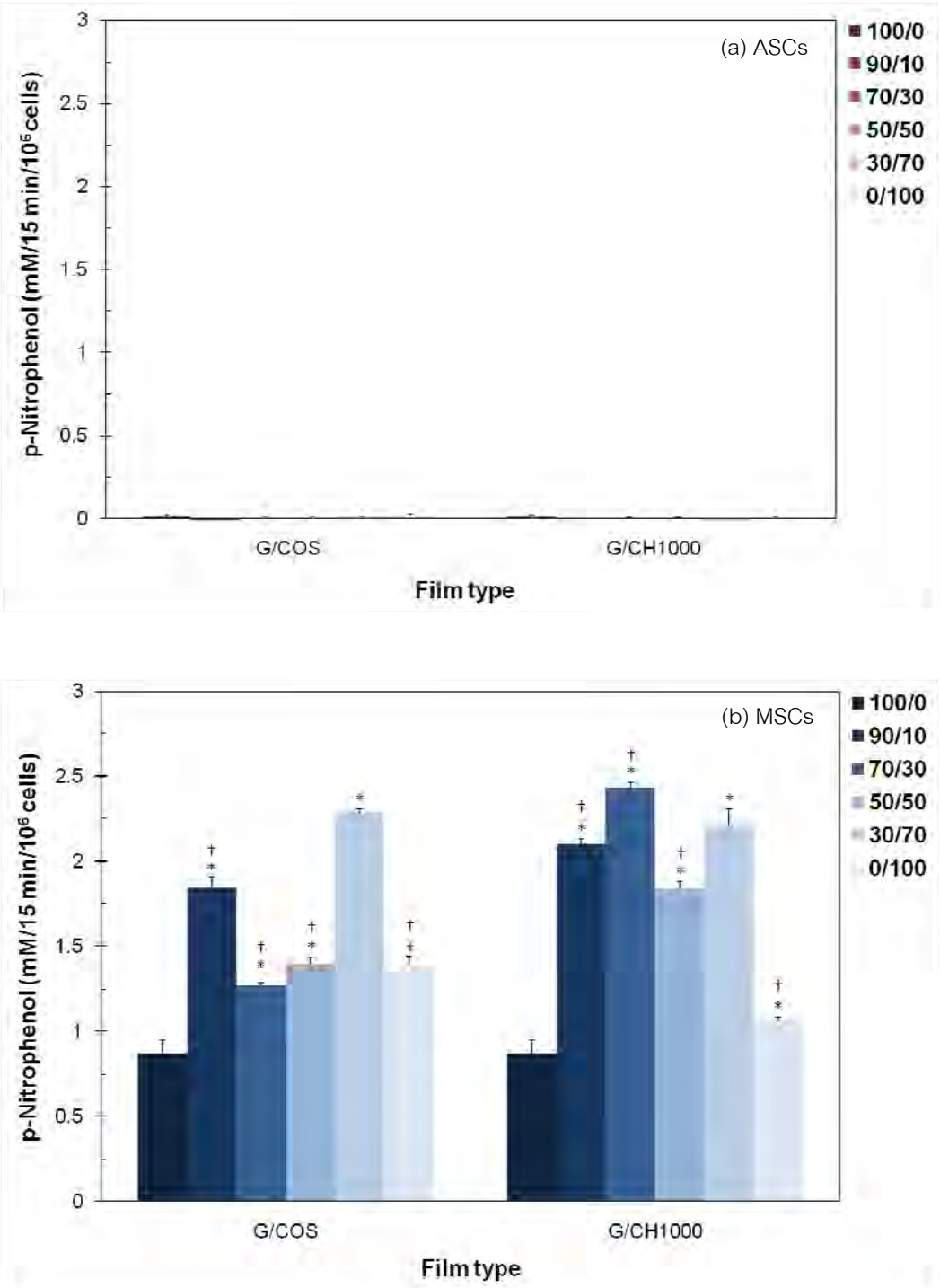

Figure 4.19 ALP activity of (a) ASCs and (b) MSCs on G/COS and G/CH1000 films at different blending ratios cultured in osteogenic medium (OM: α-MEM, 10% FBS, 10 mM β-glycerol phosphate, 50 μg/ml L-ascorbic acid and 10 nM dexamethasone) for 7 days (seeding: $2x10^4$ cells/cm^2, * represented a significant difference relative to gelatin within the same group at $p<0.05$, † represented a significant difference between G/COS and G/CH1000 at same blending ratio at $p<0.05$).

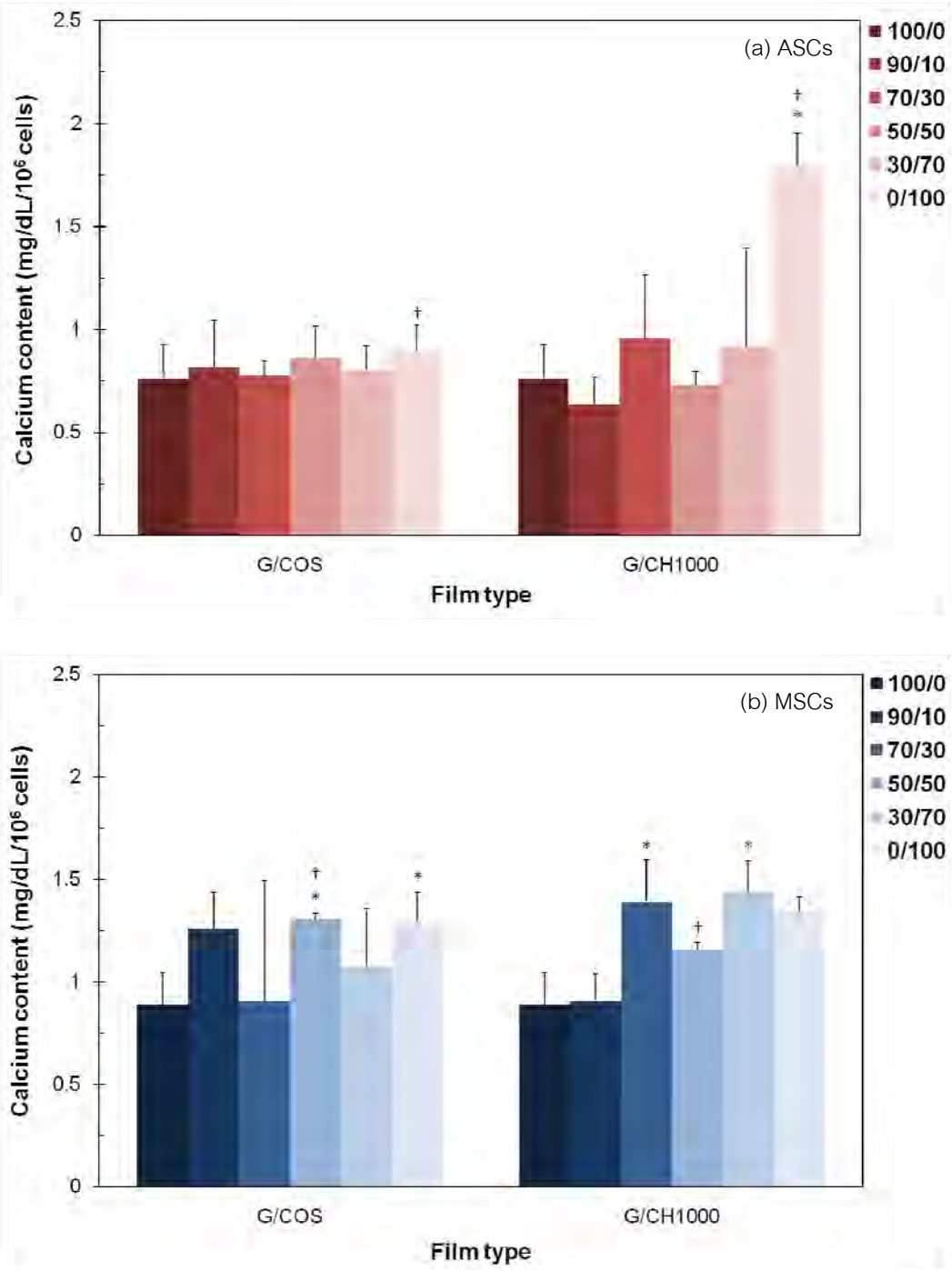

Figure 4.20 Calcium content of (a) ASCs and (b) MSCs on G/COS and G/CH1000 films at different blending ratios cultured in osteogenic medium (OM: α-MEM, 10% FBS, 10 mM β-glycerol phosphate, 50 μg/ml L-ascorbic acid and 10 nM dexamethasone) for 7 days (seeding: $2x10^4$ cells/cm^2, * represented a significant difference relative to gelatin within the same group at $p<0.05$, † represented a significant difference between G/COS and G/CH1000 at same blending ratio at $p<0.05$).

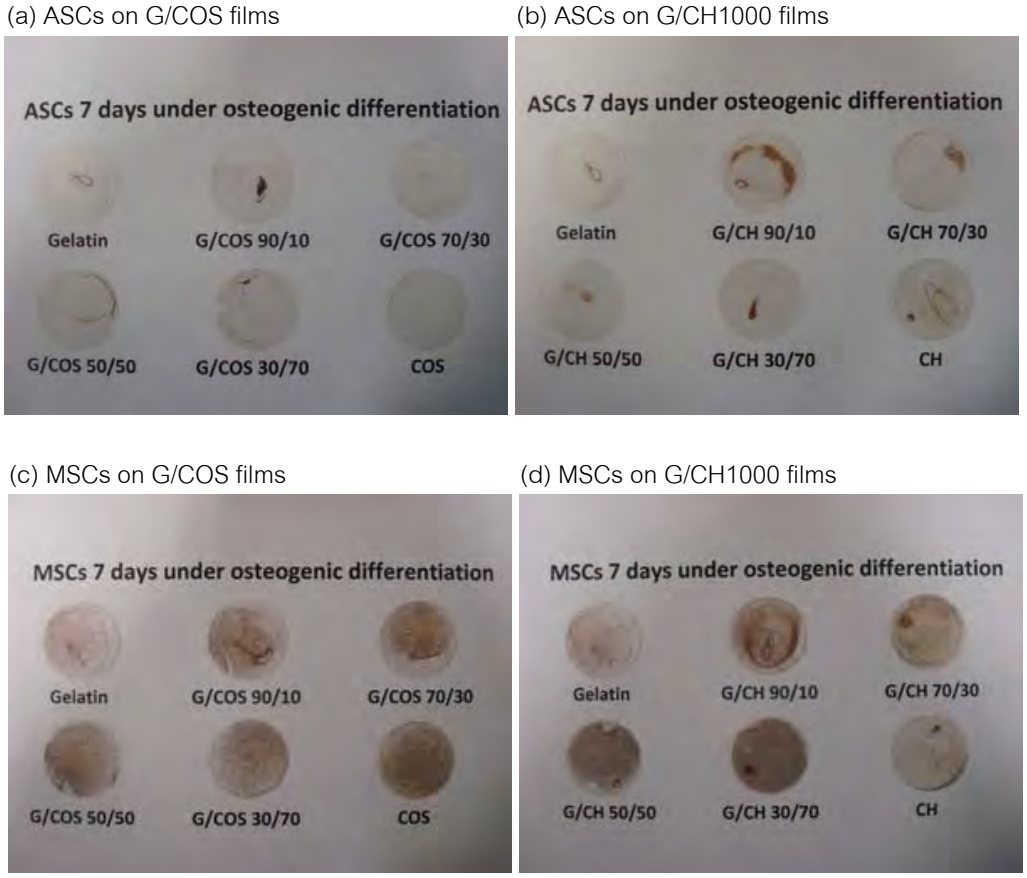

Figure 4.21 Calcium deposition of (a) ASCs on G/COS films, (b) ASCs on G/CH1000 films, (c) MSCs on G/COS films and (d) MSCs on G/CH1000 films at different blending ratios cultured in osteogenic medium (OM: α-MEM, 10% FBS, 10 mM β-glycerol phosphate, 50 µg/ml L-ascorbic acid and 10 nM dexamethasone) for 7 days, stained by Von Kossa (seeding: $2x10^4$ cells/cm^2).

From the promising results on the enhanced biocompatibility and osteoconductive property of the blended films compared to the pure films, there were some possibilities to explain it. The first factor mediated was surface properties of the films, for example, hydrophobic/hydrophilic property, surface chemistry and charge. ***Hydrophobic/ hydrophilic property*** of the films was considered as an important factor favorable to cell adhesion, proliferation and differentiation (Krakovskýa et al., 2006). Water contact angle of the DHT-crosslinked G/COS and G/CH1000 films prepared at different blending ratios was first characterized. Water contact angle of the films as presented in Table 4.5 indicated that the crosslinked gelatin film was the most hydrophobic, as seen from the highest water contact angle (102.40°). Also, it was

noticed that water contact angle tended to decrease along the increasing of chitosan ratio, representing the more hydrophilic surface. Generally, gelatin is more hydrophilic and water-soluble than chitosan. However, in this study, the films were crosslinked by DHT treatment in which chemical bondings between the amino (NH_2) and carboxyl (COOH) groups were generated due to thermal dehydration (Weadock et al., 1996; Ueda et al., 2003; Ozeki & Tabata, 2005). The result of which is the formation of crosslinks via condensation reactions either by esterification or amide formation (Weadock et al., 1983; Haugh et al., 2006). Crosslinking by DHT treatment can occur only when NH_2 and COOH groups are close to each other (Ozeki & Tabata, 2005). Gelatin is a protein of which the structural unit consists of amino acids, mainly are glycine, proline and 4-hydroxylproline residues. Then, NH_2 and COOH groups are abundant in gelatin molecules. Chitosan is a linear polysaccharide consisting of N-acetyl-glucosamine and N-glucosamine as repeating units. NH_2 and hydroxyl (OH) groups are contained in chitosan molecules while the COOH group was absent. With this molecular aspect, gelatin molecules were expected to be crosslinked by DHT treatment more than the chitosan molecules, resulting in highest crosslinking extent and hydrophobicity of pure gelatin film comparing to the blended, pure COS and pure CH1000 films. The correlation between crosslinking extent and hydrophobicity of materials was previously described by several reports (Krakovskýa et al., 2006; Liu et al., 2007). However, in this case, we found that the hydrophobic/hydrophilic property of the film surfaces was not correlated to cell attachment and proliferation.

Table 4.5 Water contact angle of G/COS and G/CH1000 films at different blending ratios.

Blending ratio	Water contact angle (°)	
	G/COS	G/CH1000
100/0	102.40 ± 2.59	102.40 ± 2.59
90/10	97.63 ± 3.35	102.83 ± 1.65
70/30	97.83 ± 3.51	89.07 ± 11.25
50/50	91.70 ± 4.72[a]	79.83 ± 8.21[a]
30/70	88.43 ± 6.83	90.20 ± 6.46
0/100	81.97 ± 0.78[a]	92.50 ± 0.44[a]

[a] represented a significant difference relative to gelatin film at $p<0.05$

Surface chemistry of the films such as the presence of free amine (NH_2) and carboxyl (COOH) groups was also reported to affect cell affinity. Several works have shown that the interaction of COOH and NH_2 groups with the cell surface could promote cell activities (Keselowsky et al., 2003; Belmonte et al., 2005; Curran et al., 2005 & 2006). In this case, the blended G/CH1000 and G/COS films might introduce more free COOH and NH_2 groups than the pure crosslinked gelatin film and resulted in better cell attachment, proliferation and osteogenic differentiation. We then characterized surface elements including nitrogen (N), oxygen (O) and carbon (C) appeared on the film surfaces using XPS. The appearance of these elements could represent the amount of NH_2, COOH and OH on film surfaces. Atomic concentration of N, O and C and the ratio of N/O and N/C on the film surfaces were shown in Table 4.6. In this case, the difference in amount of each element on the pure gelatin and the blended films would not be much enough to be quantified by this technique. In general, theoretically quantitative result from XPS technique was not much reliable, especially when peaks of element on each surface had similar shape, as illustrated in Figure 4.22-4.24. Only the N peak of pure COS and CH1000 films showed noticeable difference in shape compared to the other films, resulting in a detectably low nitrogen element (representing NH_2 group) on such surfaces. On the other hand, elemental peaks of pure gelatin and all blended films were similar, thus the quantitative results obtained from those films were not noticeably different. It was then hard to summarize that free NH_2 and COOH groups on the blended film surfaces accounted for cell attachment, proliferation and osteogenic differentiation in this study.

(a)

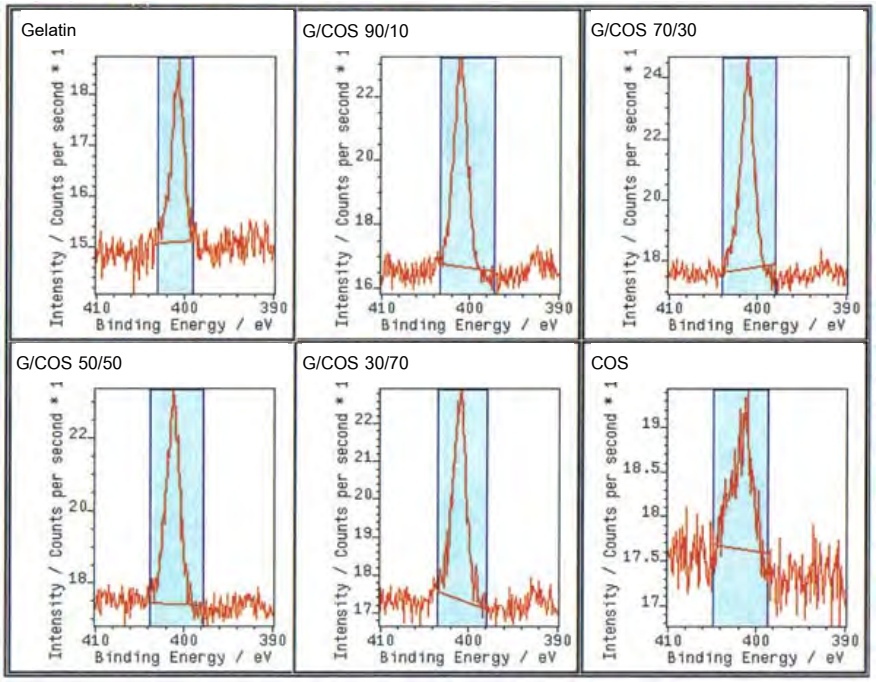

(b)

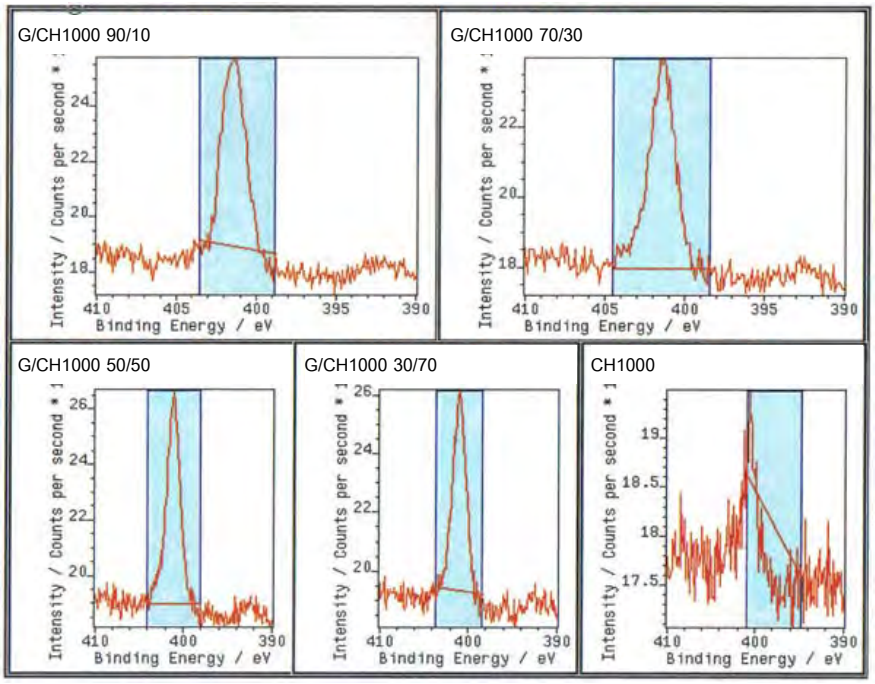

Figure 4.22 Intensity of nitrogen (N) on (a) G/COS and (b) G/CH1000 film surfaces at different blending ratios, analyzed by XPS.

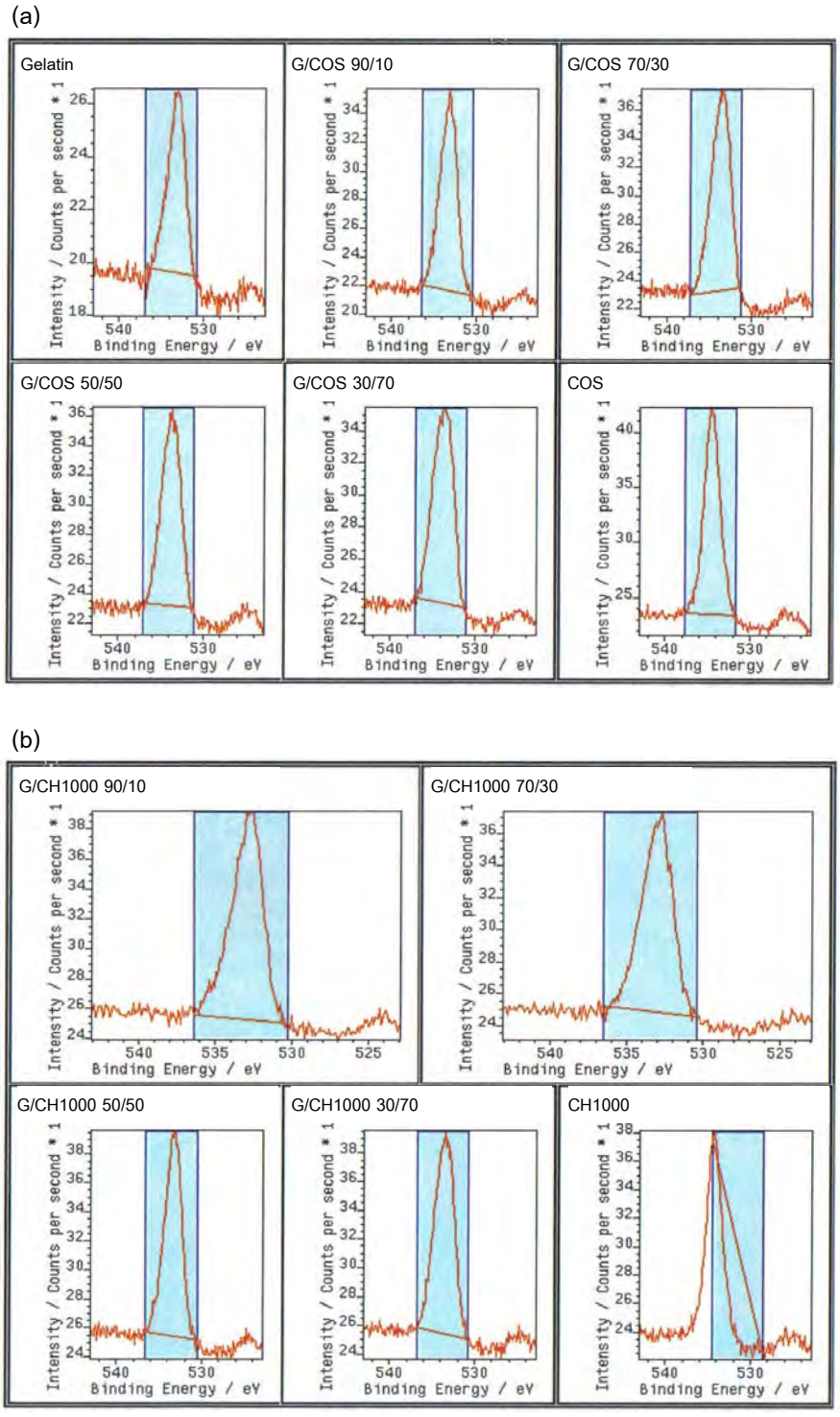

Figure 4.23 Intensity of oxygen (O) on (a) G/COS and (b) G/CH1000 film surfaces at different blending ratios, analyzed by XPS.

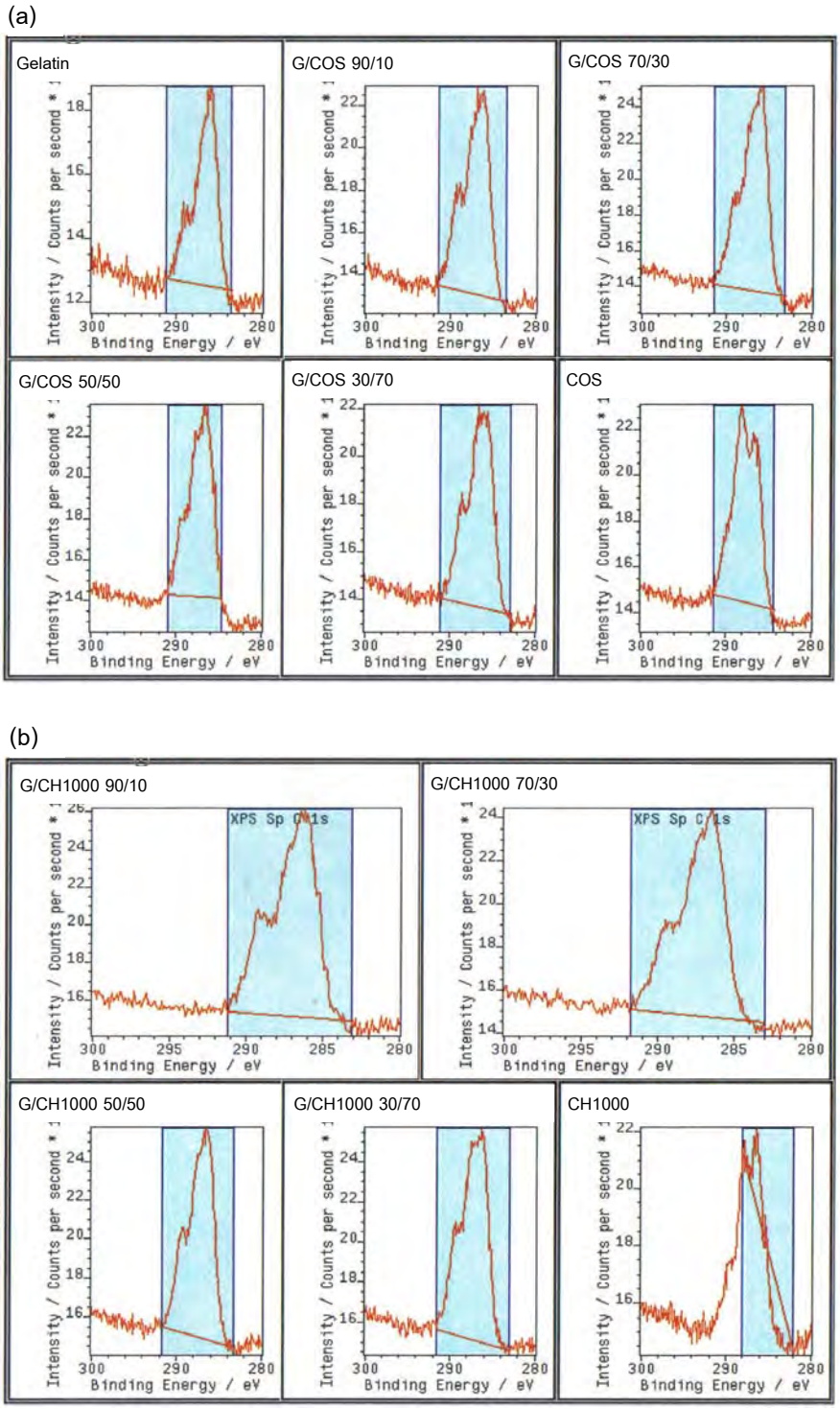

Figure 4.24 Intensity of carbon (C) on (a) G/COS and (b) G/CH1000 film surfaces at different blending ratios, analyzed by XPS.

Table 4.6 Atomic concentration of N, O, C and the ratios of N/O and N/C of G/COS and G/CH1000 film surfaces at different blending ratios quantified by XPS.

	Atomic concentration (%)			Ratio	
	N	**O**	**C**	**N/O**	**N/C**
Gelatin	12.10	22.54	65.35	0.537	0.185
G/COS 90/10	12.80	22.63	64.57	0.566	0.198
G/COS 70/30	11.12	22.66	66.23	0.491	0.168
G/COS 50/50	12.52	26.25	61.23	0.477	0.204
G/COS 30/70	12.25	26.35	61.40	0.465	0.200
COS	4.27	33.48	62.24	0.128	0.069
G/CH1000 90/10	11.28	22.75	65.97	0.496	0.171
G/CH1000 70/30	13.97	21.59	64.44	0.647	0.217
G/CH1000 50/50	13.63	21.41	64.96	0.637	0.210
G/CH1000 30/70	11.28	23.29	65.44	0.484	0.172
CH1000	3.65	30.47	65.88	0.120	0.055

Another surface property known to strongly influence the biological activities is the ***surface charge of material*** reported in term of zeta *(ζ)* potential. In this work, zeta potential of DHT-crosslinked gelatin, G/CH1000 30/70 and CH1000 films was analyzed. As shown in Table 4.7, net positive charge was found on the films of pure gelatin (+4.61 mV) and G/CH1000 30/70 (+9.00 mV). In contrast, crosslinked CH1000 film presented negative charge (-32.69 mV). It was interesting that positively charged chitosan solution should give positively charged chitosan film. The charge of non-crosslinked CH1000 film was then checked as comparatively shown in Table 4.7. It was noted that non-crosslinked CH1000 film presented positive charge as theoretically expected. Zeta potential recorded for crosslinked CH1000 could be considered to be a result of the protonation/deprotonation features of amine groups, resulted in dominant negative charge on CH1000 film surface. Zhao et al. (2008) also found that irradiation-crosslinked carboxymethyl chitosan showed negative charge depending strongly on its pH. From the results, it was no doubt that mild positive charge of DHT-crosslinked gelatin and G/CH1000 30/70 surfaces could well promote cell adhesion. Negatively charged cell surfaces would interact well with positively charged materials. Also, higher positive charge would introduce stronger interaction between material and cell surfaces. However, it is likely that there is a

critical value of the surface charge for cell adhesion. Kishida et al. (1991) have found that HeLa S3 cells could not live on highly positively charged surfaces, approximately higher than +17 mV. Therefore, mild positive charge approximately in the range of +4 to +9 mV which were found in gelatin and the blended films in this study possibly was the appropriate charge for cell attachment and proliferation. On the other hand, a negatively charged surface of DHT-crosslinked CH1000 film prohibited adhesion of negatively charged cells through electrostatic repulsion (Good, 1972). Furthermore, balance in negative/positive charges between material and cell surfaces played a key role for cell attachment and proliferation. Imbalance charge might result in unstabilized cell membrane and inhibited cell activities (Morgan et al., 1989; Choksakulnimitr et al., 1995; Nagasaki et al., 2004; Mao et al., 2005).

Table 4.7 Zeta (ζ) potential of G/CH1000 film surfaces, analyzed by ELS.

Film type	ζ potential (mV)
Gelatin	+4.61
G/CH1000 30/70	+9.00
CH1000	-32.69
Non-crosslinked CH1000	+14.89

Another possibility that could enhance cell activities on the blended films might be the affinity of films to some biological molecules like fibronectin that promoted cell activities. ***Pre-adsorption of some proteins*** such as fibronectin and vitronectin on film surfaces has been shown to affect cell behavior (Basson et al., 1990; Kirkpatric et al., 2007). Adsorption of some proteins onto a substrate is considered to be an important step for the subsequent cell adhesion to the substrate (Basson et al., 1990; Balcells & Edelman, 2002). Naturally, cells are likely to adhere onto a substrate through the integrin receptors. The integrin receptor recognizes the RGD-sequence which presents in vitronectin and fibronectin molecules (Hersel et al., 2003; Kirkpatric et al., 2007). Vitronectin and fibronectin are proteins presented in fetal bovine serum (FBS) supplemented in cell culture medium. In this study, fibronectin from FBS adsorbed onto the films was then examined using a modified ELISA method. Herein, gelatin, G/COS 30/70, COS, G/CH1000 30/70 and CH1000 films were selected for the test. Figure 4.25 presented the absorbance of fibronectin adsorbed on the films. The absorbance was directly correlated to the amount of fibronectin. From the results, the highest amount of adsorbed fibronectin was found

on pure gelatin film. This was due to the fact that fibronectin can specifically bind to RGD-sequence of gelatin and collagen molecules (Rodenberg & Pavalko, 2007). Interestingly, a remarkable difference in fibronectin adsorption between the blended film and each pure chitosan film was observed. The blended films containing 70% chitosan showed statistically higher fibronectin adsorption than pure CH and COS films. This could be the results of binding affinity of fibronectin with NH_2 and COOH groups. Faucheux et al. (2004) suggested that the adsorption of proteins onto the substrate depended on the type of functional groups on surface substrate. Keselowsky et al. (2003) have showed that fibronectin was adsorbed onto the NH_2, CH_3 and COOH surfaces with the higher extent than the OH surface. As discussed in the results of XPS, NH_2 groups were expected to be low in the cases of pure COS and CH1000 films and would result in low fibronectin adsorption onto such surfaces. This might explain the reason for great cell attachment and proliferation on the blended G/COS and G/CH1000 films compared to pure COS and CH1000 films, respectively. However, the result of fibronectin adsorbed on pure gelatin film that showed the highest amount did not correspond to the results of cell attachment and proliferation. Then, fibronectin adsorption could not completely explain the behavior of both cells attached and proliferated on all types of films.

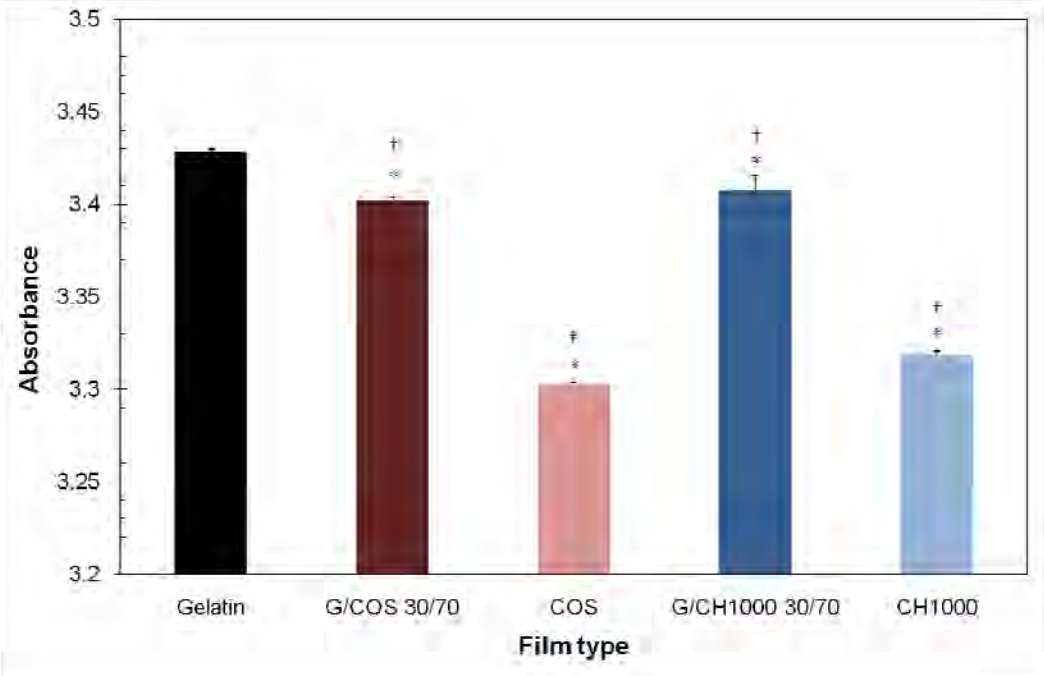

Figure 4.25 Absorbance of fibronectin adsorbed on G/COS and G/CH1000 films determined by modified ELISA method (* represented a significant difference relative to gelatin at $p<0.01$, † represented a significant difference between the blended (30/70) and pure chitosan films at $p<0.01$).

The last factor we considered was ***the secretion of growth factors*** from cells that can have paracrine effect targeting the neighboring cells to further adhere and grow on the films (Nerem, 2007). MSCs produce various growth factors such as vascular endothelial growth factor (VEGF), hepatocyte growth factor (HGF), insulin-like growth factor-1 (IGF-1), platelet derived growth factor (PDGF) and transforming growth factor-beta (TGF-β). Recently, the secretion of these growth factors has been reported as an essential function of mesenchymal stem cells (Kim et al., 2009). We here then hypothesized that IGF-1 or VEGF secreted from the initially attached MSCs signaled to neighboring MSCs and promoted further cell adhesion on the films. The films of which higher cell number attached would subsequent result in higher cell number proliferated. However, the concentration of IGF-1 and VEGF secreted from ASCs and MSCs cultured on gelatin, G/COS 30/70, COS, G/CH1000 30/70 and CH1000 films did not correlate to the above hypothesis, as exhibited in Figure 4.26. IGF-1 and VEGF concentrations of both cells cultured on G/COS 30/70 and G/CH1000 30/70 films, which showed dominant in number of cells attached and

proliferated, had similar levels to those of cells cultured on pure gelatin, COS and CH1000 films. Therefore, paracrine signaling of both IGF-1 and VEGF was not the main cause of attachment and proliferation of MSCs on the films in this study.

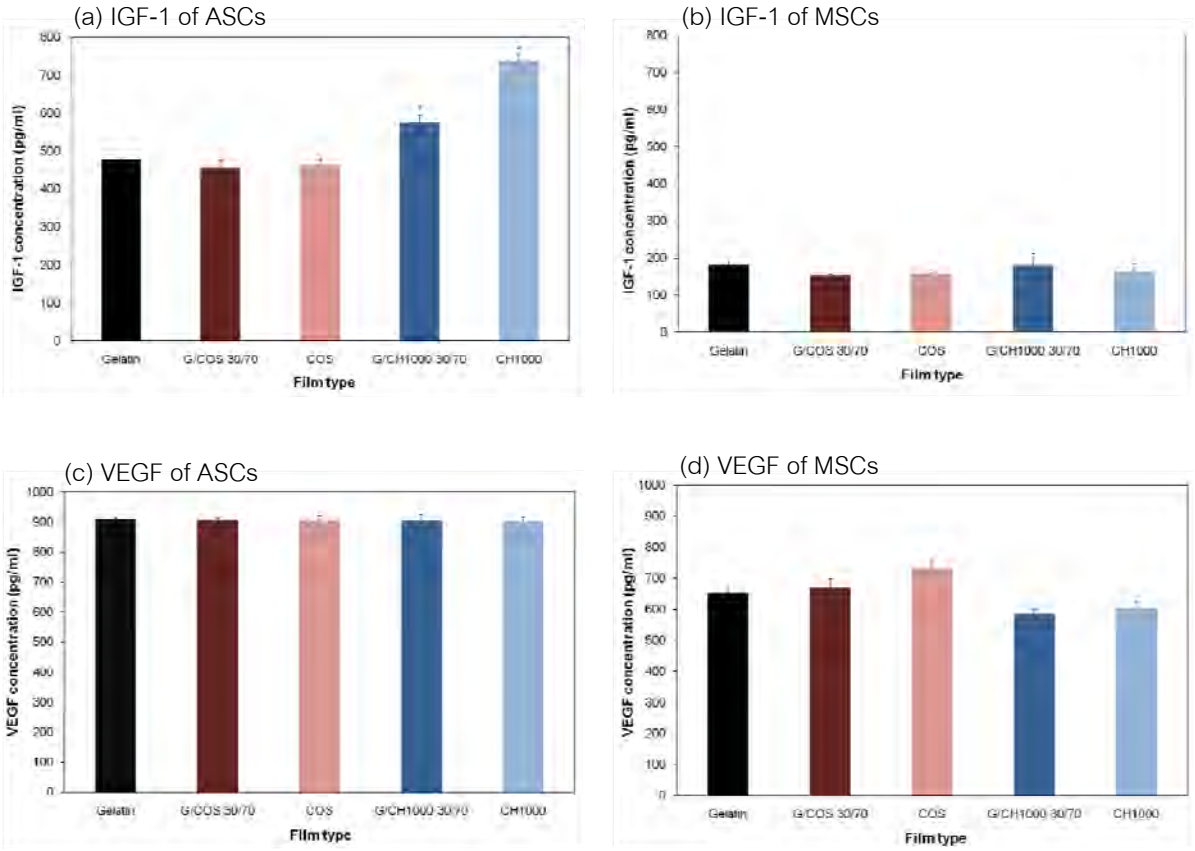

Figure 4.26 Concentration of growth factors in medium supernates of ASCs and MSCs cultured on G/COS and G/CH1000 films in α-MEM + 15% FBS for 2 days (a) IGF-1 of ASCs, (b) IGF-1 of MSCs, (c) VEGF of ASCs and (d) VEGF of MSCs (seeding: 10^5 cells/film).

Based on the possibilities discussed above, it was concluded that suitable net charge of film surfaces could be the main reason to promote cell affinity of the blended films in this study. Furthermore, in the aspect of osteogenic differentiation, it was possible that the enhanced osteogenic differentiation of the blended, pure CH1000 and COS films compared to gelatin film was due to the osteoconductive property of chitosan, as reported by Klokkevold et al. (1996).

Additionally, in this work, as it was found that high molecular weight CH1000 film did not support attachment and proliferation of both ASCs and MSCs, oppositely to the low molecular weight COS film. Then, the toxicity of both CH1000 and COS was verified by Annexin V-FITC/PI apoptosis test. The results in Figure 4.27 proved that MSCs treated with CH1000 were late apoptotic (both Annexin V-FITC and PI positive) while those treated with COS remained viable (both Annexin V-FITC and PI negative) after 24 h culture. This confirmed the higher toxicity of high molecular weight chitosan than the low molecular weight one, corresponding to the reports from several works. Richardson et al. (1999) stated that a variety of chitosans were cytotoxic in which the extent was being dependent upon their molecular weight, degree of deacetylation and salt form. Toxicity increased with increasing molecular weight and chitosan hydrochloride was the most toxic form. Subsequent study using lower molecular weight chitosan showed that toxicity could be substantially decreased (Heller et al., 1996). Some studies have proved that cationic polymers like chitosan and poly(L-lysine) were cytotoxic materials due to their unsuitable charges (Morgan et al., 1989; Choksakulnimitr et al., 1995; Nagasaki et al., 2004; Mao et al., 2005). It was believed that the cationic materials attached on negatively charged cellular membrane and destabilized their structure. The destabilization resulted in the rupture of cell membrane followed by cell death. In the case of high molecular weight chitosan, the high positively charge density may create the tight binding with the cell surface, resulting in high cytotoxic effect. In contrast, a small charge density of low molecular weight chitosan may reduce cytotoxicity.

Furthermore, interaction between chitosan and cells might be different depending on their molecular weights. Chae et al. (2005) reported that the molecular weight of water-soluble chitosan could be considered as a critical parameter of chitosan transport through the Caco-2 cell layer. Middle and low molecular weight (<22 kDa) water-soluble chitosans could penetrate through the Caco-2 cell layer, while high-molecular weight (230 kDa) water-soluble chitosan could not. Similar phenomena had been found by Schipper et al. (1997). They reported that chitosan having molecular weight higher than 30 kDa bound tightly to Caco-2 cell surface without cellular uptake. Yang et al. (2002) also demonstrated that chitosan with molecular weight of 4.2 kDa disrupted the lipid bilayer mimicked cell membrane in a concentration-dependent manner. In addition, it was shown by Porporatto et al. (2003)

that high molecular weight chitosan could be related to increased viscosity, reduced solubility or sterical hindrance, leading to a less efficient interaction with the cells.

Several works also reported on the strong effects of the molecular weight of chitin, chitosan, their derivatives, and oligosaccharides on their biological activities (Shibata et al., 1997; Richardson et al., 1999; Tangsadthakun et al., 2007; Wang et al., 2007). Low molecular weight chitosan promoted the proliferation of human skin fibroblasts and keratinocytes more than the high molecular weight ones, as reported by Tangsadthakun et al. (2007) and Wang et al. (2007), respectively. Howling et al. (2001) have also observed the proliferation of human dermal fibroblast cultured in medium containing soluble fraction of chitosan for 3 days. They found that low molecular weight chitosan (MW 13 kDa) displayed higher cell proliferation than high molecular weight chitosan (MW 263.8 kDa). The maximal stimulation was observed in fibroblasts cultured in medium containing 5 μg/mg of low molecular weight chitosan. Hsu et al. (2004) reported that the chitosan with molecular weights ranging between 180 and 330 kDa did not promote attachment and proliferation of L929 fibroblasts or rat chondrocytes. Furthermore, some *in vivo* studies suggested that low molecular weight chitosan might bind serum components, such as growth factors, and either protected them from enzymatic degradation or presented them to cells in an activated form. Growth factors bound with low molecular weight chitosan could be slowly released, supplying the cells with a sustained level of mitogenic signals (Schmidt et al., 1993; Kratz et al., 1997 & 1998).

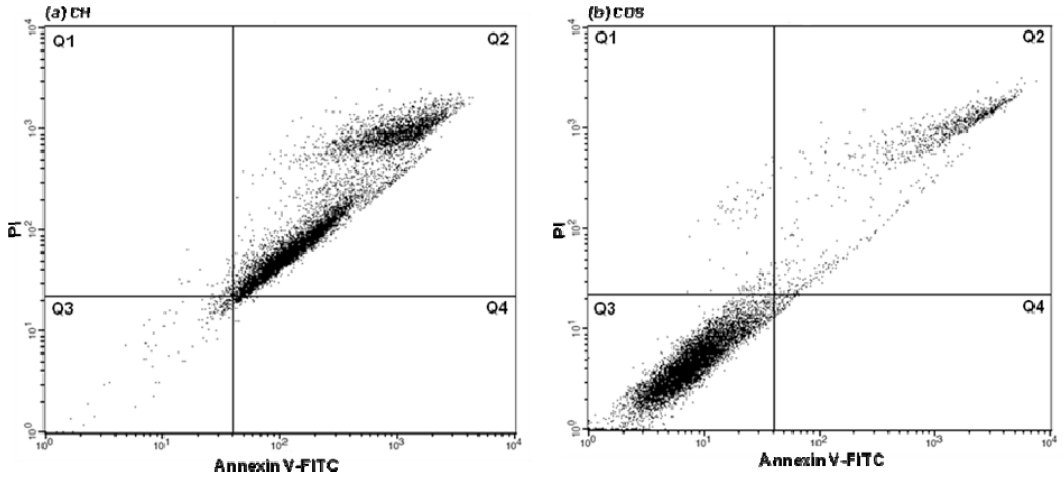

Population	% Total
Q1	0.68
Q2	96.61
Q3	1.78
Q4	0.93

Population	% Total
Q1	1.03
Q2	9.83
Q3	88.45
Q4	0.69

Figure 4.27 Apoptosis of MSCs after treated with (a) CH and (b) COS solutions for 24 h, assessed by Annexin V-FITC/PI double staining.

4.6.4 Summary

From the study on *in vitro* biocompatibility of G/COS and G/CH1000 films at different blending ratios with rat ASCs and MSCs, three interesting points were addressed. Firstly, the enhanced cell attachment and proliferation of the blended films at some curtain ratios were found to be caused by suitable charge (mild positive) of film surfaces. Secondly, the difference in toxicity of high molecular weight CH1000 and low molecular weight water-soluble COS was reported. The charge of materials might also be a main cause of cytotoxic effect of high molecular weight chitosan. The strong charge of high molecular weight chitosan could destabilize and rupture cell membrane, resulting in cell death. Last point was the diversity between rat ASCs and MSCs. ASCs showed faster proliferative rate while MSCs performed higher osteogenic differentiation potential, regardless of material types. This implied that mesenchymal stem cells derived from bone marrow had a high potential to differentiate into mature bone cells, compared to those derived from adipose tissue.

4.7 Characteristics of three-dimensional G/COS and G/CH scaffolds

After the study of material effects on cell activities in the system of two-dimensional films, morphological factor and mechanical properties of three-dimensional scaffolds prepared from the same materials associated cell behavior were considered. G/COS and G/CH1000 scaffolds at different blending ratios were further investigated systematically. Physical and chemical properties of different scaffolds were reported. Furthermore, *in vitro* biocompatibility of the scaffolds with rat ASCs and MSCs was illuminated. Behaviors of both stem cells including attachment, proliferation and osteogenic differentiation were comparatively shown here.

4.7.1 Physical characteristics of three-dimensional G/COS and G/CH scaffolds

G/COS and G/CH1000 scaffolds at different blending ratios were fabricated via freeze-drying and chemical crosslinking techniques. Glutaraldehyde was used as a crosslinking agent for these systems because it could crosslink between amino groups which were found in both gelatin and chitosan molecules. To prepare the sample solution for freeze-drying, bulk glutaraldehyde crosslinking was applied (Ozeki & Tabata, 2005). This technique resulted in higher crosslinking extent, especially when water-soluble materials like gelatin and COS were prepared. However, the glutaraldehyde-crosslinked scaffolds must be washed with glycine and water to remove the residual aldehyde groups. Non-crosslinked part of the scaffolds could be lost while washing. Then, after refreeze-drying, volume decrease and weight loss of G/COS and G/CH1000 scaffolds at different blending ratios were reported as presented in Table 4.8-4.9, comparing to the original volume and weight of scaffolds before glycine wash. However, in this present work, we found that G/COS scaffold at the blending ratio of 30/70 deformed during glycine wash so that it could not be handled, as seen in Figure 4.28. Also, pure COS scaffold dissolved completely in glycine solution. This showed that the preparation of scaffolds with high COS contents (≥ 70%) could not be achieved. Hence, G/COS scaffolds at the ratios of 100/0, 70/30 and 50/50 were further investigated. In the systems of G/CH1000 scaffolds, all blending ratios could be formed.

The results presented in Table 4.8 showed that volume of G/CH1000 scaffolds decreased around 21-27% while that of G/COS scaffolds reduced upto 65% from the original size. This indicated that, under the same preparation techniques,

G/COS scaffolds deformed easier than G/CH1000 scaffolds. Then, it could be stated that molecular weight of chitosan affected the stability of resulting scaffolds. The similar results were also found in our previous work with the systems of collagen/chitosan scaffolds (Tangsadthakun et al., 2007). Scaffolds prepared from collagen blended with medium and high molecular weight chitosans (460 and 1,450 kDa) showed higher compressive modulus and slower degradation rate than those prepared from low molecular weight one (180 kDa). Table 4.9 exhibited weight loss of G/COS and G/CH1000 scaffolds at different blending ratios after glycine washing and refreeze-drying. It was noticed that only a small amount of G/CH1000 scaffolds was lost from the processes (1-2%). At the same blending ratio, weight loss of G/COS scaffolds was more than that of G/CH1000 scaffolds, particularly at the ratio of 50/50. However, this weight loss of G/COS 50/50 scaffold (23.95%) confirmed that some amount of gelatin and COS molecules could be crosslinked by glutaraldehyde and remained in the blended scaffolds (total weight loss, 23.95% < original weight of each component, 50%). From the results, it was then referred that molecular weight of chitosan also influenced crosslinking extent of gelatin/chitosan scaffolds when crosslinked by glutaraldehyde. Very low molecular weight COS was more difficult to be crosslinked with gelatin by aldehyde groups due to the decrease in intermolecular interaction. Gupta et al. (2007) have also reported that the glutaraldehyde-crosslinked high molecular weight chitosan microspheres (2224 kg mol^{-1}) showed a low degree of swelling due to the strong intermolecular interaction and a high degree of cross-linking, comparing to the low molecular weight chitosan (260 kg mol^{-1}).

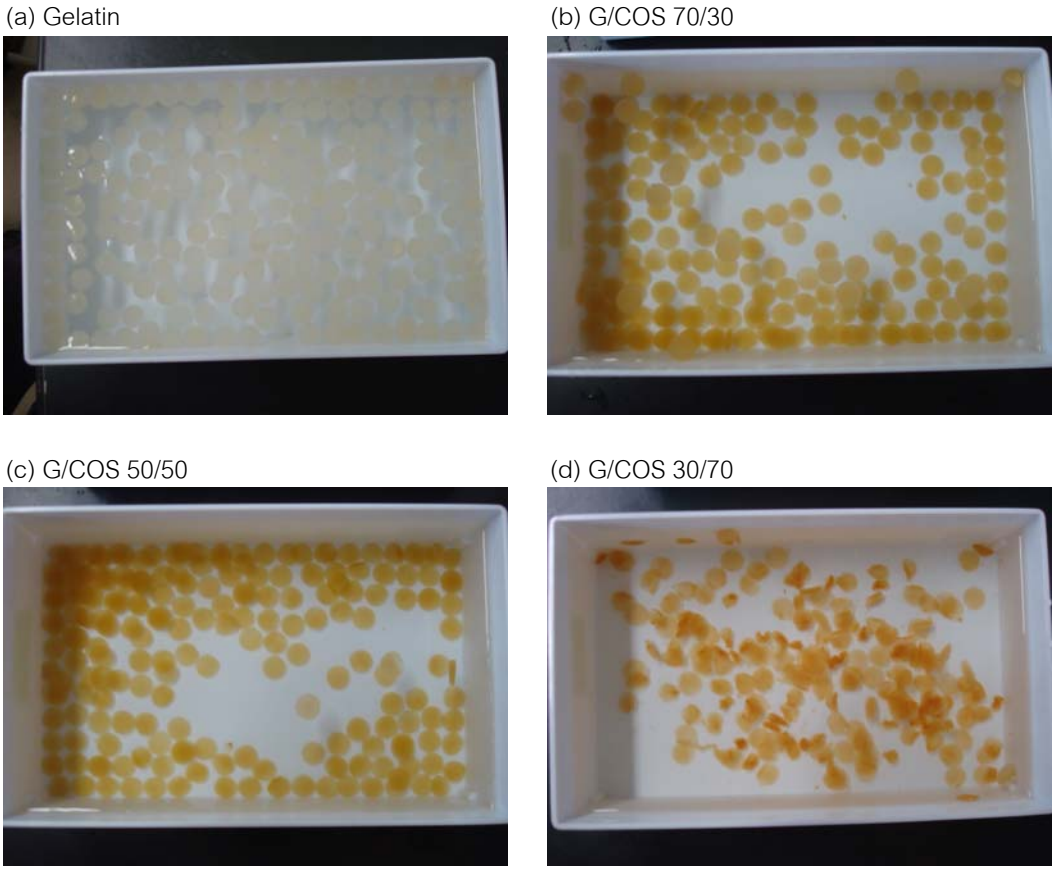

Figure 4.28 G/COS scaffolds at different blending ratios during glycine wash before refreeze-dry (a) gelatin, (b) G/COS 70/30, (c) G/COS 50/50 and (d) G/COS 30/70 scaffolds.

Table 4.8 Volume decrease of G/COS and G/CH1000 scaffolds at different blending ratios after glutaraldehyde crosslinking.

Blending ratio	Volume change of scaffolds after crosslinking (%)	
	G/COS	G/CH1000
100/0	-32.70 ± 1.33	-32.70 ± 1.33
70/30	-64.81 ± 1.39[a]	-21.25 ± 1.27[a]
50/50	-65.32 ± 0.77[a]	-27.51 ± 0.33[a]
30/70	N/A	-25.27 ± 1.44[a]
0/100	N/A	-26.47 ± 6.21

[a] represented a significant difference relative to gelatin scaffold at $p<0.05$

Table 4.9 Weight loss of G/COS and G/CH1000 scaffolds at different blending ratios after glutaraldehyde crosslinking.

Blending ratio	Weight loss of scaffolds after crosslinking (%)	
	G/COS	G/CH1000
100/0	1.60 ± 0.03	1.60 ± 0.03
70/30	4.26 ± 0.95[a]	2.12 ± 0.91
50/50	23.95 ± 0.60[a]	2.03 ± 0.72
30/70	N/A	1.59 ± 0.15
0/100	N/A	1.62 ± 0.04

[a] represented a significant difference relative to gelatin scaffold at $p<0.05$

It was known that the variation in pore topography and size of the scaffolds could have a profound effect on the attachment and long term survival of cells. Morphology of the scaffolds might have a particular pattern and pore alignment for a specific cell type. In this study, the morphology of resulting G/COS and G/CH1000 scaffolds was further observed by SEM. SEM images shown in Figure 4.29 indicated homogeneous structure for all scaffolds. G/COS scaffolds displayed a slightly more porous structure than G/CH1000 scaffolds. However, pore size of all scaffolds shown in Table 4.10 was not significantly different (approximately 70-80 μm), except that of pure gelatin scaffold which was largest (105 μm). Optimal pore size that allows bone ingrowth and vascularization throughout the scaffold was reported to be 50–150 μm (Whang et al., 1995; Holy et al., 1999). Smaller pores favored chondrogenesis followed by osteogenesis while larger pores favored direct osteogenesis (Karageorgiou and Kaplan, 2005; Hofmann et al., 2007; Jones et al., 2009). Meinig et al., (1996) also demonstrated that smaller pore size of a poly-(L-lactide) membrane (15-20 μm) was successively used to cover 1 cm defects in the

radii of rabbits. The defects had grossly healed and histologically cortical bone had been regenerated after 18–24 months.

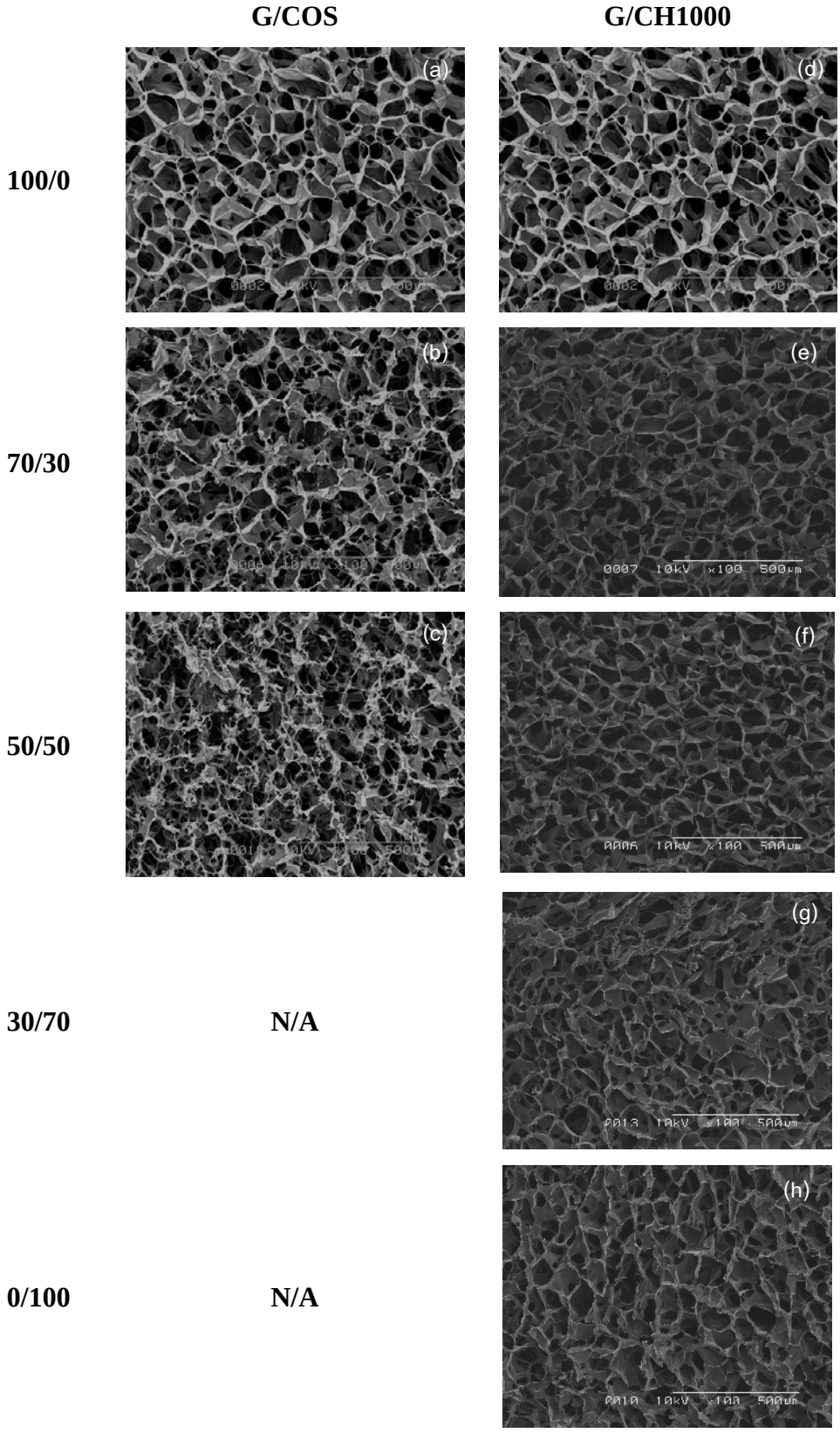

Figure 4.29 Cross-sectioned morphology of (a-c) G/COS and (d-h) G/CH1000 scaffolds at different blending ratios, observed by SEM at 100X magnification.

Table 4.10 Pore size of G/COS and G/CH1000 scaffolds at different blending ratios measured from SEM photographs.

Blending ratio	Pore size of scaffolds (μm)	
	G/COS	G/CH1000
100/0	105.33 ± 21.49	105.33 ± 21.49
70/30	83.26 ± 16.13[a]	80.42 ± 15.12[a]
50/50	71.77 ± 16.39[a]	79.16 ± 17.89[a]
30/70	N/A	80.56 ± 18.73[a]
0/100	N/A	76.40 ± 13.13[a]

[a] represented a significant difference relative to gelatin scaffold at $p<0.01$

Besides the morphology of the scaffolds, mechanical property is another significant parameter affected not only cell attachment, proliferation and phenotype, but also bone regeneration and resorption (Yaszemski et al., 1996). The scaffolds must be strong enough to support the physiological load of the body without absorbing the mechanical stimuli required for natural growth in the affected area. It is also essential that the scaffolds should allow gradual load transfer to the developing tissue for proper healing to occur (Temenoff et al., 2000). Furthermore, Sharma et al. (2005) reported that osteoblast proliferation was sensitive to strain or other mechanical stimuli. In this study, compressive modulus of both dry and wet G/COS and G/CH1000 scaffolds was comparatively illustrated in Figure 4.30 (a) and (b), respectively. In the case of dry scaffolds, compressive modulus of pure gelatin scaffold (approximately 120 kPa) was significantly higher than that of the other blended and pure CH1000 scaffolds. This might be due to the high glutaraldehyde crosslinking of abundant amino groups within gelatin molecules. The relationship between crosslinking extent and mechanical properties of materials was described elsewhere (Haugh et al., 2006; Wang et al., 2008). The difference in compressive modulus of dry G/COS and G/CH1000 scaffolds at the same blending ratio was not noticed in this work. However, in the wet state, compressive modulus of G/CH1000 scaffolds was significantly higher than that of G/COS scaffolds at the same blending ratio. This could be explained that high molecular weight chitosan presented high intermolecular chain which could lead to the higher crosslinking extent and mechanical properties (Gupta et al., 2007). This correlated to the results of our previous study reported that collagen/high molecular weight chitosan scaffolds showed higher compressive modulus than collagen/low molecular weight chitosan (180 kDa) (Tangsadthakun et al., 2007).

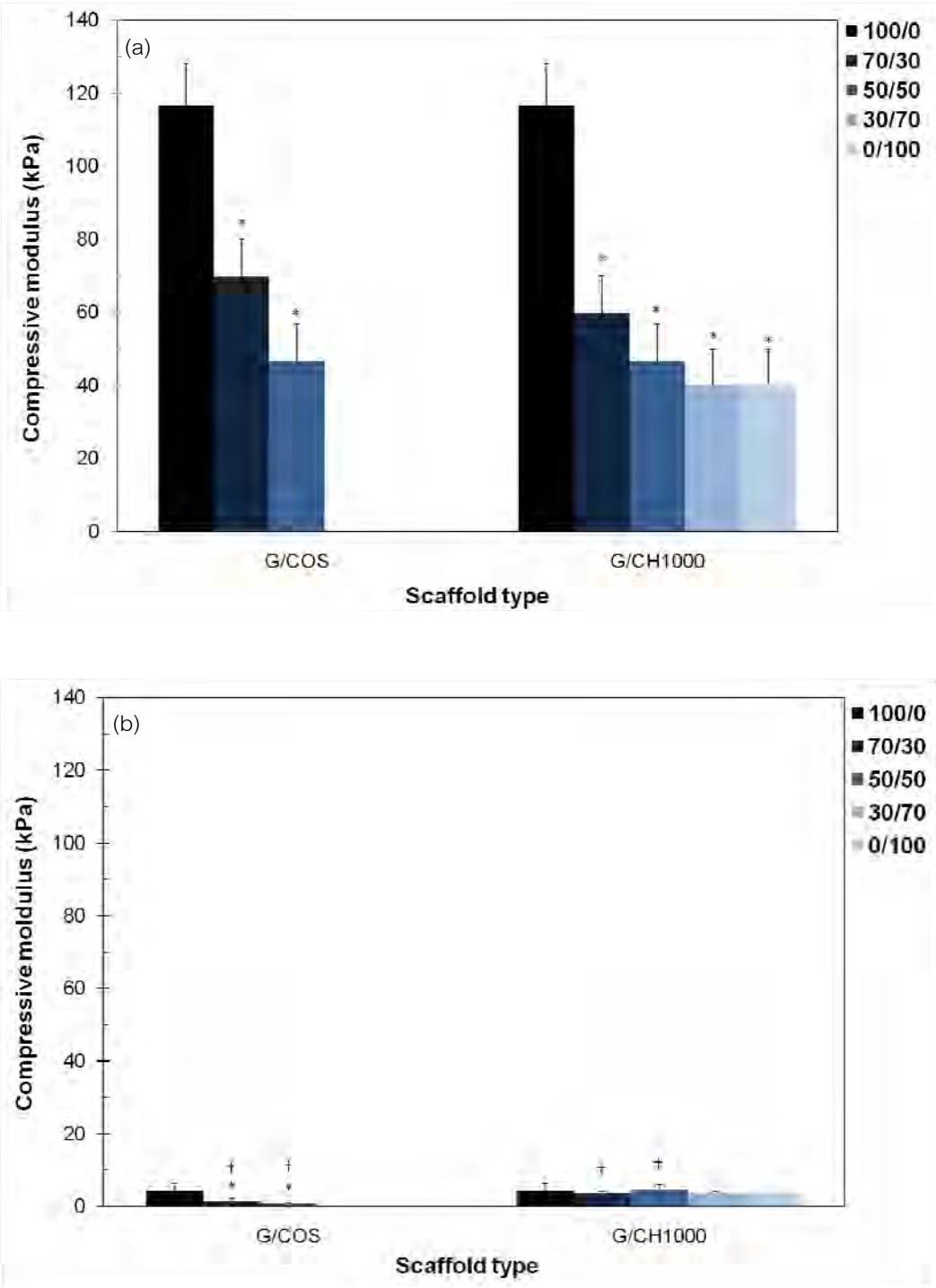

Figure 4.30 Compressive modulus of G/COS and G/CH1000 scaffolds at different blending ratios (a) dry state and (b) wet state, analyzed by a universal testing machine (* represented a significant difference relative to gelatin at $p<0.05$, † represented a significant difference between G/COS and G/CH1000 scaffolds at same blending ratio at $p<0.05$).

Swelling ability of scaffold plays an essential role during the *in vitro* culture and biological transportation *in vivo*. The scaffolds which are capable of swelling would allow the increased pore sizes, facilitating cell penetration inside the scaffolds and growing in a three-dimensional fashion. Also, the high swollen scaffolds are suitable for oxygen and waste transportation. Figure 4.31 presented swelling ability of G/COS and G/CH1000 scaffolds after 1-day incubation in PBS. It was shown that G/CH1000 scaffolds at all blending ratios could uptake more PBS solution than G/COS and gelatin scaffolds. This might due to the less deformation of G/CH1000 scaffolds, as demonstrated in Table 4.8. Less deformed G/CH1000 scaffolds possibly showed low apparent density which was easier to allow water penetration. In addition, G/CH1000 scaffolds could retain more water than G/COS scaffolds during blotting, resulting in higher swelling ratio. However, in overall, it could be indicated that all of the scaffolds in this work showed high swelling ability and were appropriate for further *in vitro* culture.

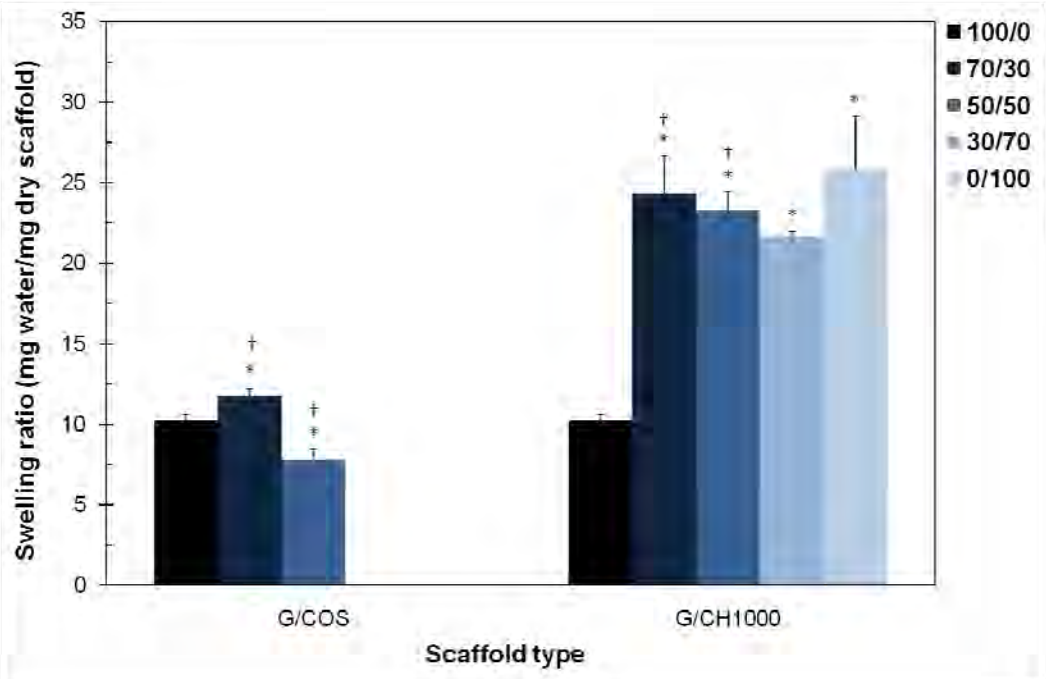

Figure 4.31 Swelling ratio of G/COS and G/CH1000 scaffolds at different blending ratios after incubation in PBS at 37°C, pH 7.4 for 24 h (* represented a significant difference relative to gelatin at $p<0.05$, † represented a significant difference between G/COS and G/CH1000 scaffolds at same blending ratio at $p<0.05$).

4.7.2 In vitro biological characteristics of three-dimensional G/COS and G/CH scaffolds with rat ASCs and MSCs

The *in vitro* biological activities of ASCs and MSCs on G/COS and G/CH1000 scaffolds at different blending ratios were systematically demonstrated. Attachment and proliferation of both cells on the scaffolds when cultured under proliferating medium (α-MEM, 15% FBS, 100 U/ml penicillin/streptomycin) were reported as the number of cells assessed by both MTT and DNA assays. Figure 4.32-4.33 illustrated the number of ASCs and MSCs attached and proliferated on G/COS and G/CH1000 scaffolds, analyzed by MTT assay. It was observed that both cells could attach and proliferate on G/COS scaffolds with the similar extent to those on pure gelatin scaffold. Also, the number of both cells slightly increased along 7-day culture period. In contrast, G/CH1000 scaffolds at all blending ratios did not support growth of ASCs and MSCs, comparing to pure gelatin scaffold. The number of cells on G/CH1000 scaffolds was significantly lower than those on gelatin scaffold, particularly after 5 and 7 days of the culture. It was also noticed that cell number gradually decreased when chitosan ratio increased. And in the case of scaffolds containing 70% and 100% CH1000, the number of cells was lower than the number of cell initially attached at 6 h, indicating the death of some cells on such scaffolds. The number of MSCs attached and proliferated on G/COS and G/CH1000 scaffolds when cultured under the same condition was confirmed by DNA assay, as comparatively shown in Figure 4.34. The results showed similar trend to those obtained from MTT assay. Thus, it could be implied from this investigation that the system of gelatin blended with high molecular weight chitosan (CH1000) at all blending ratios was not suitable for *in vitro* culture of ASCs and MSCs. Oppositely, scaffolds prepared from gelatin blended with low molecular weight COS could support cell activities. Therefore, the system of G/COS scaffold was selected for the further study on osteogenic differentiation of ASCs and MSCs.

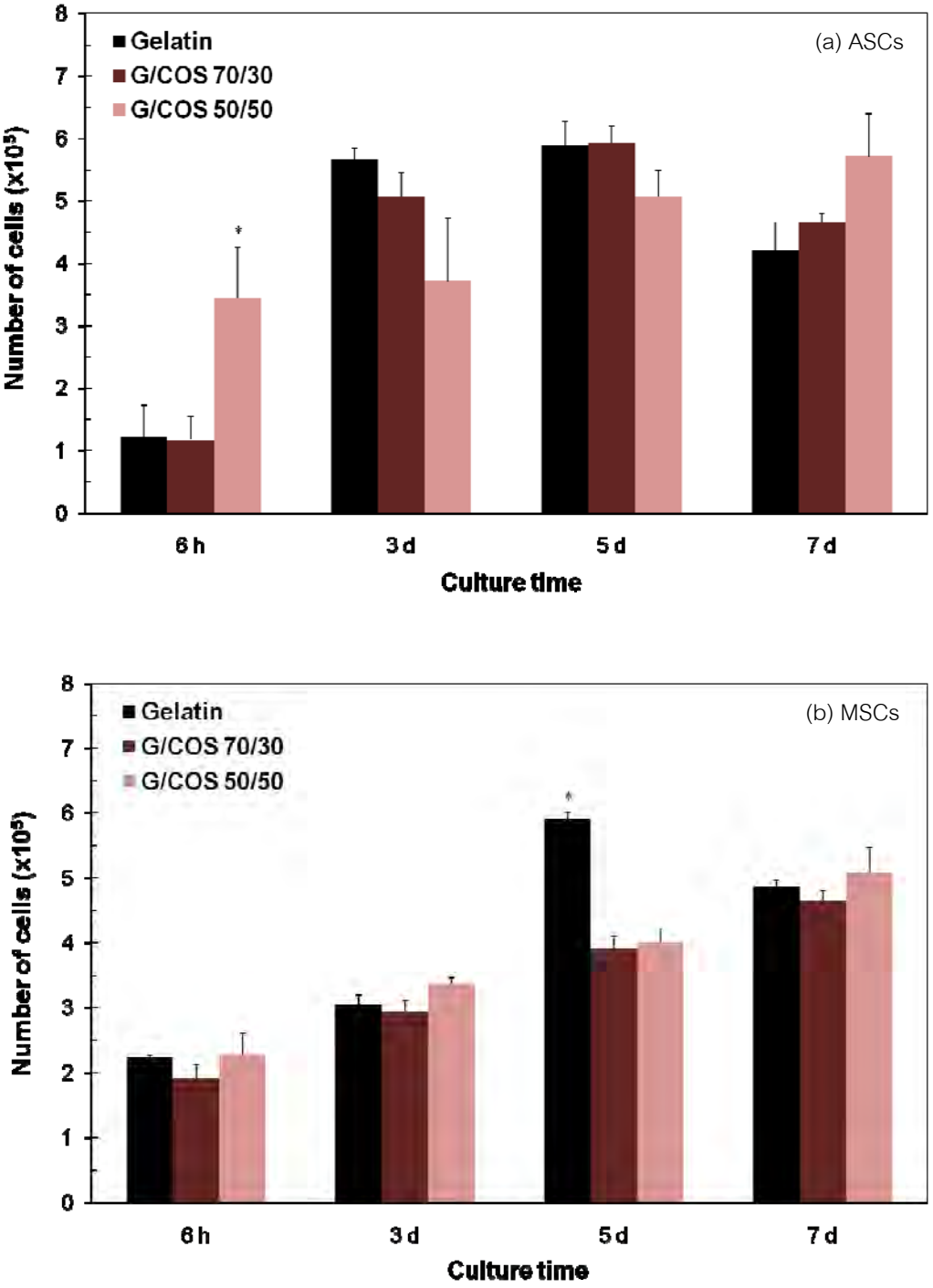

Figure 4.32 Number of (a) ASCs and (b) MSCs attached and proliferated on G/COS scaffolds at different blending ratios cultured in α-MEM + 15% FBS for 6 h, 3, 5 and 7 days, assessed by MTT assay (seeding: $5x10^5$ cells/scaffold, * represented a significant difference relative to gelatin within same culture period at $p<0.05$).

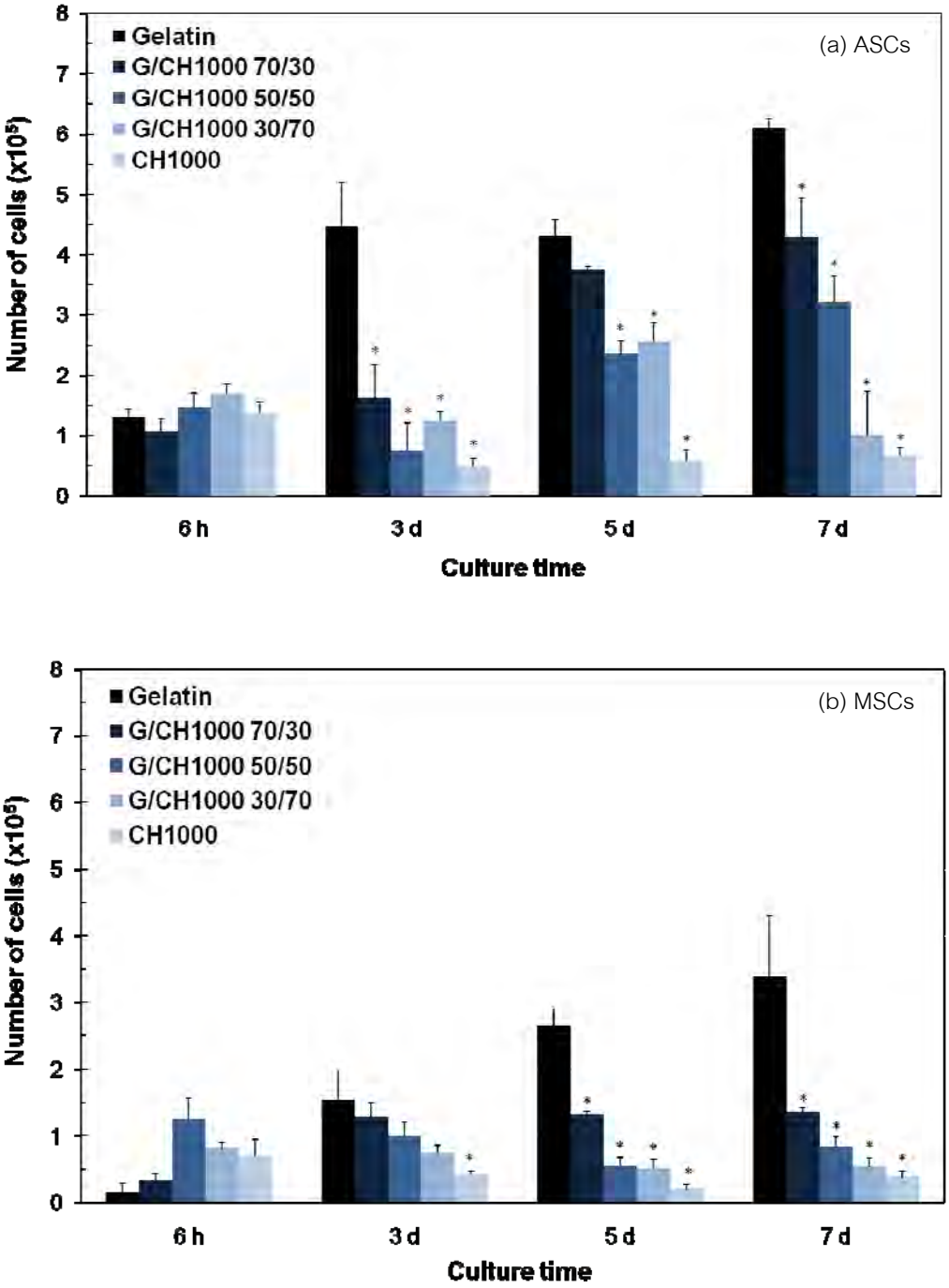

Figure 4.33 Number of (a) ASCs and (b) MSCs attached and proliferated on G/CH1000 scaffolds at different blending ratios cultured in α-MEM + 15% FBS for 6 h, 3, 5 and 7 days, assessed by MTT assay (seeding: $5x10^5$ cells/scaffold, * represented a significant difference relative to gelatin within same culture period at $p<0.05$).

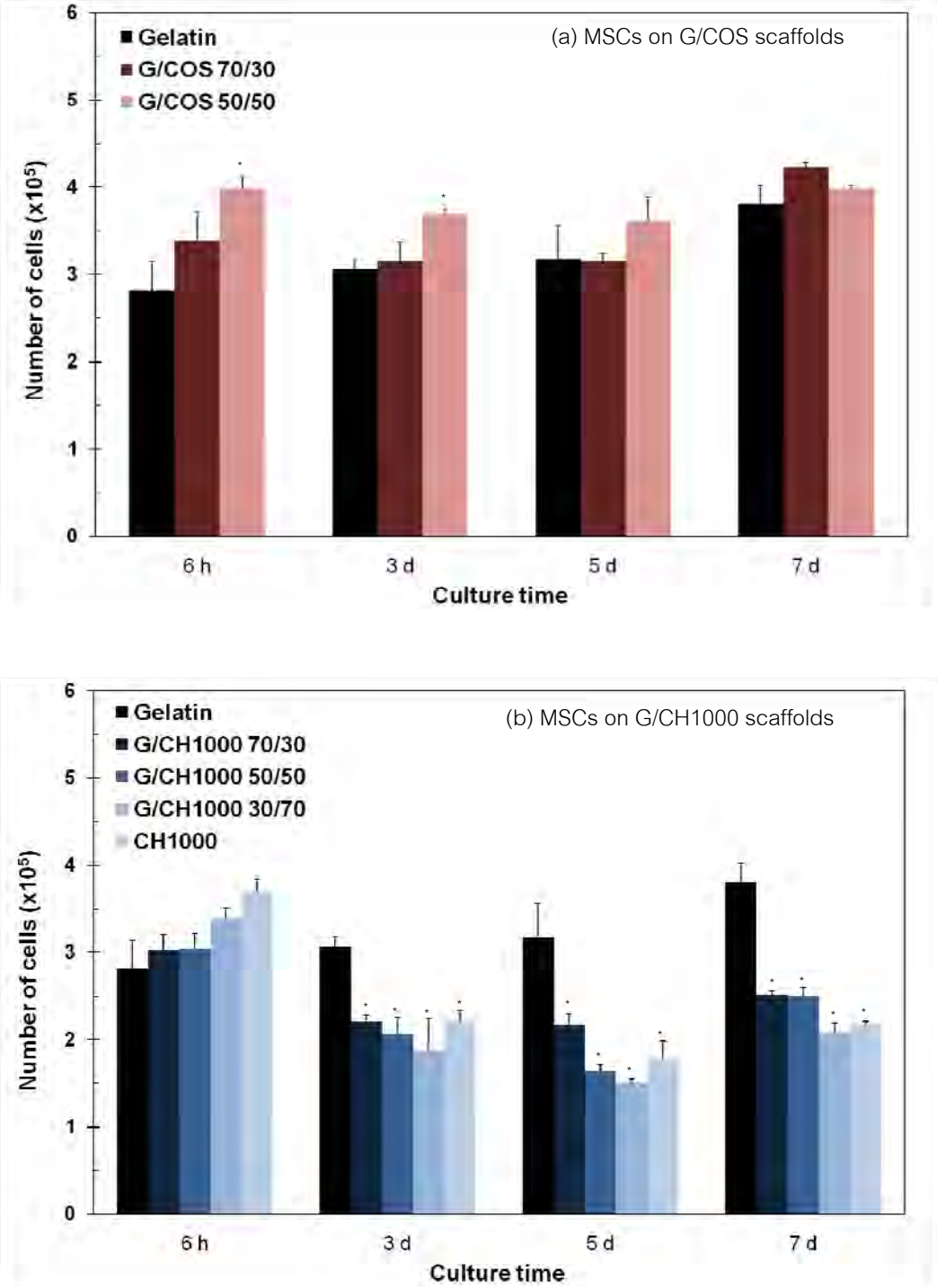

Figure 4.34 Number of MSCs attached and proliferated on (a) G/COS and (b) G/CH1000 scaffolds at different blending ratios cultured in α-MEM + 15% FBS for 6 h, 3, 5 and 7 days, assessed by DNA assay (seeding: $5x10^5$ cells/scaffold, * represented a significant difference relative to gelatin within same culture period at $p<0.05$).